WASHINGTON UNIVERSITY

SEVER INSTITUTE OF TECHNOLOGY

PERIODIC OPERATION OF HEAT REGENERATORS: A NEW METHOD FOR CALCULATION OF THERMAL EFFICIENCY

by

Shih-Ming Lai

Prepared under the direction of Professor M. P. Duduković

A thesis presented to the Sever Institute of
Washington University in partial fulfillment
of the requirements for the degree of

MASTER OF SCIENCE

August, 1983

Saint Louis, Missouri

WASHINGTON UNIVERSITY
SEVER INSTITUTE OF TECHNOLOGY

ABSTRACT

PERIODIC OPERATION OF HEAT REGENERATORS: A NEW METHOD FOR CALCULATION OF THERMAL EFFICIENCY

by Shih-Ming Lai

ADVISOR: Professor M. P. Duduković

August, 1983

Saint Louis, Missouri

Two approaches are developed for modeling of periodic operation of heat regenerators and calculation of their thermal efficiency. The first uses an approximate representation of the impulse response expressed in terms of its variance, σ_D^2, and the principle of superposition. The second consists of n-staged compartments in series.

Thermal efficiency for cocurrent and countercurrent operation is calculated for both equal and unequal products of mass flows and specific heats, $\dot{m}Cp$, of the hot and cold gas. Optimal operation is always at equal $\dot{m}Cp$'s (i.e. symmetric case). Countercurrent operation is more efficient than cocurrent and gives best efficiencies at shortest switching times. Using the thermal mean residence time as switching time gives the highest efficiency in cocurrent operation and is the most practical solution for countercurrent case also. It

is shown that thermal efficiency is primarily a function of $1/\sigma_D^2$ and switching time conditions. Agreement of the approximate solution with other methods is excellent for long regenerators and within 20% for short ones.

TABLE OF CONTENTS

TABLE OF CONTENTS
(continued)

TABLE OF CONTENTS
(continued)

List of Tables

List of Figures

List of Figures
(continued)

List of Figures
(continued)

PERIODIC OPERATION OF HEAT REGENERATORS: A NEW METHOD FOR CALCULATION OF THERMAL EFFICIENCY

1. INTRODUCTION

1.1 SCOPE AND SIGNIFICANCE

Heat regenerators have been used extensively in metallurgical industry, in air separation plants, Fischer-Tropsch synthesis, gas-turbine applications and other processes. In this type of heat exchanger, heat is not exchanged directly between a hot and cold flowing fluid through a solid wall that separates the two, as is done in heat recuperators, rather energy is periodically stored and withdrawn from the solid. Hot fluid and cold fluid flow alternately in contact with the solid, the former transmits heat to the solid and heats the solid while being cooled (heating period), the latter absorbs heat from the solid, cools the solid and is heated (cooling period).

Because solids, on a volume basis, have a very large heat capacity compared to gases, they can effectively be used as an intermediary in the transfer of heat from one gas to another. A much more compact and cheaper heat transfer area can then be used in heat regenerators compared to heat recuperators, large temperature differences between the hot and cold fluid can be tolerated and energy can be temporarily stored for later use.

Recent developments point to an increased use of heat regenerators in at least two broad areas of synthetic fuels manufacture and storage of solar energy. A variety of synthetic fuel processes, which are now in development stage, require handling, heating and cooling of large quantities of solids, generate immense volumes of hot process gas and require preheating of cold gas. Use of heat regenerators in such process schemes is required. Storage of solar and other energy forms as enthalpy of packed beds of solid material has already been tested and its usage is expected to increase.

Continuous operations can be achieved either by switching periodically from hot to cold fluid (swing regenerators) or by rotating the solid between a hot and cold flowing fluid (rotary regenerators). Both systems can be run two ways: in cocurrent operations the cold fluid and the hot fluid enter one after the other at the same end of the regenerator, in countercurrent operations the hot fluid enters at one end and the cold fluid enters at the other end of the regenerator. In order to provide a continuous exchange of heat between the two gases in the swing regenerators, at least two fixed bed regenerators must be used. The arrangement for this system is shown in Figures 1.1a and 1.1b for the countercurrent and cocurrent operations, respectively. In contrast, the arrangement for the rotating regenerator system is much more compact as shown in Figures 1.2a and 1.2b. Mathematical models for these two systems are analogous when there is no appreciable heat conduction in the angular direction of the rotary regenerator. We will concern ourselves primarily with fixed bed regenerators in this work.

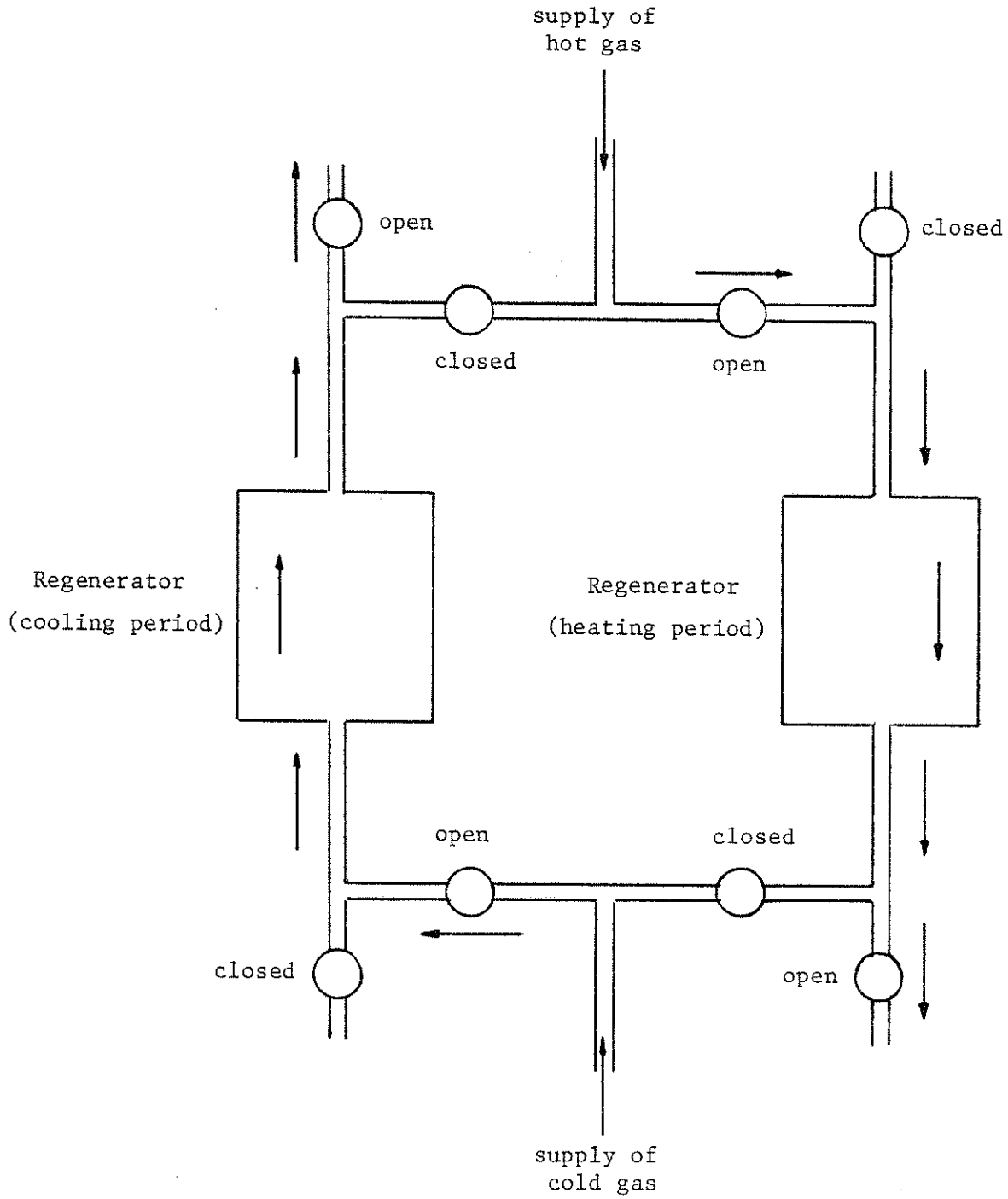

Figure 1.1a Fixed Two-Bed Regenerator

—— Countercurrent Operation

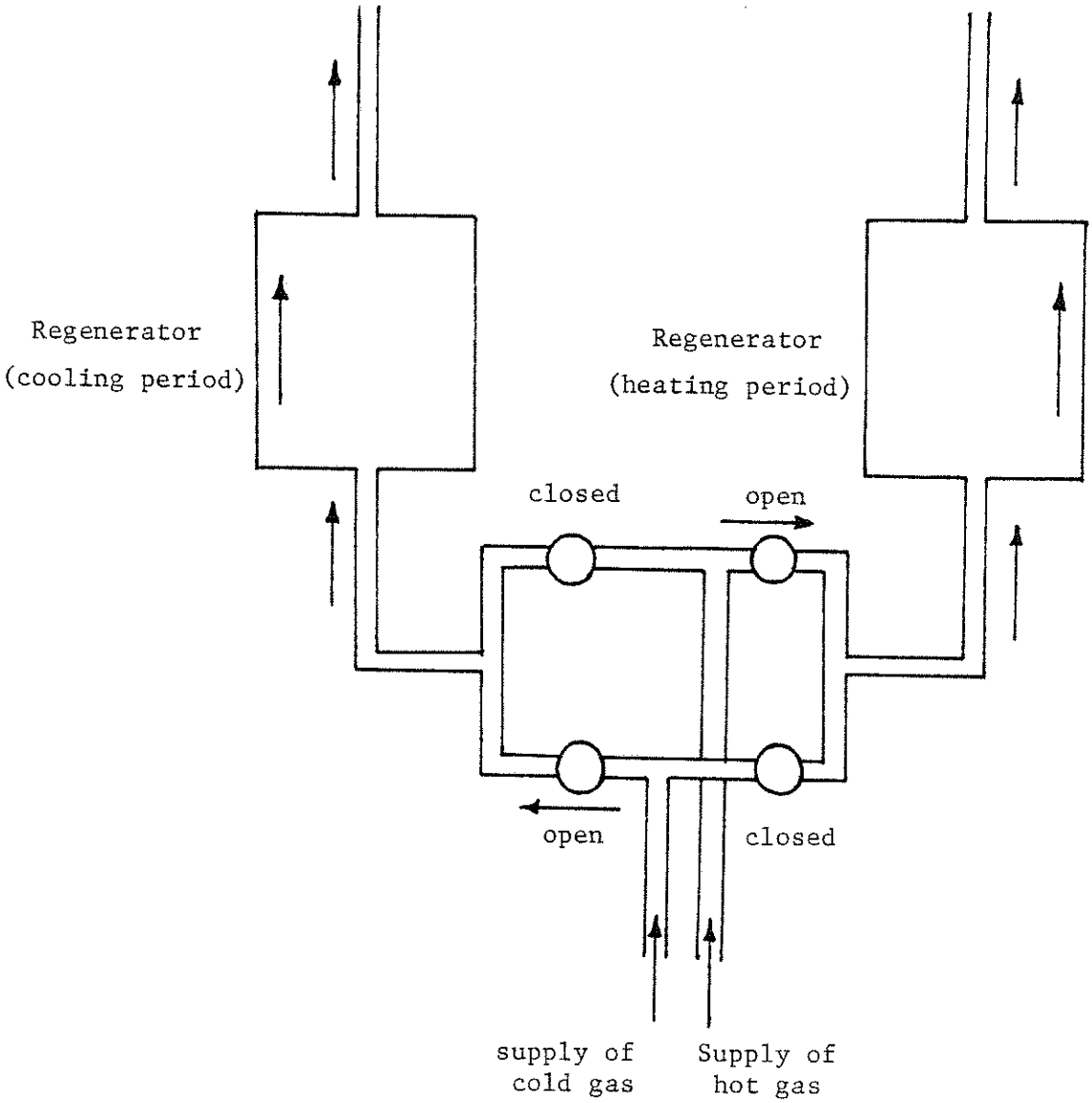

Figure 1.1b Fixed Two-Bed Regenerator

—— Cocurrent Operation

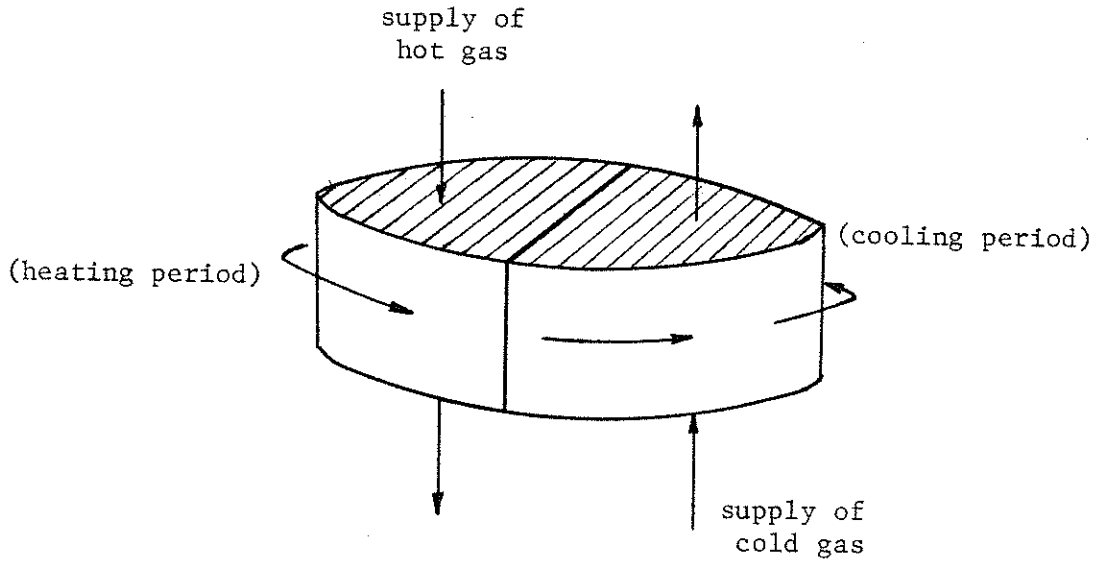

Figure 1.2a Rotary Regenerator
—— Countercurrent Operation

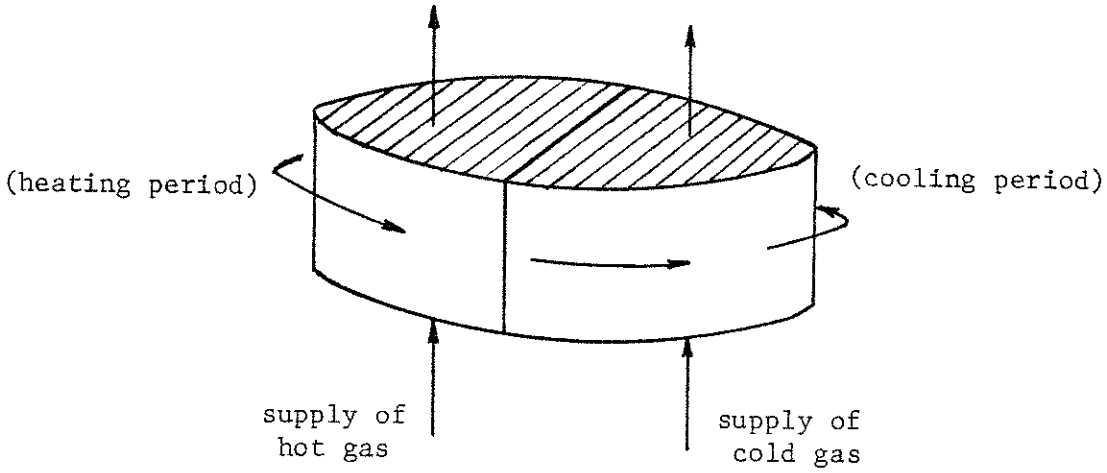

Figure 1.2b Rotary Regenerator
—— Cocurrent Operation

1.2 RESEARCH OBJECTIVES

Faced with increased use of heat regenerators it is proper to inquire whether the theory of their operation and methodology for their design is available. We have reviewed the current literature and find it somewhat wanting.

Our goals for this thesis can be summarized as follows: We want first to review and present the concepts and phenomena involved in regenerator operation. We will try next to develop a simple, approximate but accurate formula for evaluating the thermal efficiency. For cocurrent operation we will use the approximate solution in terms of the variance of impulse response based on the principle of superposition, while for countercurrent operation we will develop a model of staged fluidized beds in series (equivalent to a mixed tanks in series model) which can be used for large n as an approximation to fixed solids regenerators. Both equal and unequal flows of hot and cold gas will be considered. We will relate the variance of the impulse response to the thermal efficiency and apply the relationship to any model when the variance is available. This is the approach that we intend to follow which differs from the ones presented so far in the literature. Finally, we will indicate what are the optimal operating conditions for achievement of high thermal efficiency.

2. BACKGROUND

2.1 MATHEMATICAL MODEL FOR TWO BASIC REGENERATOR TYPES

Packed bed regenerator and plate regenerator are the two basic types of thermal regenerators. Here the general mathematical models for these two types are discussed. Under certain circumstances models can be simplified by neglecting some small heat transfer resistances and these models can then be derived as limiting cases of the general case.

All the models can be divided into two groups on the basis of how they view the solids. Some models treat the solids as a homogeneous isotropic or anisotropic phase and others view the solids to be a discrete phase consisting of particles which exchange heat with fluid only. The former model types can be used for packed beds with small particles and in a different form for plate regenerators while the latter ones based on discrete solids are appropriate for packed beds with large particles only but not for plate regenerators.

Mathematical formulation of these models follows. In the analysis the following assumptions have been made:

1. Physical properties C_p, ρ, etc. do not change with temperature
2. Constant mean fluid velocity
3. Constant heat transfer coefficient and thermal conductivity
4. Inlet temperature is a function of time only
5. No heat transfer by radiation.

2.1.1 Mathematical description of packed bed regenerators

Model IA. Solids treated as a continuous phase

Gas: $$\psi\frac{\partial t_g}{\partial \tau} = -\frac{\partial t_g}{\partial \xi} + \frac{1}{Pe_{gz}}\frac{\partial^2 t_g}{\partial \xi^2} + \frac{\ell}{Pe_{gr}}\frac{1}{\eta}\frac{\partial}{\partial \eta}\left(\eta\frac{\partial t_g}{\partial \eta}\right) - St(t_g - t_s) \qquad 2.1:1$$

Solid: $$\frac{\partial t_s}{\partial \tau} = \frac{1}{Pe_{sz}}\frac{\partial^2 t_s}{\partial \xi^2} + \frac{\ell}{Pe_{sr}}\frac{1}{\eta}\frac{\partial}{\partial \eta}\left(\eta\frac{\partial t_s}{\partial \eta}\right) + St(t_g - t_s) \qquad 2.1.2$$

$$\eta = 0 \qquad \frac{\partial t_g}{\partial \eta} = \frac{\partial t_s}{\partial \eta} = 0 \qquad 2.1.3a,b$$

$$\eta = 1 \qquad \frac{\partial t_g}{\partial \eta} = Bi_{wg}(t_w - t_g) \qquad 2.1.4a$$

$$\frac{\partial t_s}{\partial \eta} = Bi_{ws}(t_w - t_s) \qquad 2.1.4b$$

$$\xi = 0 \qquad t_g = \varphi(\tau) \qquad 2.1.5a'$$

or

$$-\frac{1}{Pe_{gz}}\frac{\partial t_g}{\partial \xi} + t_g = \varphi(\tau) \qquad 2.1.5a$$

$$\frac{\partial t_s}{\partial \xi} = Bi_{es}(t_s - t_a) \qquad 2.1.5b$$

$$\xi = 1 \qquad \frac{\partial t_g}{\partial \xi} = 0 \qquad 2.1.6a$$

$$-\frac{\partial t_s}{\partial \xi} = Bi_{es}(t_s - t_a) \qquad 2.1.6b$$

$$\tau = 0 \qquad t_g = f(\xi, \eta) \qquad 2.1.7a$$

$$t_s = g(\xi, \eta) \qquad 2.1.7b$$

where independent variables are:

$$\xi = \frac{z}{L} \quad , \quad \eta = \frac{r}{R} \quad ,$$
$$\tau = \frac{\epsilon \rho_g C_{pg}}{(1-\epsilon)\rho_s C_{ps}} \frac{\theta}{(\epsilon L/u_g)} = \psi \frac{\theta}{\theta_a} \qquad 2.1.8$$

dependent variables are:

$$t_g = \frac{T_g - T_{go}}{T_{gi} - T_{go}} \quad , \quad t_s = \frac{T_s - T_{go}}{T_{gi} - T_{go}} \qquad 2.1.9$$

dimensionless groups are

$$Pe_{gz} = \frac{LG_g C_{pg}}{Ke_{gz}} \quad , \quad Pe_{gr} = \frac{RG_g C_{pg}}{Ke_{gr}}$$

$$Pe_{sz} = \frac{LG_g C_{pg}}{Ke_{sz}} \quad , \quad Pe_{sr} = \frac{RG_g C_{pg}}{Ke_{sr}}$$

$$St = \frac{h a_s L}{G_g C_{pg}} \quad , \quad Bi_{es} = \frac{h_e L}{Ke_{sz}} \qquad 2.1.10$$

$$Bi_{wg} = \frac{h_{wg} R}{Ke_{gr}} \quad , \quad Bi_{ws} = \frac{h_{ws} R}{Ke_{sr}}$$

$$\psi = \frac{\epsilon \rho_g C_{pg}}{(1-\epsilon)\rho_s C_{ps}} \quad , \quad \ell = \frac{L}{R}$$

$$t_w = \frac{T_w - T_{go}}{T_{gi} - T_{go}} \quad , \quad t_a = \frac{T_a - T_{go}}{T_{gi} - T_{go}}$$

It should be noted that a choice of boundary conditions is given above and only one set of conditions can be used per problem e.g. only one of the equations (2.1.5a'), (2.1.5a) and (2.1.5b) can be selected in a given problem. Equation 2.1.1 contains the accumulation term for the gas phase, energy transport by the bulk flow and "effective" conduction (conduction + eddy transport) in the gas in both axial and radial directions and convective film transport from gas to solid. Equation 2.1.2 contains the accumulation term for the solid phase, "effective" conduction (conduction through points of contact + conduction through stagnant fluid film and adjacent solid) in the solid in both axial and radial directions and gas-solid convective film transport. Symmetry of the system is indicated by Equation 2.1.3, while losses at the cylindrical wall can be described by Equation 2.1.4 if an additional equation is provided for the wall temperature, T_w. At the entrance of the bed either Equations 2.1.5a' and 2.1.5b (Hulburt condition) or Equations 2.1.5a and 2.1.5b (Danckwerts condition) should be used. It suffices to say that for long beds either condition can be used and hence the simple one, Equation 2.1.5a', is preferred. For short beds Equation 2.1.5a is more appropriate. Equation 2.1.5a' assigns continuity of temperature at the entrance while Equation 2.1.5a states that transport into the bed by effective conduction and bulk flow must equal bulk flow transport to the vessel (since dispersion effects in the pipe carrying the fluid to the vessel can be neglected due to large Reynolds number). Equations 2.1.5b and 2.1.6b describe losses between

solids and surroundings at the two ends of the vessel while Equation 2.1.6a states that the gas temperature does not change at the exit. Initial conditions for the bed are prescribed by Equation 2.1.7.

The model can be used to describe either single pass operation or cyclic operation for both cocurrent and countercurrent cases.

In describing single pass operation usually one can assume that there are no losses either from the walls (which are well insulated) or from the ends of the vessel in which case $Bi_{ws} = Bi_{wg} = Bi_{es} = 0$. The initial conditions, Equations 2.1.7, normally are $t_g = t_s = 0$ (i.e. $T_{so} = T_{go}$); and boundary condition, Equation 2.1.5a' or 2.1.5a, for a step input becomes $\varphi(\tau) = 1$.

For periodic operation losses can normally be neglected $Bi_{ws} = Bi_{wg} = Bi_{es} = 0$. We now must distinguish the variables in the bed during heating periods $n\tau_p < \tau < n\tau_p + \tau_h$, denoted by t_{gh}, t_{sh}, and during the cooling periods $n\tau_p + \tau_h < \tau < (n+1)\tau_p$, denoted by t_{gc}, t_{sc}, here we use the same basis T_{hi} and T_{ci} for making variables of both periods dimensionless, i.e.,

$$t_{gh} = \frac{T_{gh} - T_{ci}}{T_{hi} - T_{ci}} \quad , \quad t_{gc} = \frac{T_{gc} - T_{ci}}{T_{hi} - T_{ci}}$$

$$t_{sh} = \frac{T_{sh} - T_{ci}}{T_{hi} - T_{ci}} \quad , \quad t_{sc} = \frac{T_{sc} - T_{ci}}{T_{hi} - T_{ci}}$$

where T_{hi} and T_{ci} are the constant inlet gas temperature during the heating and cooling periods, respectively.

There are two different methods which can be used to describe such a cyclic system: (28)*

* The numbers in parentheses in the text indicate references in the Bibliography.

1. Open method - the gas and solid temperature are evaluated in successive cycles until the mathematical model reaches the stationary state.
2. Closed method - the stationary state performance is computed directly, without any consideration of any earlier transient cycle.

For cocurrent flow operation it is possible to describe the system by either the open method or the closed method. In the case that the open method is used, the initial conditions, Equations 2.1.7, are $t_g = t_s = 0$ and the boundary condition Equation 2.1.5a' can be described by:

$$\varphi_p(\tau) = \sum_{n=0}^{\infty} \left[H(\tau - n\tau_p) - H(\tau - n\tau_p - \tau_h) \right] \qquad 2.1.11$$

The form of this boundary condition is the only difference from single pass operation model. We can solve this system period by period readily by the principle of superposition. Alternatively, when using the closed method, the boundary condition, Equation 2.1.5a', is $\varphi_h(\tau) = 1$ for the heating period and $\varphi_c(\tau) = 0$ for the cooling period. The initial conditions, Equation 2.1.7, are some temperature profiles $f_h(\xi,\eta)$ and $g_h(\xi,\eta)$ and $f_c(\xi,\eta)$ and $g_c(\xi,\eta)$ for the heating and cooling period, respectively. We will show later how to determine these functions.

For countercurrent flow operation the convection term of Equation 2.1.1 and the boundary conditions, Equations 2.1.5a and 2.1.6a, vary periodically:

Heating period, $n\tau_p < \tau < n\tau_p + \tau_h$

$$\psi \frac{\partial t_{gh}}{\partial \tau} = -\frac{\partial t_{gh}}{\partial \xi} + \frac{1}{Pe_{gz}} \frac{\partial^2 t_{gh}}{\partial \xi^2} + \frac{\ell}{Pe_{gr}} \frac{1}{\eta} \frac{\partial}{\partial \eta} \left(\eta \frac{\partial t_{gh}}{\partial \eta} \right) - St \left(t_{gh} - t_{sh} \right) \qquad 2.1.1$$

$$\xi = 0 \qquad t_{gh} = \varphi_h(\tau) \qquad 2.1.5a'$$

or

$$-\frac{1}{Pe_{gz}} \frac{\partial t_{gh}}{\partial \xi} + t_{gh} = \varphi_h(\tau) \qquad 2.1.5a$$

$$\xi = 1 \qquad \frac{\partial t_{gh}}{\partial \xi} = 0 \qquad 2.1.6a$$

Cooling period, $n\tau_p + \tau_h < \tau < (n+1)\tau_p$

$$\psi \frac{\partial t_{gc}}{\partial \tau} = +\frac{\partial t_{gc}}{\partial \xi} + \frac{1}{Pe_{gz}} \frac{\partial^2 t_{gc}}{\partial \xi^2} + \frac{\ell}{Pe_{gr}} \frac{1}{\eta} \frac{\partial}{\partial \eta} \left(\eta \frac{\partial t_{gc}}{\partial \eta} \right) - St \left(t_{gc} - t_{sc} \right) \qquad 2.1.12$$

$$\xi = 0 \qquad \frac{\partial t_{gc}}{\partial \xi} = 0 \qquad 2.1.13$$

$$\xi = 1 \qquad t_{gc} = \varphi_c(\tau) \qquad 2.1.14'$$

or

$$+\frac{1}{Pe_{gz}} \frac{\partial t_{gc}}{\partial \xi} + t_{gc} = \varphi_c(\tau) \qquad 2.1.14$$

The closed method can also be applied here in the same way as in the cocurrent case. However, the open method is now more difficult to apply because we cannot readily make use of the principle of superposition

and we have to start from the beginning to solve for $t_{gh}\ (\xi,\eta,\tau_h)$ and $t_{sh}\ (\xi,\eta,\tau_h)$ and $t_{gc}\ (\xi,\eta,\tau_c)$ and $t_{sc}\ (\xi,\eta,\tau_c)$ periodically until the stationary state has been reached.

Model IB. Solids treated as a discrete phase

gas: $$\psi\frac{\partial t_g}{\partial \tau} = -\frac{\partial t_g}{\partial \xi} + \frac{1}{Pe_{gx}}\frac{\partial^2 t_g}{\partial \xi^2} + \frac{l}{Pe_{g\eta}}\frac{1}{\eta}\frac{1}{\partial \eta}\left(\eta\frac{\partial t_g}{\partial \eta}\right) - St_\rho\left(t_g - t_\rho\big|_{\varphi=1}\right) \qquad 2.1.15$$

particle: $$\frac{\partial t_\rho}{\partial \tau} = \frac{1}{Pe_\rho}\frac{1}{\varphi^\mu}\frac{\partial}{\partial \varphi}\left(\varphi^\mu\frac{\partial t_\rho}{\partial \varphi}\right) \qquad 2.1.16$$

$$\eta=0 \qquad \frac{\partial t_g}{\partial \eta} = 0 \qquad 2.1.17$$

$$\eta=1 \qquad \frac{\partial t_g}{\partial \eta} = Bi_{wg}(t_w - t_g) \qquad 2.1.18$$

$$\varphi=0 \qquad \frac{\partial t_\rho}{\partial \varphi} = 0 \qquad 2.1.19$$

$$\varphi=1 \qquad \frac{\partial t_\rho}{\partial \varphi} = Bi_\rho(t_g - t_s) \qquad 2.1.20$$

where $t_s = t_\rho\ (\xi,\eta,\varphi = 1,\tau)$

$$\xi=0 \qquad t_g = \Phi(\tau) \qquad 2.1.21'$$

or $$-\frac{1}{Pe_{gx}}\frac{\partial t_g}{\partial \xi} + t_g = \Phi(\tau) \qquad 2.1.21$$

$$\xi=1 \qquad \frac{\partial t_g}{\partial \xi} = 0 \qquad 2.1.22$$

$$\tau = 0 \qquad t_g = f(\xi, \eta) \tag{2.1.23a}$$

$$t_p = g(\xi, \eta, \varphi) \tag{2.1.23b}$$

where independent variables are:

$$\xi = \frac{z}{L} \ , \qquad \eta = \frac{r}{R} \ ,$$

$$\varphi = \frac{r_p}{r_{po}} \ , \qquad \tau = \frac{\epsilon \rho_g C_{pg}}{(1-\epsilon)\rho_p C_{pp}} \frac{\theta}{\epsilon L / u_g} \tag{2.1.24}$$

dependent variables are:

$$t_g = \frac{T_g - T_{go}}{T_{gi} - T_{go}} \ , \qquad t_p = \frac{T_p - T_{go}}{T_{gi} - T_{go}} \tag{2.1.25}$$

dimensionless groups are

$$Pe_{gz} = \frac{L G_g C_{pg}}{K e_{gz}} \ , \qquad Pe_{gr} = \frac{R G_g C_{pg}}{K e_{gr}}$$

$$Pe_p = \frac{r_{po} G_g C_{pg}}{K_p (1-\epsilon)} \ , \qquad St_p = \frac{(1-\epsilon)(\nu+1) h_p L_j}{r_{po} G_g C_{pg}} = \frac{h_p a_s L_j}{G_g C_{pg}}$$

$$Bi_p = \frac{h_p r_{po}}{K_p} \ , \qquad Bi_{wg} = \frac{h_{wg} R}{K e_{gr}}$$

$$\psi = \frac{\epsilon \rho_g C_{pg}}{(1-\epsilon)\rho_p C_{pp}} \ , \qquad \ell = \frac{L_j}{R} \tag{2.1.26}$$

$$t_w = \frac{T_w - T_{go}}{T_{gi} - T_{go}} \ , \qquad \text{Shape factor } \nu = \begin{matrix} 0 \ , \text{ Plate} \\ 1 \ , \text{ cylinder} \\ 2 \ , \text{ sphere} \end{matrix}$$

This approach extends directly the models used in the theory of chromatography and mass regenerators as developed by Kubin and Kucera (12, 13) and applies them to heat regenerators. In doing so, solids are considered to be a discrete phase and conduction in an individual particle is modeled. Transport from particle to particle by conduction through points of contact and through the stagnant film is neglected.

The same discussion regarding the boundary and initial condition when describing single pass operation and cocurrent or countercurrent periodic operation as given for Model IA is pertinent in this case and hence will not be repeated.

As mentioned earlier when continuous regenerator operation is described, losses can frequently be neglected and $Bi_{wg} = 0$. Then one can average t_g and t_ρ overall the vessel cross section and due to new homogeneous Neumann conditions given by Equations 2.1.17 and 2.1.18, the third term on the right hand side of Equation 2.1.15 drops out completely. In this situation there is no dependence of variables on the radial position in the vessel and the dimensionality of the problem is reduced. This is the model treated by Sagara et al (26) which has its analog in the theory of chromatography.

2.1.2 Mathematical Description of Parallel Plate Regenerators

Model IIA. Gas temperature is not uniform across the cross-section of the channel

$$\text{gas:}\quad \psi' \frac{\partial t_g}{\partial \tau'} = -\frac{u_g'(\eta)}{\bar{u}_g'} \frac{\partial t_g}{\partial \xi} + \frac{1}{Pe_{gz}'} \frac{\partial^2 t_g}{\partial \xi^2} + \frac{1}{Pe_{gx}'} \left(\frac{L}{T}\right)\left(\frac{\pi_c}{T}\right) \frac{\partial^2 t_g}{\partial \eta'^2} \qquad 2.1.27$$

plates: $$\frac{\partial t_s}{\partial \tau'} = \frac{1}{Pe'_{sz}} \frac{\partial^2 t_s}{\partial \xi^2} + \frac{1}{Pe'_{sx}} \left(\frac{L}{T}\right)\left(\frac{R\rho}{T}\right) \frac{\partial^2 t_s}{\partial \eta'^2} \qquad 2.1.28$$

$$\xi = 0 \qquad t_g = \varphi(\tau') \qquad 2.1.29a'$$

or $$-\frac{1}{Pe'_{gz}} \frac{\partial t_g}{\partial \xi} + \frac{u'_g}{\bar{u}'_g} t_g = \frac{u'_g}{\bar{u}'_g} \varphi(\tau') \qquad 2.1.29a$$

$$\frac{\partial t_s}{\partial \xi} = Bi'_s (t_s - t_a) \qquad 2.1.29b$$

$$\xi = 1 \qquad \frac{\partial t_g}{\partial \xi} = 0 \qquad 2.1.30a$$

$$-\frac{\partial t_s}{\partial \xi} = Bi'_s (t_s - t_a) \qquad 2.1.30b$$

$$\eta' = 0 \qquad \frac{\partial t_g}{\partial \eta} = 0 \qquad 2.1.31$$

$$\eta' = \frac{\pi c}{T} \quad (= \rho) \qquad t_g = t_s \qquad 2.1.32a$$

$$\frac{\partial t_g}{\partial \eta'} = \frac{\partial t_s}{\partial \eta'} \qquad 2.1.32b$$

$$\eta' = 1 \qquad \frac{\partial t_s}{\partial \eta'} = 0 \qquad 2.1.33$$

$$\tau' = 0 \qquad t_g = f(\xi, \eta') \qquad 2.1.34a$$

$$t_s = g(\xi, \eta') \qquad 2.1.34b$$

where independent variables are:

$$\xi = \frac{z}{L} \quad , \quad \eta' = \frac{x}{T} \quad ,$$

$$\tau' = \frac{\rho_g C_{pg} \bar{u}_g'}{\rho_s C_{ps} L} \theta = \psi \frac{\theta}{\theta_a'} \qquad 2.1.35$$

dependent variables are:

$$t_g = \frac{T_g - T_{go}}{T_{gi} - T_{go}} \quad , \quad t_s = \frac{T_s - T_{go}}{T_{gi} - T_{go}} \qquad 2.1.36$$

dimensionless groups are:

$$Pe_{gz}' = \frac{L \rho_g C_{pg} \bar{u}_g'}{K_{gz}'} \quad , \quad Pe_{gx}' = \frac{r_c \rho_g C_{pg} \bar{u}_g'}{K_{gx}'}$$

$$Pe_{sz}' = \frac{L \rho_g C_{pg} \bar{u}_g'}{K_{sz}'} \quad , \quad Pe_{sx}' = \frac{R_\rho \rho_g C_{pg} \bar{u}_g'}{K_{sx}'}$$

$$Bi_s' = \frac{h_e L}{K_{sz}'} \quad , \quad \psi' = \frac{\rho_g C_{pg}}{\rho_s C_{ps}} \qquad 2.1.37$$

Here L is the large length in Z direction, d_c is the small height in X direction ($d_c = 2\ r_c$) of the rectangular channel. The half thickness of the plates around the channel is R_ρ, their length and width equal those for the channel. T is the basis in X direction equal to the sum of half width of the channel and half thickness of the plate and is defined as $T = r_c + R_\rho$. We can distinguish two situations. In one, the Reynolds number is small and we have laminar flow $u_g'(\eta') = \frac{3}{2} \bar{u}_g' (1-\eta'^2)$. In

the other, the Reynolds number is large and we have turbulent flow $u'_g(\eta') \simeq \bar{u}'_g = \text{const.}$

It is possible to average the gas temperature across the cross-section and in the process drops its dependence on η'. The cross sectional average gas temperature is:

$$\bar{t}_g = \frac{1}{\rho}\int_0^{\rho} t_g \, d\eta' \quad , \quad \rho = \frac{r_c}{r} \qquad 2.1.38$$

The overall heat transfer coefficient h is introduced by the assumption

$$-\left.\frac{\partial t_g}{\partial \eta'}\right|_{\eta'=\rho} = -\left.\frac{\partial t_s}{\partial \eta'}\right|_{\eta'=\rho} = Bi'\left(\frac{r}{R\rho}\right)\left(\bar{t}_g - t_s\Big|_{\eta'=\rho}\right) \qquad 2.1.39$$

where $Bi' = \frac{R\rho h}{K'_{esx}}$ and define $St' = \frac{h}{\rho_g C_{pg} \bar{u}'_g}$

We also introduce a new Peclet number, Pe'_{go}, based on the effective axial gas conductivity:

$$Pe'_{ego} = \frac{L \rho_g C_{pg} \bar{u}'_g}{K'_{egz}} \qquad 2.1.40$$

Then we can describe the system by a simpler model.

The above approach is only applicable for turbulent flow. In case of laminar flow a different approach using the extensions of the Graetz problem has been used by Gidaspow and coworkers (23).

Model IIB. Averaged gas temperature is considered across the cross-section of the channel

gas: $$\psi' \frac{\partial \bar{t}_g}{\partial \tau'} = -\frac{\partial \bar{t}_g}{\partial \xi} + \frac{1}{Pe'_{go}} \frac{\partial^2 \bar{t}_g}{\partial \xi^2} - St' \left(\frac{L}{r_c}\right) \left(\bar{t}_g - t_s\Big|_{\eta'=\rho}\right) \qquad 2.1.41$$

plates: $$\frac{\partial t_s}{\partial \tau'} = \frac{1}{Pe'_{sz}} \frac{\partial^2 t_s}{\partial \xi^2} + \frac{1}{Pe'_{sx}} \left(\frac{L}{r}\right) \left(\frac{R\rho}{r}\right) \frac{\partial^2 t_s}{\partial \eta'^2} \qquad 2.1.28$$

$$\xi = 0 \qquad \bar{t}_g = \psi(\tau') \qquad 2.1.42'$$

or $$-\frac{1}{Pe'_{go}} \frac{\partial \bar{t}_g}{\partial \xi} + \bar{t}_g = \psi(\tau') \qquad 2.1.42$$

$$\frac{\partial t_s}{\partial \xi} = B'_{is} (t_s - t_a) \qquad 2.1.29b$$

$$\xi = 1 \qquad \frac{\partial \bar{t}_g}{\partial \xi} = 0 \qquad 2.1.43$$

$$-\frac{\partial t_s}{\partial \xi} = B'_{is} (t_s - t_a) \qquad 2.1.30b$$

$$\eta' = \rho \qquad -\frac{\partial t_s}{\partial \eta'} = B'_i \left(\frac{r}{R\rho}\right) (\bar{t}_g - t_s) \qquad 2.1.44$$

$$\eta' = 1 \qquad \frac{\partial t_s}{\partial \eta'} = 0 \qquad 2.1.45$$

$$\tau' = 0 \qquad \bar{t}_g = f(\xi) \qquad 2.1.46$$

$$t_s = g(\xi, \eta') \qquad 2.1.34b$$

The previous discussion under model MIA regarding boundary and initial conditions for single pass, cocurrent and countercurrent cyclic operation is also pertinent to this case and hence will not be repeated.

In packed bed regenerator models, MIA and MIB, all transport properties are based on the total cross-sectional areas perpendicular to the direction of transport while in plate regenerators these quantities are based on areas of a particular phase in question. The following relationship can then be established among various dimensionless quantities:

$$\psi' \frac{\epsilon}{1-\epsilon} = \psi \qquad 2.1.47a$$

$$\tau' \frac{\epsilon}{1-\epsilon} = \tau \qquad 2.1.47b$$

and $$\epsilon = \frac{\pi_c}{\Gamma} \qquad 2.1.47c$$

$$a_s = \frac{1}{\Gamma} \qquad \text{for parallel plates} \qquad 2.1.47d$$

$$u_g/\epsilon = \bar{u}_g' \qquad 2.1.47e$$

We have reviewed so far the possible, general, mathematical descriptions of packed bed and plate regenerators in either single pass or cyclic operation. The choice of the model depends on the problem on hand. However, because of the complexity of the analysis models had to be simplfied in all cases to obtain any kind of analytical or

semianalytical solution. Following is a listing of the various investigations and main types of solutions classified according to their principle assumptions and restrictions.

1. Single pass operation, only film resistance considered (h = finite, $K_s = 0$ in direction of flow, $K_s = \infty$ normal to flow):

   Anzelius - 1926 (1), Nusselt - 1927 (21), Hausen - 1929, 1930 (3,4), Schumann - 1929 (25), Klinkenberg - 1954 (11), Larsen - 1967 (16).

2. Single pass operation, h = finite, $K_s = 0$ in direction of flow, K_s = finite normal to flow:

   Nusselt - 1927 (21), Handley and Heggs - 1966 (8), Schmidt and Szego - 1978 (27).

3. Periodic operations, only film resistance considered (h = finite, $K_s = 0$ in direction of flow, $K_s = \infty$ normal to flow):

   (i) Cocurrent case -

   Hausen - 1950 (6), Nahavandi and Weinstein - 1961 (22), Willmott - 1969 (29), Kumar - 1978 (15).

   (ii) Countercurrent case -

   Hausen - 1950 (6), Nusselt - 1927 (21), Iliffe - 1948 (9), Nahavandi and Weinstein - 1961 (22), Willmott and Thomas - 1974 (30).

4. Periodic operations, h = finite, $K_s = 0$ in direction of flow, K_s = finite normal to flow:

   (i) Cocurrent case -

   Kardas - 1966 (14), Kumar - 1978 (15).

(ii) Countercurrent case -

Hausen - 1942 (5), Bahnke and Howard - 1964 (2),

Willmott - 1969 (29).

Because all the cases neglected the heat conduction of the solid in the direction of flow ($K_s = 0$ in the direction of flow), that is the same condition as if we treat the solid as a discrete phase that exchanges heat with the fluid and may have a heat transfer resistance due to conduction only in directions perpendicular to the direction of flow.

2.2 PRINCIPLES OF OPERATION AND DEFINITION OF THERMAL EFFICIENCY

Unfortunately, at present there is no generally accepted notation for regenerator problems. Here, we will introduce our own which to a great extent follows the symbolism used in Chemical Engineering.

Ideally one would like to transfer energy with perfect efficiency and heat an equivalent amount of cold fluid to the inlet temperature of the hot fluid thus utilizing all the available energy of the hot fluid. The overall energy balance for such an ideal regenerator can be written as:

$$\dot{M}_c C_{pc} (T_{c,e} - T_{c,i}) \theta_c = \dot{M}_h C_{ph} (T_{h,i} - T_{h,e}) \theta_h = M_s C_{ps} (\overline{T}_{s,f} - \overline{T}_{s,o}) \qquad 2.2.1$$

with $$T_{c,e} = T_{h,i} = \overline{T}_{s,f} \qquad 2.2.2a$$

$$T_{c,i} = T_{h,e} = \overline{T}_{s,o} \qquad 2.2.2b$$

where $\dot{m}$ - mass flow rate of gas streams, C_p - specific heat, T - temperature, θ - switching time, M_s - total mass of solids. Subscripts c and h indicate fluid variables during cooling and heating periods, respectively. Subscript s indicates quantities for the solid and a bar indicates an averaged quantity. Second subscripts e, i indicate fluid exit and inlet quantities, while f, o indicate variables at the end and the beginning of the heating period, respectively.

It should be noted that Equation 2.2.1 besides the assumption of an ideal regenerator with step changes in exit temperatures and constant inlet temperatures also rests on the assumptions that specific heats can be considered constant and that the overall heat capacity of the fluid in the regenerator is small compared to the total heat capacity of the solid. This last assumption is certainly justified for gas-solid system.

Equation 2.2.1 for the ideal regenerator, when dealing with gases and hence when the gas heat capacity in the regenerator can be neglected, requires that the "water equivalents" of the cold gas, hot gas and solids be all equal as indicated by the following equation:

$$\dot{m}_c C_{pc} \theta_c = \dot{m}_h C_{ph} \theta_h = M_s C_{ps} \qquad 2.2.3$$

So the thermal mean residence time, μ_i, is defined as:

$$\mu_i \equiv \theta_i = \frac{M_s C_{ps}}{\dot{m}_i C_{pi}} \quad ; \quad i = c, h \qquad 2.2.4$$

i.e.the characteristic time needed to cool all the initially hot solids or to heat all the initially cold solids for an ideal regenerator.

Such ideal performance would be attained by a regenerator in which

(i) the fluid is in plug flow:
(i.e. moves as a front perfectly mixed in the direction perpendicular to flow with no mixing in the direction of flow)

(ii) no heat transfer resistance perpendicular to flow direction either between fluid and solid or within the solid:
(i.e. infinite fluid-solid heat transfer coefficient and solid conductivity)

(iii) no heat transfer (other than by bulk gas flow) in the direction of flow either in the gas or solid;
(i.e. no dispersion in the gas, no conduction in the solid)

(iv) no losses to the surroundings.

The periodic input and output temperatures in an ideal regenerator, with switching time equal to the thermal mean residence time, are sketched in Figure 2.1.

We can see that all of the energy of a hot fluid can be utilized to heat the solids and the cold fluid can receive the whole energy from the solids for both cocurrent and countercurrent ideal regenerators. It means that the mode of operation, i.e., cocurrent or countercurrent flow, does not affect the performance of an ideal regenerator if the switching time is the thermal mean residence time.

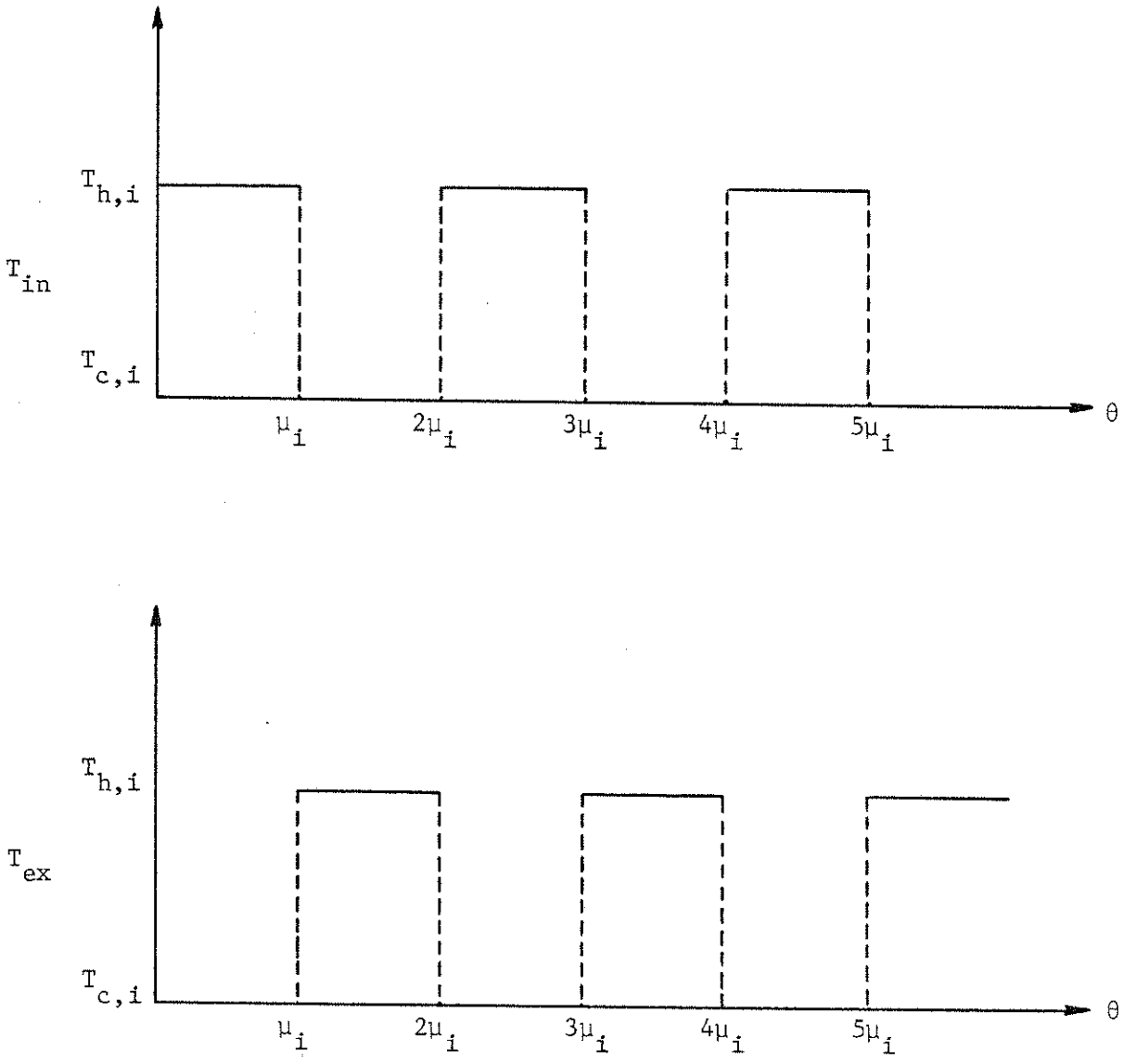

Figure 2.1 The Periodic Input and Output Temperatures for Both Cocurrent and Countercurrent Ideal Regenerators with $\theta_i = \mu_i$

This ideal limit of an ideal regenerator cannot be reached in practice due to finite heat transfer resistances perpendicular to flow, finite heat transfer area, dispersion in the fluid caused by nonuniform velocity profile and/or turbulence, transfer of heat in the direction of flow and possibly due to losses to surroundings. Therefore the response curve for exit temperatures is not a step change of an ideal regenerator, rather it is smearing and broadening due to the above effects. The overall energy balance for such an nonideal regenerator should be written as:

$$\dot{m}_c C_{pc} \int_0^{\theta_c} (T_{c,e} - T_{c,i})\, d\theta = \dot{m}_h C_{ph} \int_0^{\theta_h} (T_{h,i} - T_{h,e})\, d\theta = M_s C_{ps} (\bar{T}_{s,f} - \bar{T}_{s,o}) \qquad 2.2.5$$

Here the exit temperatures change during cooling and heating periods.

It is thus customary to use some measures of regenerator thermal efficiency, η_{th}, and it has been defined as (10):

$$\eta_{th} = \frac{Q}{Q_{id}} = \frac{\text{(heat actually exchanged)}}{\left(\begin{array}{l}\text{ideal amount of heat that would be}\\ \text{exchanged if the temperature of the}\\ \text{cold (hot) gas could be increased}\\ \text{(decreased) to the entrance}\\ \text{temperature of the hot (cold) gas}\end{array}\right)} \qquad 2.2.6$$

According to this definition, the thermal efficiency for the heating period, η_h, is:

$$\eta_h = \frac{\dot{m}_h C_{ph} \int_0^{\theta_h} (T_{h,i} - T_{h,e})\, d\theta}{\dot{m}_h C_{ph}\, \theta_h\, (T_{h,i} - T_{c,i})}$$

$$= \frac{1}{\theta_h} \int_0^{\theta_h} (1 - t_{h,e})\, d\theta \qquad 2.2.7$$

where $t_{h,e} = \frac{T_{h,e} - T_{c,i}}{T_{h,i} - T_{c,i}}$ is the normalized exit temperature of the heating period.

Similarly the thermal efficiency for the cooling period, η_c, is:

$$\eta_c = \frac{\dot{m}_c C_{pc} \int_0^{\theta_c} (T_{c,e} - T_{c,i}) d\theta}{\dot{m}_c C_{pc}\, \theta_c (T_{h,i} - T_{c,i})}$$

$$= \frac{1}{\theta_c} \int_0^{\theta_c} t_{c,e}\, d\theta \qquad 2.2.8$$

where $t_{c,e} = \frac{T_{c,e} - T_{c,i}}{T_{h,i} - T_{c,i}}$ is the normalized exit temperature of the cooling period.

Let us relate these efficiences. From the overall energy balance, Equation 2.2.5, and the thermal efficiency for the heating and cooling periods, Equation 2.2.7 and 2.2.8, we have

$$\eta_c = \eta_h \left(\frac{\dot{m}_h C_{ph}}{\dot{m}_c C_{pc}}\right)\left(\frac{\theta_h}{\theta_c}\right)$$

$$= \eta_h \left(\frac{\mu_c}{\mu_h}\right)\left(\frac{\theta_h}{\theta_c}\right) = \eta_h \left(\frac{\tau_h}{\tau_c}\right) \qquad 2.2.9$$

where $\tau_h = \theta_h/\mu_h$, $\tau_c = \theta_c/\mu_c$ are dimensionless switching times based on thermal mean residence time of the heating and cooling period, respectively. When $\mu_h = \mu_c$ and $\theta_h = \theta_c$, i.e. same switching time and same thermal mean residence time, we have the same efficiences for the

heating and cooling periods. We can call this a "symmetric regenerator". In some cases, although $\mu_h \neq \mu_c$ and $\theta_h \neq \theta_c$, but the dimensionless switching times τ_h, τ_c are the same and we still have the same efficiencies for the heating and cooling periods. This is called a "balanced regenerator" (28). Other situations are called an "unbalanced regenerator".

The thermal regenerator problem is simplified by consideration of the symmetric case, i.e. $\mu_h = \mu_c$ and $\theta_h = \theta_c$. Here for cocurrent flow in periodic operation the solids temperature profile at the beginning and at the end of the heating period is symmetric with respect to a horizontal line at $t_s = 0.5$ as shown in Figure 2.2a,

where $t_s = \frac{T_s - T_{c,i}}{T_{h,i} - T_{c,i}}$ is the normalized solid temperature, $\xi = \frac{Z}{L}$ is the dimensionless axial position and $t_s(0,\xi)$, $t_s(\tau_h,\xi)$ are the solid temperature profiles at the beginning and at the end of the heating period, respectively. Because of symmetry, we have:

$$t_s(\tau_h,\xi) = 1 - t_s(0,\xi) \qquad 2.2.10a$$

For countercurrent flow, the solids temperature profile at the beginning and at the end of the heating period is symmetric with respect to the diagonal as shown in Figure 2.2b.

From the property of symmetry, we have:

$$t_s(\tau_h,\xi) = 1 - t_s(0,1-\xi) \qquad 2.2.10b$$

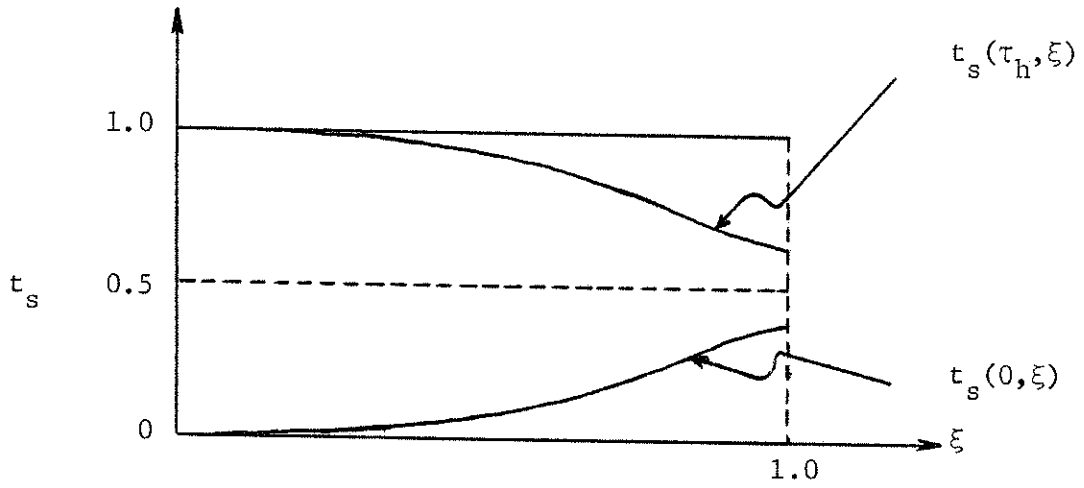

Figure 2.2a Solid Temperature Profile at the Beginning and End of the Heating Period in Cocurrent Flow

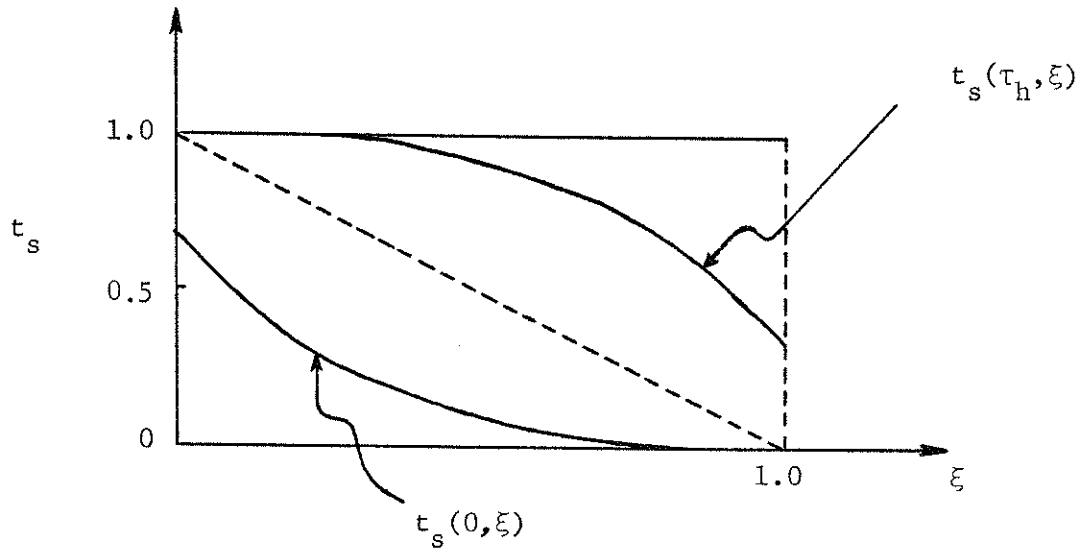

Figure 2.2b Solid Temperature Profile at the Beginning and End of the Heating Period in Countercurrent Flow

We will also define overall thermal efficiency, η_o, as:

$$\eta_o = \frac{Q_h + Q_c}{Q_{h,id} + Q_{c,id}} = \frac{\text{(Heat actually exchanged for two periods)}}{\text{(Ideal amount of heat exchanged for two periods)}}$$

From the overall energy balance, Equation 2.2.5, $Q_h = Q_c$

and

$$\frac{Q_{h,id}}{Q_{c,id}} = \frac{\eta_c}{\eta_h} = \frac{\tau_h}{\tau_c}$$

Therefore,

$$\eta_o = 2\frac{Q_h}{Q_{h,id} + Q_{c,id}} \quad \text{or} \quad 2\frac{Q_c}{Q_{h,id} + Q_{c,id}}$$

$$= 2\frac{Q_h}{Q_{h,id}}\frac{1}{1+\frac{Q_{c,id}}{Q_{h,id}}} \quad \text{or} \quad 2\frac{Q_c}{Q_{c,id}}\frac{1}{1+\frac{Q_{h,id}}{Q_{c,id}}}$$

$$= 2\,\eta_h\frac{1}{1+\left(\frac{\tau_c}{\tau_h}\right)} \quad \text{or} \quad 2\,\eta_c\frac{1}{1+\left(\frac{\tau_h}{\tau_c}\right)} \qquad 2.2.11$$

and we have

$$\eta_o = \eta_h = \eta_c = \eta_{reg}$$

for symmetric and balanced regenerators.

Although the ideal regenerator cannot be quite approached in practice, it is a good model for illustrating the importance of switching time on thermal efficiency. In Figure 2.3 there are several sketches showing ideal regenerator performance in cocurrent and countercurrent flow with different switching times.

Thus we see that in cocurrent flow an ideal regenerator may have efficiencies below 1.0 when $\theta_i \neq \mu_i$ according to the following formula:

Case 1. $\frac{\theta_i}{\mu_i} = \frac{p}{q}$ and $p > q$ (i.e. $\theta_i > \mu_i$)

then $\eta_{reg} = q/p$

Case 2. $\frac{\theta_i}{\mu_i} = \frac{p}{q}$ and $p < q$ (i.e. $\theta_i < \mu_i$)

if we define q/p = Q (Quotient) + R (Residual)

then (i) Q is even

$\eta_{reg} = R/p$

(ii) Q is odd

$\eta_{reg} = (p-R)/p$

In contrast for countercurrent operation the ideal regenerator efficiency is:

Case 1. $\frac{\theta_i}{\mu_i} = \frac{p}{q}$ and $p > q$ (i.e. $\theta_i > \mu_i$)

then $\eta_{reg} = q/p$

(*i*) Cocurrent Flow: $\theta_i/\mu_i = 1/2$, $\eta_{reg} = 0$

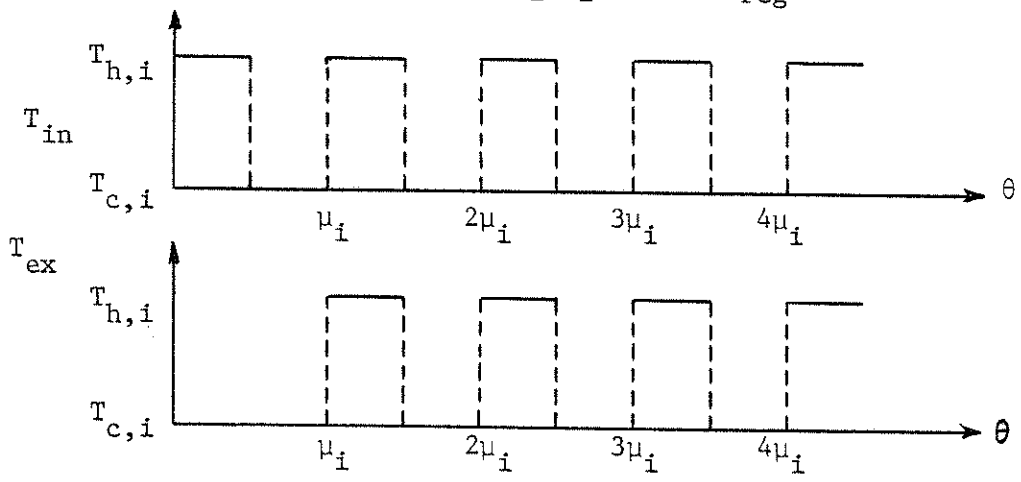

(*ii*) Cocurrent Flow: $\theta_i/\mu_i = 1/3$, $\eta_{reg} = 1$

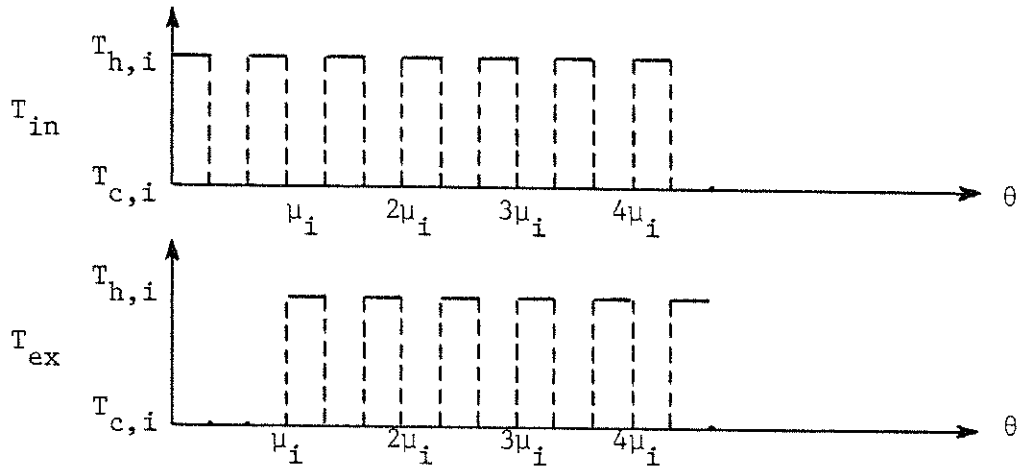

(*iii*) Cocurrent Flow: $\theta_i/\mu_i = 3/4$, $\eta_{reg} = 2/3$

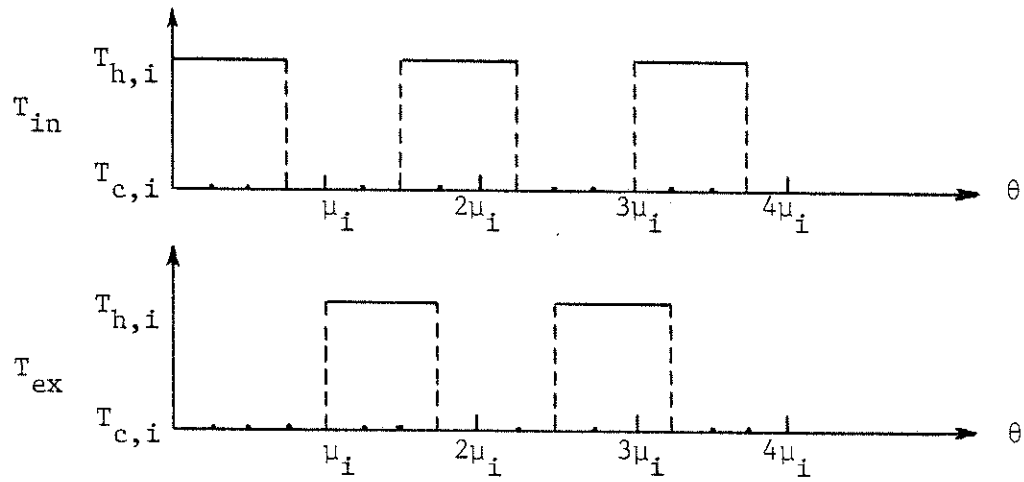

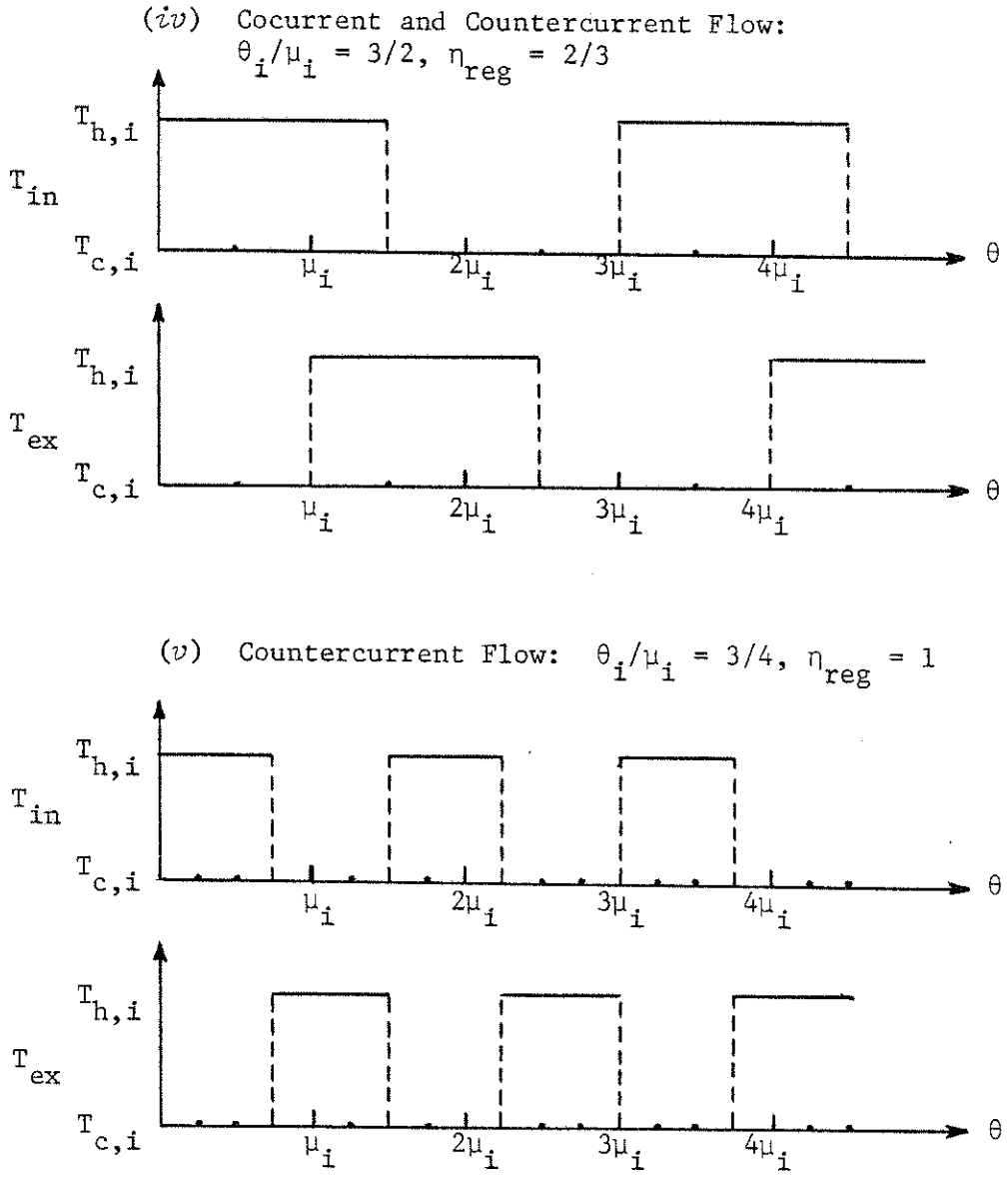

Figure 2.3 The Periodic Input and Output Temperatures for Cocurrent and Countercurrent Ideal Symmetric Regenerators with $\theta_i \neq \mu_i$

Case 2. $\frac{\theta_i}{\mu_i} = \frac{p}{q}$ and $p < q$ (i.e. $\theta_i < \mu_i$)

then $\eta_{reg} = 1$

We can realize that the mode of operation does not affect the performance of an ideal regenerator when $\theta_i > \mu_i$ but the efficiency is smaller than one and decreases with increasing the switching time. In the case of $\theta_i < \mu_i$ we can have $\eta_{reg} = 1$ for some particular cases, e.g. $\frac{\theta_i}{\mu_i} = \frac{1}{3}, \frac{1}{5}, \ldots$ etc. in cocurrent flow and in every case in countercurrent flow but we could have done better by using smaller regenerators in these cases.

It is thus clear that for an ideal regenerator of a given size the optimal operation is to switch the flow at $\theta_i = \mu_i$.

Sometimes we have to deal with the heat exchange between two gases with different products of mass flow rate and specific heat, i.e., different thermal mean residence times. Practically, when only two regenerators are used, we need to operate at the same real switching times for both periods. So we would also like to consider the ideal regenerator performance in cocurrent and countercurrent flow with different ratios of $\dot{m}C_p$ and different switching times for the unbalanced regenerator. Several sketches are shown in Figure 2.4.

For ideal unbalanced regenerators the maximum overall efficiency will be smaller than 1.0 from the following two formulas:

(*i*) Cocurrent Flow: $\mu_h/\mu_c = 2.0$, $\tau_h = 7/10$, $\tau_c = 7/5$

—— $\eta_h = 1.0$, $\eta_c = 0.5$, $\eta_o = 0.667$

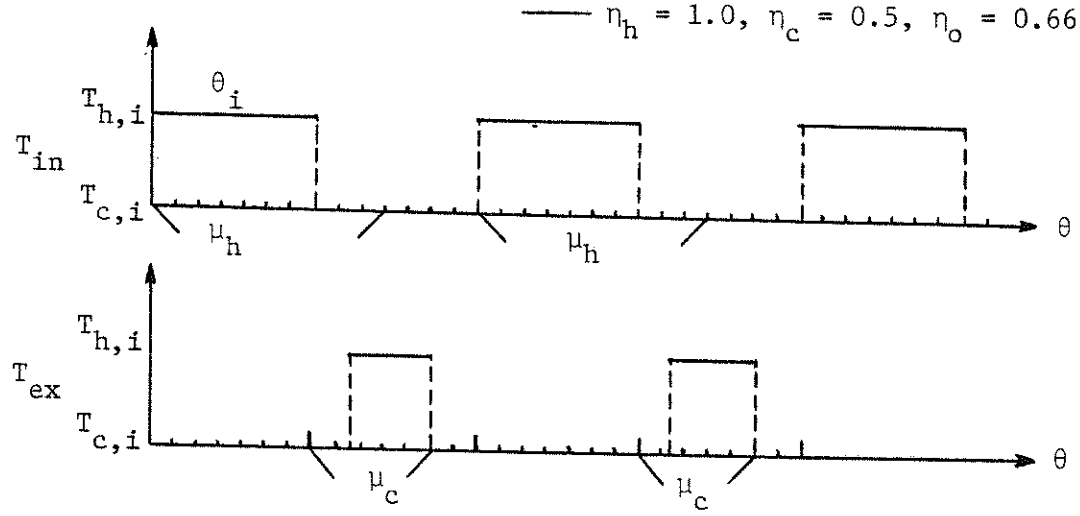

Similar result for the case of $\mu_h/\mu_c = 0.5$, $\tau_h = 7/5$, $\tau_c = 7/10$

—— $\eta_h = 0.5$, $\eta_c = 1.0$, $\eta_o = 0.667$

(*ii*) Cocurrent Flow: $\mu_h/\mu_c = 2.0$, $\tau_h = 2/5$, $\tau_c = 4/5$

—— $\eta_h = 0.5$, $\eta_c = 0.25$, $\eta_o = 0.333$

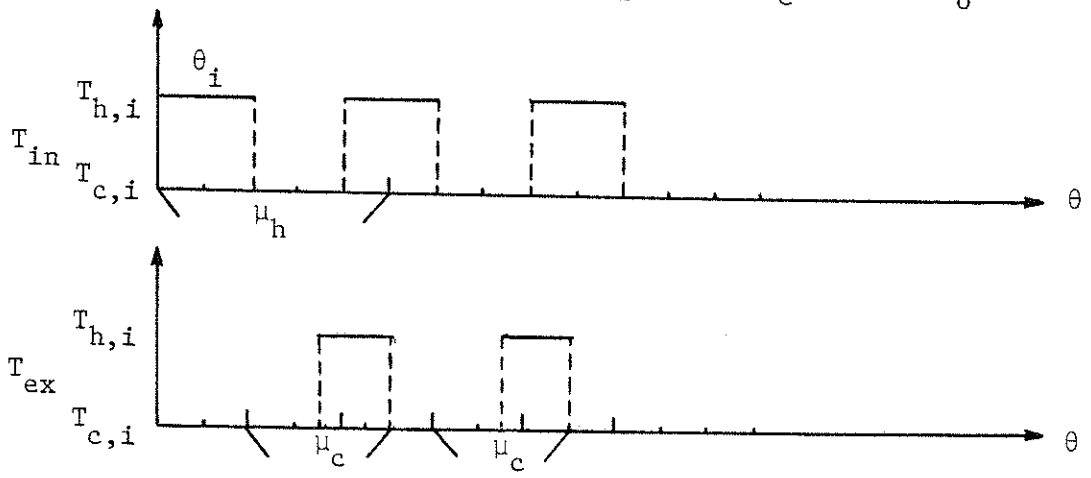

Similar result for the case of $\mu_h/\mu_c = 0.5$, $\tau_h = 4/5$, $\tau_c = 2/5$

—— $\eta_h = 0.25$, $\eta_c = 0.5$, $\eta_o = 0.333$

(*iii*) Cocurrent and Countercurrent Flow:
$\mu_h/\mu_c = 2.0$, $\tau_h = 6/5$, $\tau_c = 12/5$

—— $\eta_h = 0.833$, $\eta_c = 0.417$, $\eta_o = 0.556$

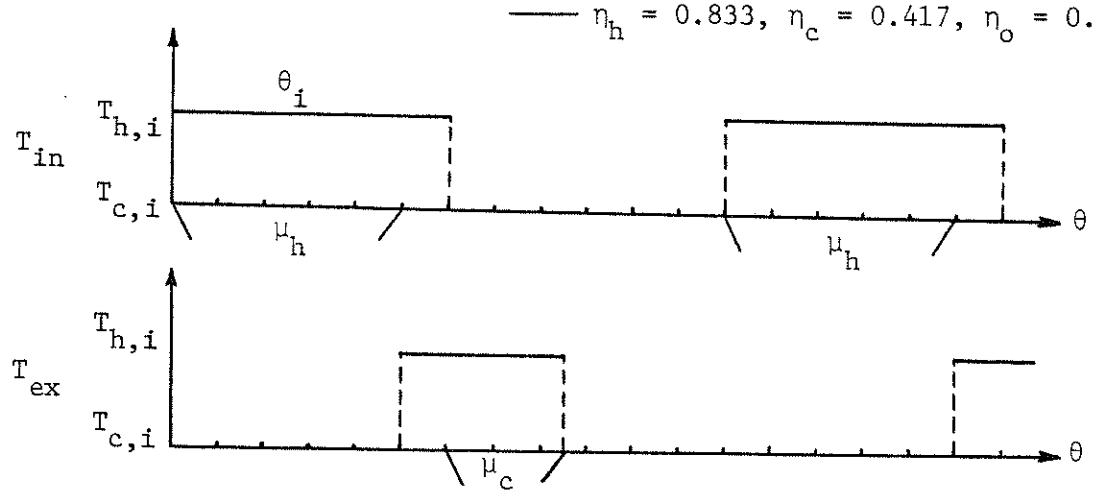

Similar results for the case of $\mu_h/\mu_c = 0.5$, $\tau_h = 12/5$, $\tau_c = 6/5$

—— $\eta_h = 0.417$, $\eta_c = 0.833$, $\eta_o = 0.556$

(*iv*) Countercurrent Flow: $\mu_h/\mu_c = 2.0$, $\tau_h = 7/10$, $\tau_c = 7/5$

—— $\eta_h = 1.0$, $\eta_c = 0.5$, $\eta_o = 0.667$

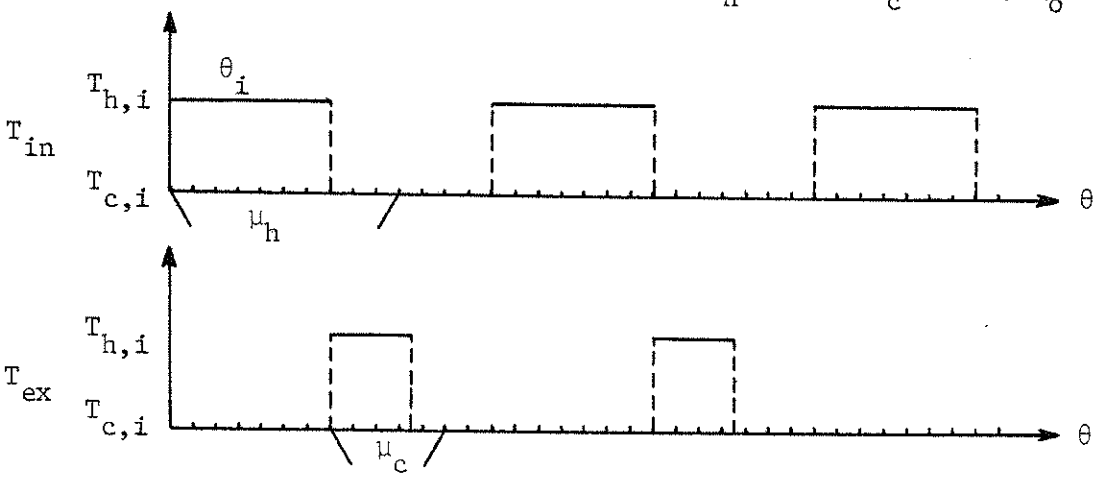

Similar result for the case of $\mu_h/\mu_c = 0.5$, $\tau_h = 7/5$, $\tau_c = 7/10$

—— $\eta_h = 0.5$, $\eta_c = 1.0$, $\eta_o = 0.667$

(*v*) Countercurrent Flow: $\mu_h/\mu_c = 2.0$, $\tau_h = 2/5$, $\tau_c = 4/5$

—— $\eta_h = 1.0$, $\eta_c = 0.5$, $\eta_o = 0.667$

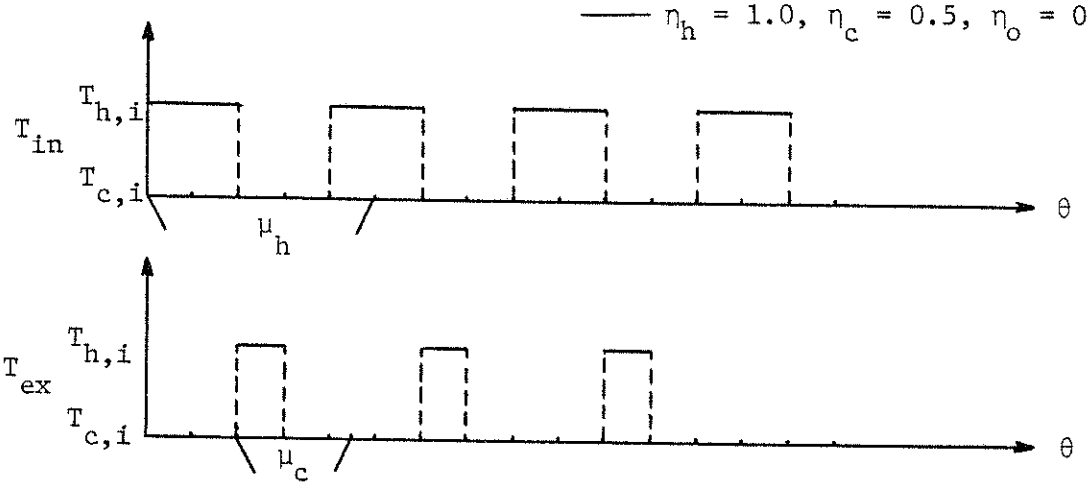

Similar result for the case of $\mu_h/\mu_c = 0.5$, $\tau_h = 4/5$, $\tau_c = 2/5$

—— $\eta_h = 0.5$, $\eta_c = 1.0$, $\eta_o = 0.667$

Figure 2.4 The Periodic Input and Output Temperatures for Cocurrent and Countercurrent Ideal Unbalanced Regenerators

Case 1. $\mu_h/\mu_c > 1.0$

then $\eta_h = 1.0$, $\eta_c = \eta_h \left(\frac{\tau_h}{\tau_c}\right) = \eta_h \left(\frac{\mu_c}{\mu_h}\right)$

and $\eta_o < 1.0$

Case 2. $\mu_h/\mu_c < 1.0$

then $\eta_c = 1.0$, $\eta_h = \eta_c \left(\frac{\tau_c}{\tau_h}\right) = \eta_c \left(\frac{\mu_h}{\mu_c}\right)$

and $\eta_o < 1.0$

The maximum overall efficiences with different μ_h/μ_c values are shown in Figure 2.5.

We can show that the above optimal operations can be reached in case of:

(i) Cocurrent operation at $\tau_h \leq 1.0$ and $\tau_c \geq 1.0$ or

$\tau_h \geq 1.0$ and $\tau_c \leq 1.0$

(ii) Countercurrent operation at $\tau_h \leq 1.0$ or $\tau_c \leq 1.0$

These two conditions can be satisfied simultaneously at $\tau_h \leq 1.0$ and $\tau_c \geq 1.0$ or $\tau_h \geq 1.0$ and $\tau_c \leq 1.0$ where we have the same efficiencies for both cocurrent and countercurrent operations. For the case of nonoptimal operations with $\tau_h > 1.0$ and $\tau_c > 1.0$, the efficiencies are also the same for both cocurrent and countercurrent operation. The mode of operation does not affect the performance of an ideal regenerator for the above situations.

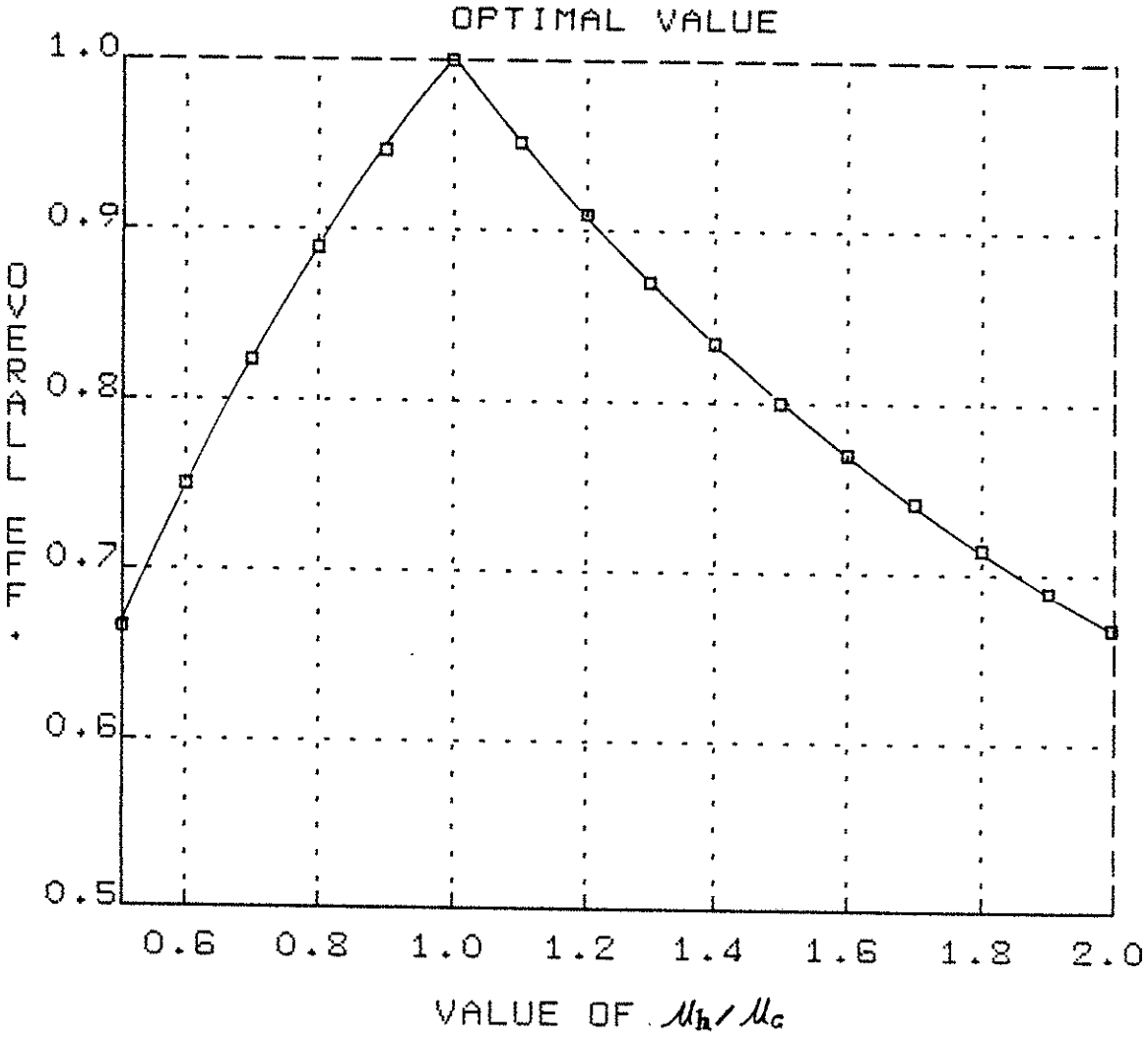

FIGURE 2.5

MAXIMUM OVERALL EFFICIENCY WITH DIFFERENT μ_h/μ_c VALUES FOR COCURRENT AND COUNTERCURRENT IDEAL REGENERATOR

3. IMPULSE RESPONSE, STEP RESPONSE AND SINGLE PASS EFFICIENCY

As already mentioned, the model equations described in Chapter 2 are rather complex. Analytical solutions are available even for simple single pass operation only for some limiting cases described by models which have been further simplified by neglecting certain terms. However, they are frequently expressed in terms of slowly convergent series or certain higher transcendental functions which are cumbersome to be evaluated numerically. Numerical solutions are always possible but different numerical schemes and special algorithms have to be used for different models in order to guarantee convergence and accuracy. Thus, it is desirable to have an approximate method which allows a rapid computation of breakthrough curves and thermal efficiencies for any model of heat regenerators.

We would also like to be able to assess approximately the effect of various heat transfer resistances on the deviation of the breakthrough curve from an ideal one. Since the moments of the impulse response are generally available in terms of the parameters of the model, and especially for some models the variance of the impulse response can be represented as the sum of various heat transfer resistances, an approximate solution that utilizes the moments and variance is of particular interest. Such an approach was suggested by Razavi et al (24) in modeling of fixed bed adsorbers.

3.1 APPROXIMATE SOLUTIONS FOR IMPULSE AND STEP RESPONSES

The impulse response $E(\theta)$ of any model of a nonideal regenerator can be characterized by its mean:

$$\mu = \frac{M_s C_{ps}}{\dot{m}_g C_{pg}} \qquad 2.2.4$$

and variance:

$$\sigma^2 = f\left(Pe_{gz}, St_p, Bi_p, \epsilon, \frac{d_p}{L}\right) \qquad 3.1.1$$

Linek and Dudukovic (20), based on the work of Hulburt and Katz (7), suggested that the impulse response can be approximated by:

$$E(\theta) \cong \frac{\left(\frac{\mu}{\sigma^2}\right)\left(\frac{\mu}{\sigma^2}\theta\right)^{\frac{\mu^2}{\sigma^2}-1} e^{-\frac{\mu}{\sigma^2}\theta}}{\Gamma\left(\frac{\mu^2}{\sigma^2}\right)} \qquad 3.1.2$$

This represents the leading term of the expansion of $E(\theta)$ in Laguerre series which is a series of Laguerre polynomials which are orthogonal on the interval $(0,\infty)$ when the Gamma distribution function is used as a weighting function. The approximation agrees well with analytical solutions of some limiting cases for both long and short packed bed adsorbers and reactors (20).

The important point is that for some models the variance of the impulse response can be represented as the sum of various heat transfer resistances. If for example we used a model of packed bed regenerators that treats the solids as a discrete medium (Model IB) and assumed spherical particles in an analogy to mass regenerators the variance can be expressed as (26):

$$\sigma^2 = 2\mu^2\left\{\frac{1}{5}\frac{Bi_p}{St_p} + \frac{1}{St_p} + \frac{1}{Pe_{gz}}\right\} \qquad 3.1.3a$$

Here Hulburt's condition is used. For short regenerators Danckwerts condition needs to be considered for more accuracy and the expression for the variance will be (18):

$$\sigma^2 = 2\mu^2 \left\{ \frac{1}{5}\frac{Bi_\rho}{St_\rho} + \frac{1}{St_\rho} + \left[\frac{1}{Pe_{gz}} - \frac{1}{Pe_{gz}^2}\left(1 - e^{-Pe_{gz}}\right) \right] \right\} \qquad 3.1.3a$$

where

$$Pe_{gz} = \frac{LG_g C_{pg}}{Ke_{gz}} = \frac{\text{(convective heat transfer)}}{\text{("eddy" dispersion heat transfer)}}$$

$$St_\rho = \frac{h_\rho a_s L}{G_g C_{pg}} = \frac{\text{(gas-solid heat transfer)}}{\text{(convective heat transfer)}} \qquad 3.1.4$$

and

$$a_s \equiv \frac{(1-\epsilon)(1+\Gamma)}{\Pi_{\rho o}} = \frac{3(1-\epsilon)}{\Pi_{\rho o}} \quad \text{for spherical particles}$$

$$Bi_\rho = \frac{h_\rho \Pi_{\rho o}}{K_\rho} = \frac{\text{(gas-solid heat transfer)}}{\text{(intraparticle heat transfer by conduction)}}$$

Dimensionless variance then is (assuming that the regenerator is long enough):

$$\sigma_D^2 = \frac{\sigma^2}{\mu^2} = 2\left\{ \frac{1}{5}\frac{Bi_\rho}{St_\rho} + \frac{1}{St_\rho} + \frac{1}{Pe_{gz}} \right\} \qquad 3.1.3b$$

i.e. $\sigma_D^2 = \sigma_{D\ \text{particle conduction}}^2 + \sigma_{D\ \text{film resistance}}^2 + \sigma_{D\ \text{gas dispersion}}^2$

$$= \frac{\text{(conduction resistance in particles)}}{\text{(convective resistance)}} + \frac{\text{(gas-solid film resistance)}}{\text{(convective resistance)}}$$

$$+ \frac{\text{("eddy" axial dispersion resistance)}}{\text{(convective resistance)}} \qquad 3.1.5$$

Thus when

(conduction resistance in particles) << (convective resistance)

(gas-solid film resistance) << (convective resistance)

("eddy"axial dispersion resistance) << (convective resistance)

we have an ideal regenerator.

Instead of resistances we can talk about "characteristic times":

$$\tau_t \equiv \frac{\sigma^2}{\mu} = 2\left\{\frac{1}{5}\frac{Bi_\rho}{St_\rho}\mu + \frac{1}{St_\rho}\mu + \frac{1}{Pe_{gz}}\mu\right\} \qquad 3.1.6$$

$$= \tau_c + \tau_f + \tau_d$$

where characteristic convection time is μ,

characteristic particle conduction time is $\tau_c = \frac{2}{5}\frac{Bi_\rho}{St_\rho}\mu$,

characteristic film heat transfer time is $\tau_f = \frac{2}{St_\rho}\mu$,

characteristic heat dispersion time is $\tau_d = \frac{2}{Pe_{gz}}\mu$.

In order to approach an ideal regenerator, we need:

$$\frac{\tau_c}{\mu} \ll 1 \quad ; \quad \frac{\tau_f}{\mu} \ll 1 \quad ; \quad \frac{\tau_d}{\mu} \ll 1 \qquad 3.1.7$$

$$\frac{\tau_c}{\mu} = \sigma_D^2{}_{\substack{\text{particle}\\ \text{conduction}}} = \frac{2}{5}\frac{Bi_\rho}{St_\rho} = \frac{2\rho_{po}G_gC_{pg}}{5a_sK_\rho L} \qquad 3.1.8a$$

$$\frac{\tau_f}{\mu} = \sigma_D^2{}_{\substack{\text{film}\\ \text{resistance}}} = \frac{2}{St_\rho} = \frac{2G_gC_{pg}}{h_\rho a_s L} \qquad 3.1.8b$$

$$\frac{\tau_d}{\mu} = \sigma_D^2{}_{\substack{\text{gas}\\ \text{dispersion}}} = \frac{2}{Pe_{gz}} = \frac{2K_{egz}}{LG_gC_{pg}} \qquad 3.1.8c$$

Thus if we want to approach an ideal regenerator we should build a long heat regenerator to reduce $\frac{\tau_t}{\mu}$ i.e. σ_D^2. Naturally there are practical limitations on the regenerator length.

Since the variance is additive for various heat transfer resistances, it is possible to simplify the complex model by breaking it into several limiting cases. We can readily develop the expression for individual variances from the simple models and finally sum them up to find the expression for the total variance. However, if we use the models that treat the solids as a continuous medium (MIA and plate regenerators MII) the variance is no longer additive if the heat conduction in the solid phase in the axial direction is not negligible. Then we have to treat the whole complex model in order to find the expression for the total variance. Except for some limiting cases the variances of these models have not been solved yet and the above approach cannot be applied for these complex systems until that is done.

From the convolution theory a step response $u(\theta)$ is defined as:

$$\mathcal{U}(\theta) = \int_0^\theta E(\theta')\,d\theta' = \frac{\mu}{\sigma^2}\frac{1}{\Gamma\left(\frac{\mu^2}{\sigma^2}\right)}\int_0^\theta \left(\frac{\mu}{\sigma^2}\theta'\right)^{\frac{\mu^2}{\sigma^2}-1} e^{-\frac{\mu}{\sigma^2}\theta'}\,d\theta' \qquad 3.1.9$$

After a change of variable, $x = \frac{\mu}{\sigma^2}\theta'$,

$$\mathcal{U}(\theta) = \frac{1}{\Gamma\left(\frac{\mu^2}{\sigma^2}\right)}\int_0^{\frac{\mu}{\sigma^2}\theta} x^{\frac{\mu^2}{\sigma^2}-1} e^{-x}\,dx \equiv P\left(\frac{\mu^2}{\sigma^2};\frac{\mu}{\sigma^2}\theta\right) \qquad 3.1.10a$$

and the dimensionless form is: $u(\tau) = P\left[\frac{1}{\sigma_D^2}\,;\,\frac{1}{\sigma_D^2}\,\tau\right]$ where 3.1.10b

P(a,x) is an incomplete gamma function which can be related to tabulated χ^2 probability distribution, $\mathcal{P}(X^2/\nu)$, by the relationship:

$$P(a;x) = \mathcal{P}(X^2|\nu) \qquad 3.1.11$$

if $\quad a=\frac{\nu}{2} \quad , \quad x=\frac{X^2}{2}$

3.2 SINGLE PASS EFFICIENCY

For a single pass operation, i.e., a single step input of hot fluid, the regenerator response is:

$$t_{h,e\ \text{single pass}}(\theta) = u(\theta) = P\left(\frac{\mu^2}{\sigma^2};\frac{\mu}{\sigma^2}\theta\right) = \mathcal{P}\left(\frac{2\mu\theta}{\sigma^2}\middle|\frac{2\mu^2}{\sigma^2}\right) \qquad 3.2.1$$

The thermal efficiency of single pass operation, defined in Equation 2.2.7, is:

$$\eta_s(\theta_i) = \frac{1}{\theta_i}\int_0^{\theta_i}\left[1-P\left(\frac{\mu^2}{\sigma^2};\frac{\mu}{\sigma^2}\theta\right)\right]d\theta \qquad 3.2.2$$

where θ_i now represents the switch-off time i.e., the time when the input is terminated. After several manipulations (see Appendix A), we have the following expression:

$$\eta_s(\theta_i) = 1-\left(1-\frac{\mu}{\theta_i}\right)P\left(\frac{\mu^2}{\sigma^2};\frac{\mu}{\sigma^2}\theta_i\right)-\frac{\mu}{\theta_i}\frac{\left(\frac{\mu}{\sigma^2}\theta_i\right)^{\frac{\mu^2}{\sigma^2}}e^{-\frac{\mu}{\sigma^2}\theta_i}}{\Gamma\left(\frac{\mu^2}{\sigma^2}+1\right)} \qquad 3.2.3a$$

The incomplete gamma function function can readily be obtained either by integration or from tabulated values.

It is convenient to use the dimensionless form:

$$\eta_s(\tau_i) = 1 - \left(1 - \frac{1}{\tau_i}\right) P\left(\frac{1}{\sigma_D^2}; \frac{\tau_i}{\sigma_D^2}\right) - \frac{1}{\tau_i} \frac{\left(\frac{\tau_i}{\sigma_D^2}\right)^{\frac{1}{\sigma_D^2}} e^{-\frac{\tau_i}{\sigma_D^2}}}{\Gamma\left(\frac{1}{\sigma_D^2}+1\right)} \qquad 3.2.3b$$

Here τ_i is the dimensionless switching time and σ_D^2 is the dimensionless variance.

For long heat regenerators ($1/\sigma_D^2 > 15$) the gamma density function of $E(\theta)$ can be approximated by the Gaussian probability density function, i.e.:

$$E(\theta) \cong \frac{1}{\sigma\sqrt{2\pi}} e^{-\frac{(\theta-\mu)^2}{2\sigma^2}} \qquad 3.2.4$$

and the step response $u(\theta)$ can be integrated as:

$$u(\theta) \cong \frac{1}{2}\left[1 + \operatorname{erf}\left(\frac{\theta-\mu}{\sqrt{2}\sigma}\right)\right] = 1 - \frac{1}{2}\operatorname{erfc}\left(\frac{\theta-\mu}{\sqrt{2}\sigma}\right) \qquad 3.2.5a$$

The dimensionless form of the step response is:

$$u(\tau) \cong \frac{1}{2}\left[1 + \operatorname{erf}\left(\frac{\tau-1}{\sqrt{2}\sigma_D}\right)\right] = 1 - \frac{1}{2}\operatorname{erfc}\left(\frac{\tau-1}{\sqrt{2}\sigma_D}\right) \qquad 3.2.5b$$

where error function is defined as $\operatorname{erf}(x) = \frac{2}{\sqrt{\pi}} \int_0^x e^{-x^2} dx$ and complementary error function is defined as $\operatorname{erfc}(x) = 1 - \operatorname{erf}(x)$. The thermal efficiency can be approximated as (see Appendix A):

$$\eta_s(\theta_i) \cong \frac{\mu}{2\theta_i}\left[\frac{\theta_i}{\mu} + \operatorname{erf}\left(\frac{\mu}{\sqrt{2}\sigma}\right) - \left(\frac{\theta_i}{\mu} - 1\right)\operatorname{erf}\left(\frac{\theta_i-\mu}{\sqrt{2}\sigma}\right)\right] - \frac{\sigma}{\theta_i\sqrt{2\pi}}\left[e^{-\frac{(\theta_i-\mu)^2}{2\sigma^2}} - e^{-\frac{\mu^2}{2\sigma^2}}\right] \qquad 3.2.6a$$

and the dimensionless form is:

$$\eta_s(\tau_i) \cong \frac{1}{2\tau_i}\left[\tau_i + \operatorname{erf}\left(\frac{1}{\sqrt{2}\sigma_D}\right) - (\tau_i - 1)\operatorname{erf}\left(\frac{\tau_i - 1}{\sqrt{2}\sigma_D}\right)\right] - \frac{\sigma_D}{\tau_i\sqrt{2\pi}}\left[e^{-\frac{(\tau_i-1)^2}{2\sigma_D^2}} - e^{-\frac{1}{2\sigma_D^2}}\right] \qquad 3.2.6b$$

The results of the step response $u(\tau)$ and the thermal efficiency η_s as a function of dimensionless inverse variance $(1/\sigma_D^2)$ for different values of dimensionless switching time for a single pass operation are shown in Figures 3.1 and 3.2, respectively. It can be seen that the single pass efficiency is reduced with increasing switching time for a fixed value of $1/\sigma_D^2$. At constant switching time the longer the heat regenerator (larger $1/\sigma_D^2$), the higher will be its thermal efficiency. For long regenerators (small variance, $1/\sigma_D^2 > 15$) the thermal efficiencies at long switching times ($\tau_i \geq 1.6$) approach and are almost equal to the efficiency of an ideal regenerator in single pass approach. For the ideal regenerator in single pass operation the efficiency is:

$$\eta_{ideal}\ (\tau_i \leq 1.0) = 1.0$$

$$\eta_{ideal}\ (\tau_i > 1.0) = \frac{1.0}{\tau_i}$$

This result for an ideal regenerator is intuitively obvious. If switch-off time is less than the mean thermal residence time ($\tau_i \leq 1$) the step cannot break through and all of the energy of the hot fluid has been utilized to heat the solids. If switch-off time is larger than mean residence time ($\tau_i > 1$) energy of the hot fluid is only utilized to heat the solids for the duration equal to mean residence time.

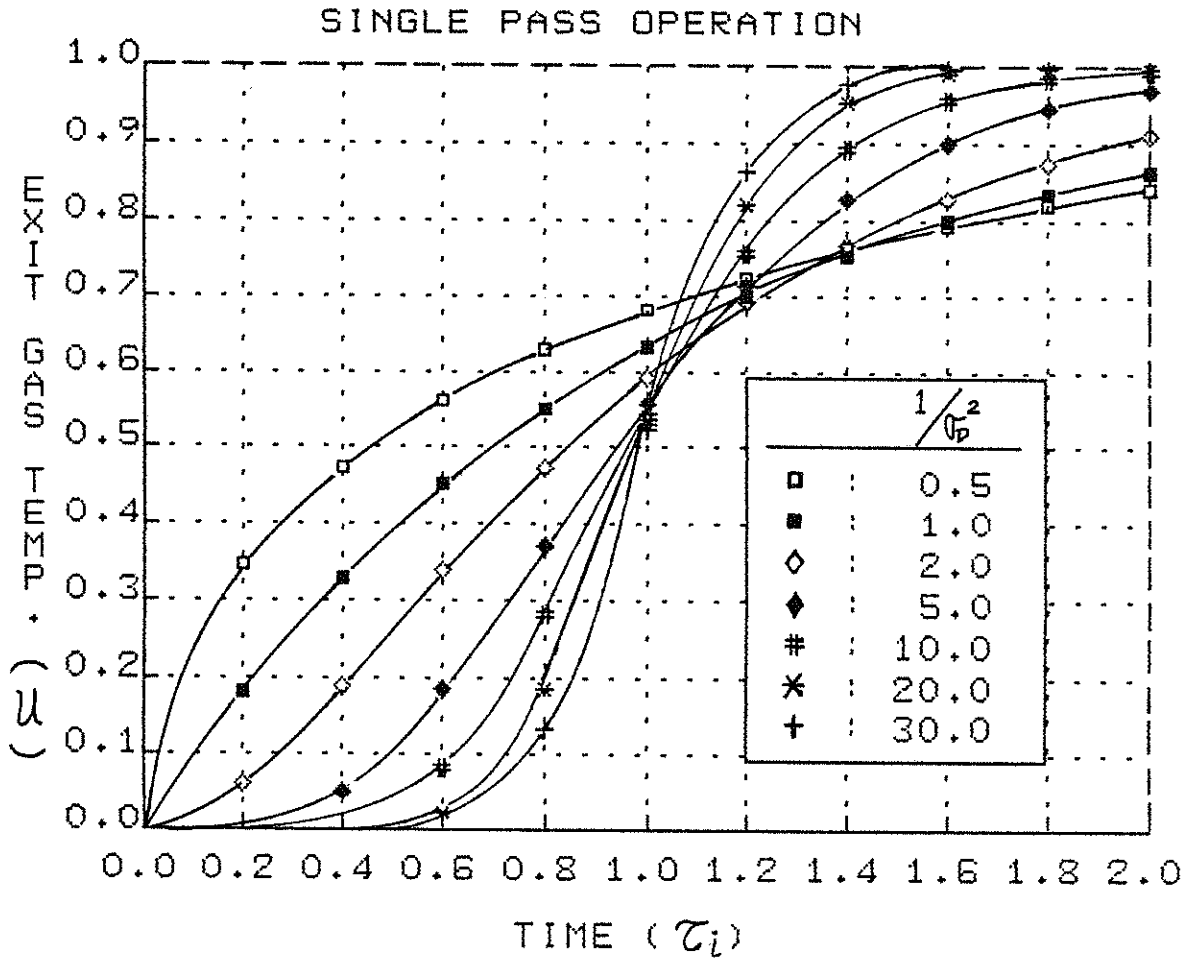

FIGURE 3.1

STEP RESPONSE OF SINGLE PASS OPERATION

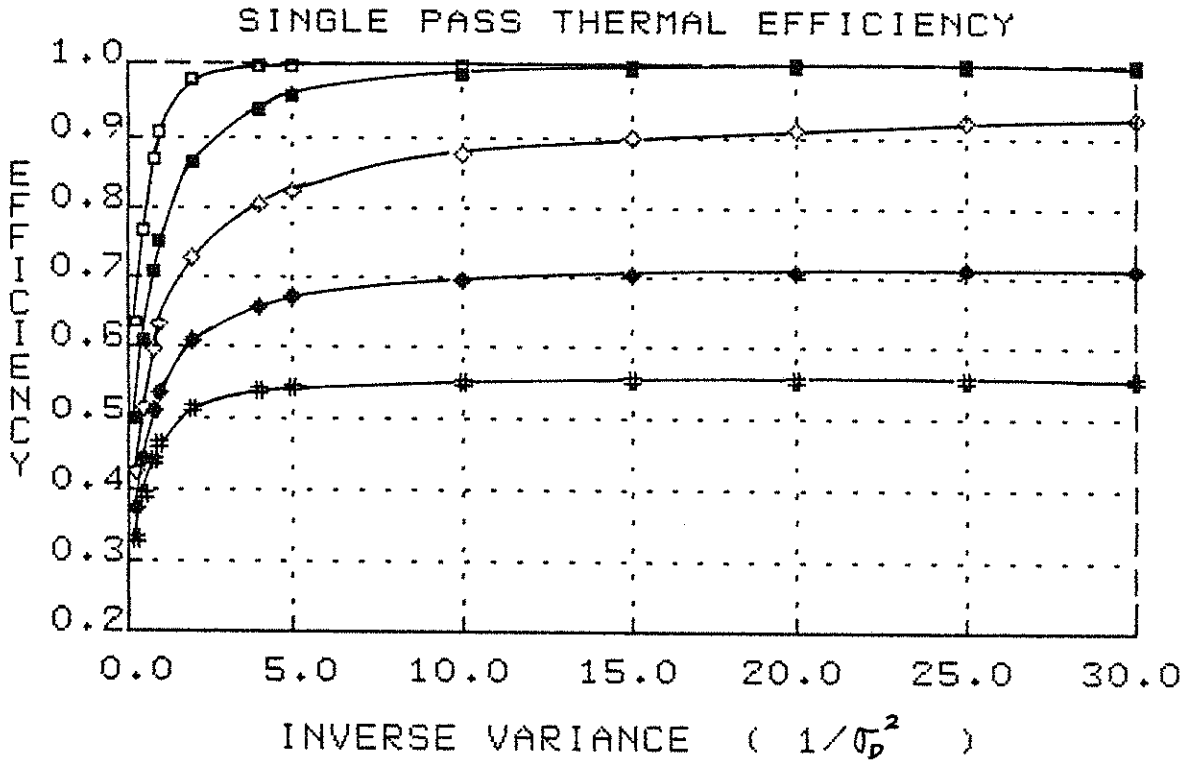

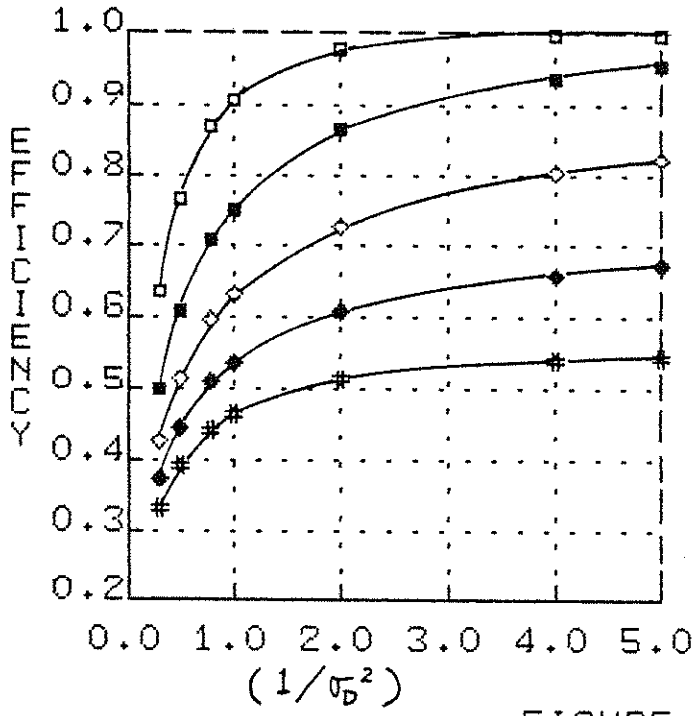

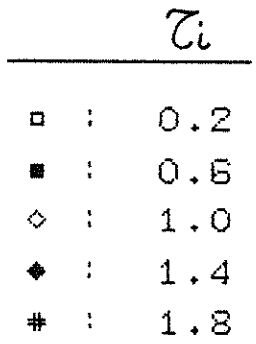

FIGURE 3.2

THERMAL EFFICIENCIES OF SINGLE PASS OPERATION

4. COCURRENT OPERATION

We have derived the response of the regenerator to a single step input of hot gas of duration θ_h by assuming that all the bed is at inlet cold gas temperature. Equivalent results would be obtained by assuming a single step input of cold gas into a bed initially at inlet hot gas temperature. In cocurrent operation the regenerator unit is subjected to a periodic, square wave, inlet gas temperature (Figure 4.1) and the mathematical treatment can be considered to be an extension of the single pass operation model. Since the system is linear and the unit impulse response, $E(\theta)$, is known in terms of the mean and variance, one can construct an approximate solution based on the convolution theory and superposition principle. This solution can then be used to determine the thermal efficiency of cocurrent operation in terms of the variance of the impulse response.

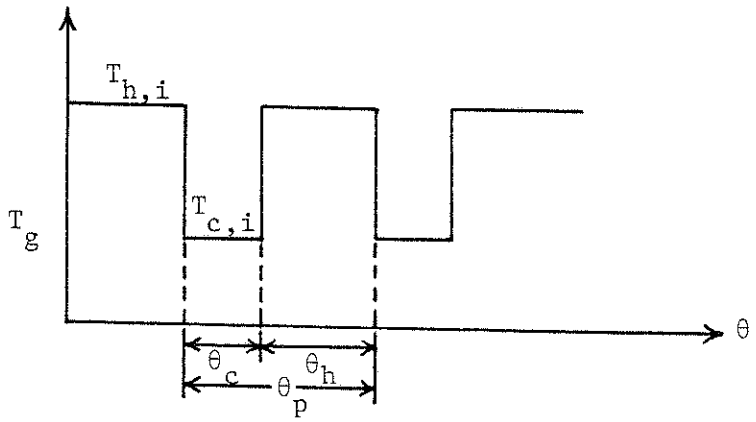

Figure 4.1

Inlet Gas Temperature for Cocurrent Operation

We will also consider a discrete representation for the regenerator consisting of n mixed tanks (cells) in series. This representation will allow us to apply both open and closed methods in calculation of regenerator efficiency. It is also of interest to compare the results at large n with those obtained based on the above discussed approximate method and with other results of more complex computational schemes reported in the literature (10,28). Finally, there are situations where gases carry a considerable amount of particulates and staged fluidized beds need to be used as regenerators. For small n then our model will be useful for representation of such systems.

In practice, as mentioned before, if only two regenerators are used the real switching times of the hot and cold periods should be the same. Therefore in case of equal product of mass flow rate and specific heat of the two gas streams (hot and cold) we will consider symmetric regenerators only. In the case of unequal product of mass flow rate and specific heat only unbalanced regenerators will be considered.

4.1 PRINCIPLE OF SUPERPOSITION

Superposition techniques can be used for the prediction of the transient response of a heat regenerator subject to any input provided that the impulse response is known and that the physical properties of the gas and solids are independent of temperature. Under these conditions the differential energy equations for the gas and solids and the initial and boundary conditions are linear for all the models discussed in Chapter 2 and the convolution theory can be applied.

The varying inlet gas temperature, as shown in Figure 4.1, is broken up into a series of step changes in temperature. Each step represents a subproblem that has a step change in inlet temperature, with the unit considered to be initially at a given temperature. The response of the unit with a variation in inlet gas temperature is the sum of the responses of all the subproblems (28).

4.1.1 Equal Product of Mass Flow Rate and Specific Heat - Symmetric Regenerators

The periodic input in the cocurrent operation is:

$$t_{in}(\theta) = \sum_{n=0}^{\infty} \left[H(\theta - n\theta_p) - H(\theta - n\theta_p - \theta_h) \right] \qquad 4.1.1a$$

For a symmetric regenerator, i.e. $\theta_h = \theta_c = \theta_i$ and $\theta_p = 2\theta_i$, we have:

$$t_{in}(\theta) = \sum_{n=0}^{\infty} \left[H(\theta - 2n\theta_i) - H(\theta - (2n+1)\theta_i) \right] \qquad 4.1.2a$$

The exit temperature can be found by applying the superposition principle, which yields:

$$t_{ex}(\theta) = \sum_{n=0}^{\infty} \left[u(\theta - 2n\theta_i) H(\theta - 2n\theta_i) - u(\theta - (2n+1)\theta_i) H(\theta - (2n+1)\theta_i) \right] \qquad 4.1.3a$$

where $u(\theta)$ is the single pass step response of the regenerator discussed in Chapter 3.

The thermal efficiency of the heating period, defined in Equation 2.2.7 is:

$$\eta_h(\theta_i) = \frac{1}{\theta_i} \int_{2N\theta_i}^{(2N+1)\theta_i} \left[t_{in}(\theta) - t_{ex}(\theta) \right] d\theta \qquad 4.1.4a$$

where $t_{in}(\theta) = 1$ in the heating period and N is a number large enough so that stationary state is obtained.

After several manipulations (see Appendix B), we get:

$$\eta_h(\theta_i) = \eta_s(\theta_i) + \frac{1}{\theta_i}\sum_{j=1}^{N}\left\{\left[-\left((2j-1)\theta_i - \mu\right)P\left(\frac{\mu^2}{\sigma^2};\frac{\mu}{\sigma^2}(2j-1)\theta_i\right)\right.\right.$$
$$+2\left(2j\theta_i-\mu\right)P\left(\frac{\mu^2}{\sigma^2};\frac{\mu}{\sigma^2}2j\theta_i\right)-\left((2j+1)\theta_i-\mu\right)P\left(\frac{\mu^2}{\sigma^2};\frac{\mu}{\sigma^2}(2j+1)\theta_i\right)\Big]$$
$$-\frac{\mu}{\Gamma\left(\frac{\mu^2}{\sigma^2}+1\right)}\left[\left(\frac{\mu}{\sigma^2}(2j-1)\theta_i\right)^{\frac{\mu^2}{\sigma^2}}e^{-\frac{\mu}{\sigma^2}(2j-1)\theta_i}\right. \qquad 4.1.5a$$
$$\left.\left.-2\left(\frac{\mu}{\sigma^2}2j\theta_i\right)^{\frac{\mu^2}{\sigma^2}}e^{-\frac{\mu}{\sigma^2}2j\theta_i}+\left(\frac{\mu}{\sigma^2}(2j+1)\theta_i\right)^{\frac{\mu^2}{\sigma^2}}e^{-\frac{\mu}{\sigma^2}(2j+1)\theta_i}\right]\right\}$$

The dimensionless form of the above equation is:

$$\eta_h(\tau_i) = \eta_s(\tau_i) + \frac{1}{\tau_i}\sum_{j=1}^{N}\left\{\left[-\left((2j-1)\tau_i - 1\right)P\left(\frac{1}{\sigma_D^2};\frac{1}{\sigma_D^2}(2j-1)\tau_i\right)\right.\right.$$
$$+2\left(2j\tau_i-1\right)P\left(\frac{1}{\sigma_D^2};\frac{1}{\sigma_D^2}2j\tau_i\right)-\left((2j+1)\tau_i-1\right)P\left(\frac{1}{\sigma_D^2};\frac{1}{\sigma_D^2}(2j+1)\tau_i\right)\Big]$$
$$-\frac{1}{\Gamma\left(\frac{1}{\sigma_D^2}+1\right)}\left[\left(\frac{1}{\sigma_D^2}(2j-1)\tau_i\right)^{\frac{1}{\sigma_D^2}}e^{-\frac{1}{\sigma_D^2}(2j-1)\tau_i}\right. \qquad 4.1.5b$$
$$\left.\left.-2\left(\frac{1}{\sigma_D^2}2j\tau_i\right)^{\frac{1}{\sigma_D^2}}e^{-\frac{1}{\sigma_D^2}2j\tau_i}+\left(\frac{1}{\sigma_D^2}(2j+1)\tau_i\right)^{\frac{1}{\sigma_D^2}}e^{-\frac{1}{\sigma_D^2}(2j+1)\tau_i}\right]\right\}$$

For a long heat regenerator ($1/\sigma_D^2 > 15$), the thermal efficiency can be approximated using the Gaussian distribution as (see Appendix B):

$$\eta_h(\theta_i) = \eta_s(\theta_i) + \frac{1}{\theta_i}\sum_{j=1}^{N}\left\{\frac{1}{2}\left[\left((2j-1)\theta_i-\mu\right)\operatorname{erfc}\left(\frac{(2j-1)\theta_i-\mu}{\sqrt{2}\,\sigma}\right)\right.\right.$$
$$\left.-2(2j\theta_i-\mu)\operatorname{erfc}\left(\frac{2j\theta_i-\mu}{\sqrt{2}\,\sigma}\right)+\left((2j+1)\theta_i-\mu\right)\operatorname{erfc}\left(\frac{(2j+1)\theta_i-\mu}{\sqrt{2}\,\sigma}\right)\right] \qquad 4.1.6a$$
$$\left.-\frac{\sigma}{\sqrt{2\pi}}\left[e^{-\frac{((2j-1)\theta_i-\mu)^2}{2\sigma^2}}-2e^{-\frac{(2j\theta_i-\mu)^2}{2\sigma^2}}+e^{-\frac{((2j+1)\theta_i-\mu)^2}{2\sigma^2}}\right]\right\}$$

The dimensionless form is:

$$\eta_h(\tau_i) = \eta_s(\tau_i) + \frac{1}{\tau_i}\sum_{j=1}^{N}\left\{\frac{1}{2}\left[\left((2j-1)\tau_i-1\right)\operatorname{erfc}\left(\frac{(2j-1)\tau_i-1}{\sqrt{2}\,\sigma_D}\right)\right.\right.$$
$$\left.-2(2j\tau_i-1)\operatorname{erfc}\left(\frac{2j\tau_i-1}{\sqrt{2}\,\sigma_D}\right)+\left((2j+1)\tau_i-1\right)\operatorname{erfc}\left(\frac{(2j+1)\tau_i-1}{\sqrt{2}\,\sigma_D}\right)\right] \qquad 4.1.6b$$
$$\left.-\frac{\sigma_D}{\sqrt{2\pi}}\left[e^{-\frac{((2j-1)\tau_i-1)^2}{2\sigma_D^2}}-2e^{-\frac{(2j\tau_i-1)^2}{2\sigma_D^2}}+e^{-\frac{((2j+1)\tau_i-1)^2}{2\sigma_D^2}}\right]\right\}$$

For symmetric heat regenerators we have $\eta_h = \eta_c = \eta_o$. The results of the thermal efficiency as a function of $1/\sigma_D^2$ for different values of switching time for cocurrent operation are shown in Figure 4.2. In this evaluation N is determined from the convergence criterion in the summation. We find that N is large for small $1/\sigma_D^2$ values and short switching times but is small for large $1/\sigma_D^2$ values and long switching times.

Figure 4.2 indicates that the longer the regenerator, i.e., the larger $1/\sigma_D^2$ the better the efficiency except at short switching times. The curve for $\tau_i = 1$ ($\theta_i = \mu_i$) seems to form an upper bound on efficiency except at large variance ($\sigma_D^2 > 1/3$). Later on we show that this is true at $\sigma_D^2 < 0.05$ and approximately true at other variances. The behavior

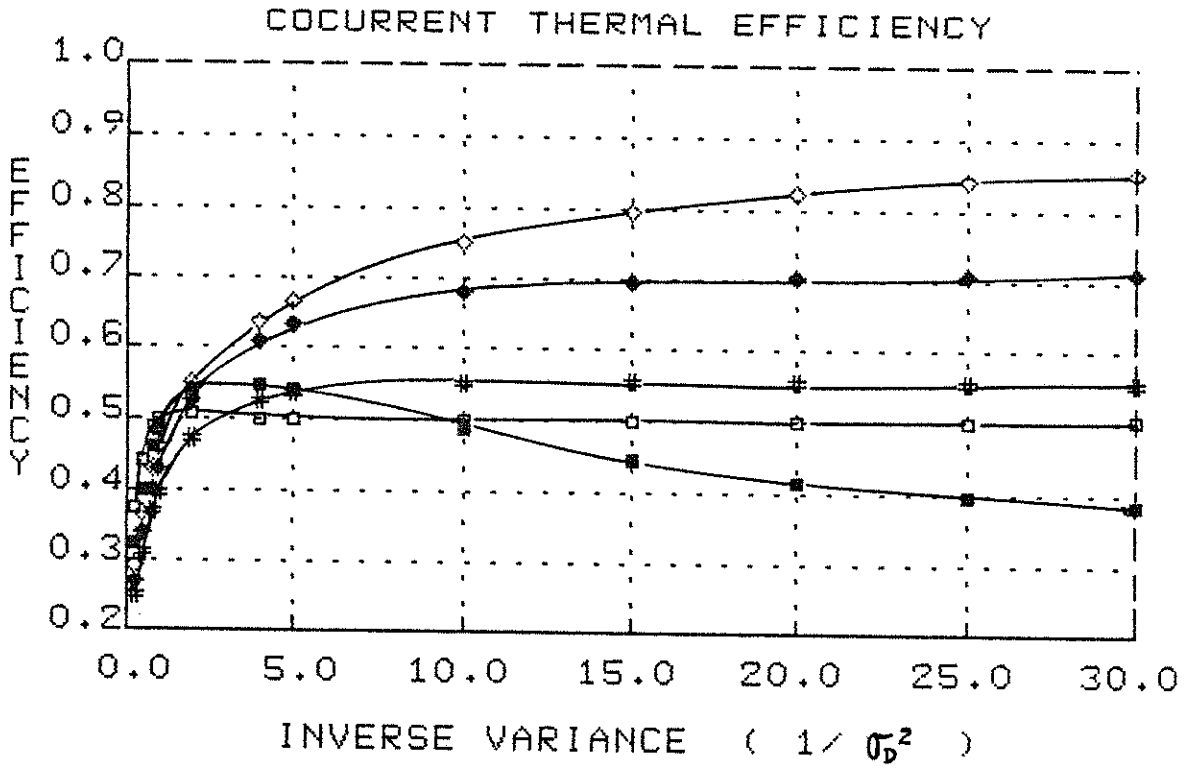

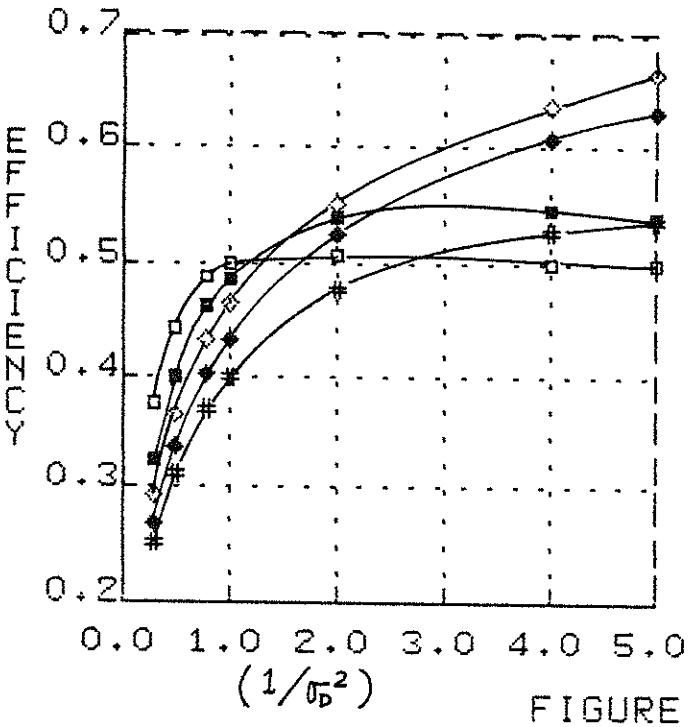

$\tau_h = \tau_c = \tau_i$

- □ : 0.2
- ■ : 0.6
- ◇ : 1.0
- ◆ : 1.4
- # : 1.8

FIGURE 4.2

THERMAL EFFICIENCIES OF COCURRENT OPERATION
——APPROXIMATE SOLUTION USING THE PRINCIPLE OF SUPERPOSITION , SYMMETRIC CASE

at large variance (expanded view of Figure 4.2) seems to be due to model inability to simulate physical reality as shown later by n-staged bed model.

All these findings are in agreement with those of Hausen (6) and Nusselt (21) as presented by Jakob (10). The simple model considered by these authors contained only the film resistance, hence, $\sigma_D^2 = \frac{2}{St}$ and $\frac{1}{\sigma_D^2} = \frac{St}{2}$. The reduced length in Jakob's book is $\Lambda = St = \frac{hA}{\dot{m}_g C_{pg}} = 2\left(\frac{1}{\sigma_D^2}\right)$ and the reduced period is $\pi = \Lambda.\tau_i = \frac{hA}{\dot{m}_g C_{pg}} \frac{\theta}{M_s C_{ps}/\dot{m}_g C_{pg}} = \frac{hA\theta}{M_s C_{ps}}$ and good agreement with these charts is evident.

The method using the approximate solutions in terms of the variance of impulse response based on the principle of superposition is much simpler to solve and can determine the periodic cocurrent performance of heat regenerators for any model when the variance is available.

4.1.2 Unequal Product of Mass Flow Rate and Specific Heat - Unbalanced Regenerators

We always want to operate the heat regenerator with the same switching time for the heating and cooling periods. Once the products of mass flow rate and specific heat in these two periods are unequal, we call this an "unbalanced regenerator". We have found that the principle of superposition can still be applied for this case if we have the dimensionless times based on μ_h and μ_c for the heating and cooling periods, respectively.

The dimensionless form of the periodic input is now defined as:

$$t_{in}(\tau) = \sum_{n=0}^{\infty} \left[H(\tau - n\tau_p) - H(\tau - n\tau_p - \tau_h) \right] \qquad 4.1.1b$$

and the dimensionless output can then be found by applying the superposition principle:

$$t_{ex}(\tau) = \sum_{n=0}^{\infty} \left[u_h(\tau - n\tau_p) H(\tau - n\tau_p) - u_c(\tau - n\tau_p - \tau_h) H(\tau - n\tau_p - \tau_h) \right] \qquad 4.1.7$$

where τ is the dimensionless time based on the μ_h and μ_c periodically and $\tau_p = \tau_h + \tau_c = \theta_i/\mu_h + \theta_i/\mu_c = \tau_h + (\mu_h/\mu_c)\tau_h$; u_h is the step response to the single step input of hot gas in a bed initially at inlet cold gas temperature while u_c is the step response of cold gas in a bed initially at inlet hot gas temperature. From Equation 3.1.10b we have:

$$u_h(\tau) = P\left(\frac{1}{\sigma_{D,h}^2}; \frac{1}{\sigma_{D,h}^2}\tau\right) \quad ; \quad u_c(\tau) = P\left(\frac{1}{\sigma_{D,c}^2}; \frac{1}{\sigma_{D,c}^2}\tau\right) \qquad \begin{matrix} 3.1.10c; \\ 3.1.10d \end{matrix}$$

where $\sigma_{D,h}^2 = \sigma_h^2/\mu_h^2$ and $\sigma_{D,c}^2 = \sigma_c^2/\mu_c^2$ are the dimensionless variances of the heating and cooling periods, respectively.

The thermal efficiency of heating period is then defined as:

$$\eta_h(\tau_h) = \frac{1}{\tau_h} \int_{N\tau_p}^{N\tau_p + \tau_h} \left[t_{in}(\tau) - t_{ex}(\tau) \right] d\tau \qquad 4.1.8$$

where N is the number large enough to reach the stationary state.

After similar manipulations as before (see Appendix C), we get:

$$\eta_h(\tau_h) = \eta_s(\tau_h) + \frac{1}{\tau_h}\sum_{j=1}^{N}\left\{\left[-(j\tau_p-\tau_h-1)P\left(\frac{1}{\sigma_{D,c}^2};\frac{1}{\sigma_{D,c}^2}[j\tau_p-\tau_h]\right)+(j\tau_p-1)P\left(\frac{1}{\sigma_{D,c}^2};\frac{1}{\sigma_{D,c}^2}[j\tau_p]\right)\right.\right.$$

$$\left.+(j\tau_p-1)P\left(\frac{1}{\sigma_{D,h}^2};\frac{1}{\sigma_{D,h}^2}[j\tau_p]\right)-(j\tau_p+\tau_h-1)P\left(\frac{1}{\sigma_{D,h}^2};\frac{1}{\sigma_{D,h}^2}[j\tau_p+\tau_h]\right)\right]$$

$$-\frac{1}{\Gamma\left(\frac{1}{\sigma_{D,c}^2}+1\right)}\left[\left(\frac{1}{\sigma_{D,c}^2}[j\tau_p-\tau_h]\right)^{\frac{1}{\sigma_{D,c}^2}}e^{-\frac{1}{\sigma_{D,c}^2}[j\tau_p-\tau_h]}-\left(\frac{1}{\sigma_{D,c}^2}[j\tau_p]\right)^{\frac{1}{\sigma_{D,c}^2}}e^{-\frac{1}{\sigma_{D,c}^2}[j\tau_p]}\right]$$

$$\left.-\frac{1}{\Gamma\left(\frac{1}{\sigma_{D,h}^2}+1\right)}\left[\left(\frac{1}{\sigma_{D,h}^2}[j\tau_p+\tau_h]\right)^{\frac{1}{\sigma_{D,h}^2}}e^{-\frac{1}{\sigma_{D,h}^2}[j\tau_p+\tau_h]}-\left(\frac{1}{\sigma_{D,h}^2}[j\tau_p]\right)^{\frac{1}{\sigma_{D,h}^2}}e^{-\frac{1}{\sigma_{D,h}^2}[j\tau_p]}\right]\right\} \qquad 4.1.9$$

where $\eta_s(\tau_h)$ is the single pass efficiency:

$$\eta_s(\tau_h) = 1-\left(1-\frac{1}{\tau_h}\right)P\left(\frac{1}{\sigma_{D,h}^2};\frac{1}{\sigma_{D,h}^2}\tau_h\right)-\frac{1}{\tau_h}\frac{\left(\frac{1}{\sigma_{D,h}^2}\tau_h\right)^{\frac{1}{\sigma_{D,h}^2}}e^{-\frac{1}{\sigma_{D,h}^2}\tau_h}}{\Gamma\left(\frac{1}{\sigma_{D,h}^2}+1\right)} \qquad 3.2.3C$$

For long heat regenerators ($1/\sigma_D^2 > 15$), the thermal efficiency can be approximated as (see Appendix C):

$$\eta_h(\tau_h) = \eta_s(\tau_h) + \frac{1}{\tau_h}\sum_{j=1}^{N}\left\{\frac{1}{2}\left[(j\tau_p-\tau_h-1)\,\mathrm{erfc}\left(\frac{j\tau_p-\tau_h-1}{\sqrt{2}\,\sigma_{D,c}}\right)-(j\tau_p-1)\,\mathrm{erfc}\left(\frac{j\tau_p-1}{\sqrt{2}\,\sigma_{D,c}}\right)\right.\right.$$

$$\left.-(j\tau_p-1)\,\mathrm{erfc}\left(\frac{j\tau_p-1}{\sqrt{2}\,\sigma_{D,h}}\right)+(j\tau_p+\tau_h-1)\,\mathrm{erfc}\left(\frac{j\tau_p+\tau_h-1}{\sqrt{2}\,\sigma_{D,h}}\right)\right]$$

$$-\frac{\sigma_{D,c}}{\sqrt{2\pi}}\left[e^{-\frac{(j\tau_p-\tau_h-1)^2}{2\sigma_{D,c}^2}}-e^{-\frac{(j\tau_p-1)^2}{2\sigma_{D,c}^2}}\right]$$

$$\left.-\frac{\sigma_{D,h}}{\sqrt{2\pi}}\left[e^{-\frac{(j\tau_p+\tau_h-1)^2}{2\sigma_{D,h}^2}}-e^{-\frac{(j\tau_p-1)^2}{2\sigma_{D,h}^2}}\right]\right\} \qquad 4.1.10$$

where

$$\eta_s(\tau_h) = \frac{1}{2\tau_h}\left[\tau_h + \text{erf}\left(\frac{1}{\sqrt{2}\sigma_{D,h}}\right) - (\tau_h - 1)\,\text{erf}\left(\frac{\tau_h - 1}{\sqrt{2}\sigma_{D,h}}\right)\right]$$

$$- \frac{\sigma_{D,h}}{\tau_h\sqrt{2\pi}}\left[e^{-\frac{(\tau_h-1)^2}{2\sigma_{D,h}^2}} - e^{-\frac{1}{2\sigma_{D,h}^2}}\right] \qquad 3.2.6c$$

We need both $\sigma_{D,h}^2$ and $\sigma_{D,c}^2$ to calculate the thermal efficiency. If we have heat transfer parameters in hands, we can calculate $\sigma_{D,h}^2$ and $\sigma_{D,c}^2$ from Equation 3.1.3 for different values of the ratio of mass flow rates ($\dot{m}_c C_{pc}/\dot{m}_h C_{ph}$ or μ_h/μ_c). We have selected the variances shown in Table 4.1a and 4.1b for the cases $\mu_h/\mu_c = 0.5$ and $\mu_h/\mu_c = 2.0$, respectively. These values allow us to compare the results of this method to the ones obtained by using 30 tanks in series.

The results for the overall thermal efficiency η_o as a function of dimensionless inverse variance of the heating period ($1/\sigma_{D,h}^2$) for different τ_h and τ_c values are shown in Figure 4.3a and 4.3b for the cases $\mu_h/\mu_c = 0.5$ and $\mu_h/\mu_c = 2.0$, respectively. Because of unequal $\dot{m}C_p$, the highest thermal efficiency is no longer at $\tau_h \simeq 1.0$. Instead, for the case of $\mu_h/\mu_c = 0.5$, $\eta_{o,max}$ occurred between $\tau_h = 1.4$ and $\tau_h = 1.5$ while for the case of $\mu_h/\mu_c = 2.0$, $\eta_{o,max}$ occurred between $\tau_h = 0.7$ and $\tau_h = 0.9$ and is slightly different for different $1/\sigma_D^2$ value. These values, however, are all lower than $\eta_{o,max}$ ($\tau_i \cong 1.0$) in the symmetric case.

Table 4.1

The Relationship Between $1/\sigma_{D,h}^2$ and $1/\sigma_{D,c}^2$ From 30-Staged Fluidized Bed Model

(a) $\mu_h/\mu_c = 0.5$

$1/\sigma_{D,h}^2$	0.500	0.800	1.000	2.000	4.000	5.000	10.000	15.000	20.000	25.000	30.000
$1/\sigma_{D,c}^2$	0.984	1.558	1.935	3.750	7.059	8.571	15.000	20.000	24.000	27.273	30.000

(b) $\mu_h/\mu_c = 2.0$

$1/\sigma_{D,h}^2$	0.500	0.800	1.000	2.000	4.000	5.000	10.000	15.000	20.000	25.000	30.000
$1/\sigma_{D,c}^2$	0.252	0.405	0.508	1.034	2.143	2.727	6.000	10.000	15.000	21.429	30.000

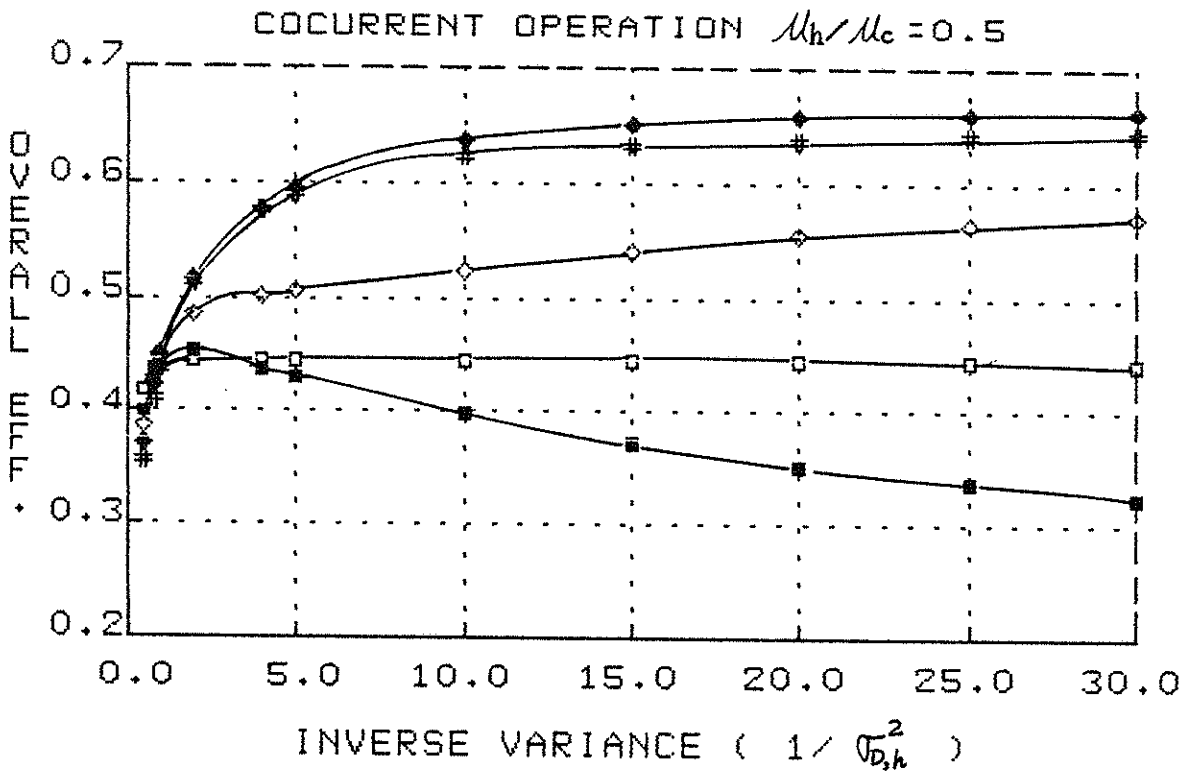

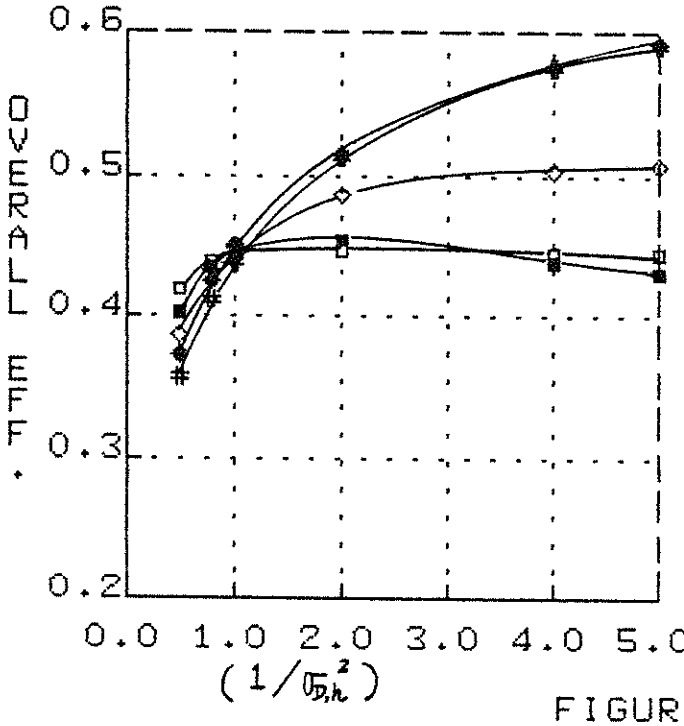

	τ_h	τ_c
□ :	0.2	0.1
■ :	0.6	0.3
◇ :	1.0	0.5
◆ :	1.4	0.7
# :	1.8	0.9

FIGURE 4.3a

THERMAL EFFICIENCIES OF COCURRENT OPERATION
——APPROXIMATE SOLUTION USING THE PRINCIPLE OF SUPERPOSITION ,
UNBALANCED CASE ($M_h/M_c = 0.5$)

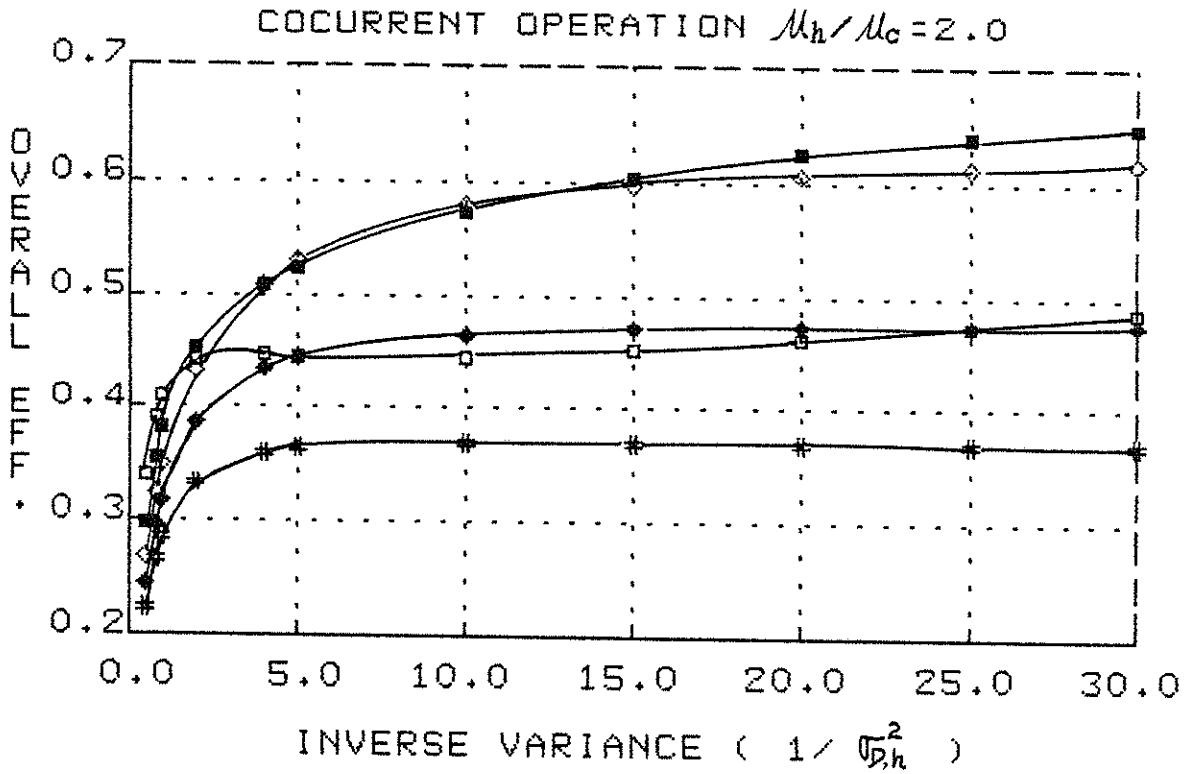

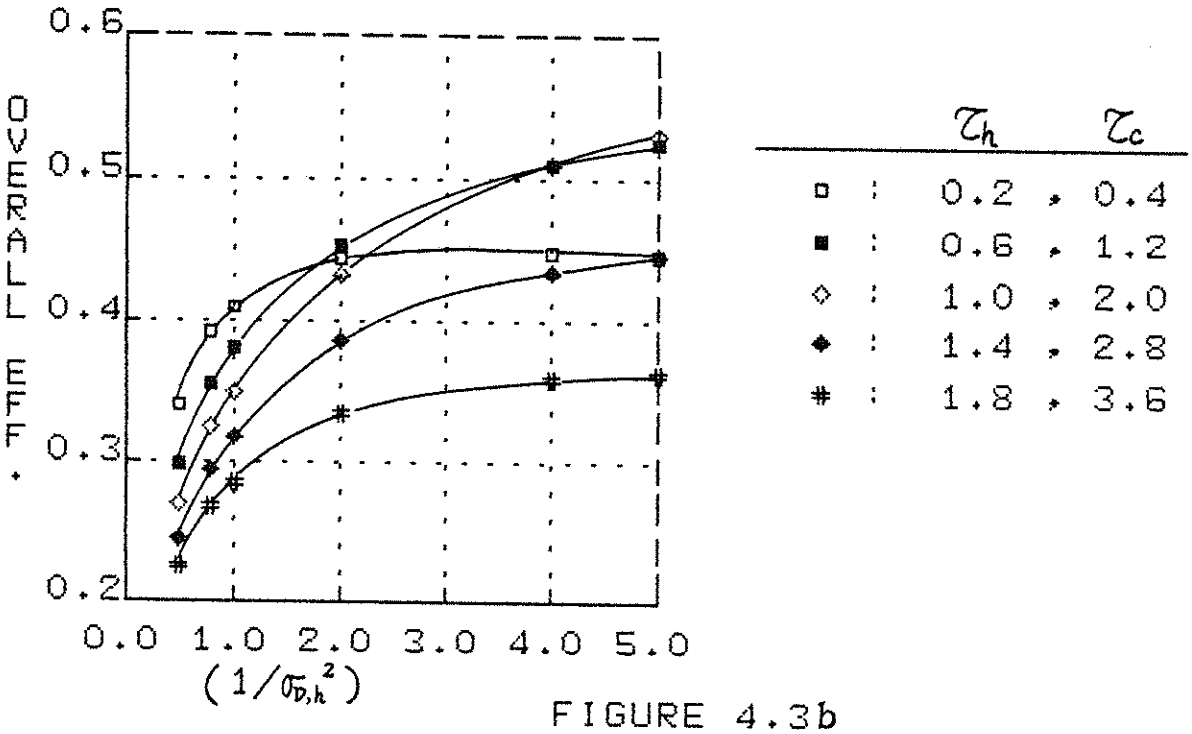

FIGURE 4.3b

THERMAL EFFICIENCIES OF COCURRENT OPERATION
——APPROXIMATE SOLUTION USING THE PRINCIPLE OF SUPERPOSITION ,
UNBALANCED CASE ($M_h/M_c = 2.0$)

We cannot predict precisely where $\eta_{o,max}$ will occur for each $1/\sigma_{D,h}^2$ until we do some optimization searches for Equation 4.1.9, but it can be seen that for the case of $\mu_h/\mu_c < 1.0$, we have a larger product of $\dot{m}_h$ and C_p in the heating period and $\eta_{o,max}$ will occur at larger switching times than μ_h, i.e., $\tau_h > 1.0$; while for the case of $\mu_h/\mu_c > 1.0$, we have a smaller product of $\dot{m}_h$ and C_p in the heating period and $\eta_{o,max}$ will occur at smaller switching times than μ_h, i.e., $\tau_h < 1.0$.

We are always interested in the overall thermal efficiency which can give us the best measure for the periodic performance of heat regenerator in the unequal $\dot{m}C_p$ case. However, based on Equation 2.2.11, we know that the higher the thermal efficiency of the heating or cooling period, the higher will be its overall thermal efficiency when τ_h/τ_c is fixed. So, if we just consider the maximum for the thermal efficiency in the heating or cooling period, i.e., $\eta_{h,max}$ or $\eta_{c,max}$, we still have the same optimal switching time conditions as those from $\eta_{o,max}$. If it is the case that $\mu_h/\mu_c = 0.5$, then $\eta_{c,max} = 2\eta_{h,max}$; while if it is the case that $\mu_h/\mu_c = 2.0$, then $\eta_{h,max} = 2\eta_{c,max}$. Both maximum values, i.e., $\eta_{c,max}$ for the case of $\mu_h/\mu_c < 1.0$ and $\eta_{h,max}$ for the case of $\mu_h/\mu_c > 1.0$, however, are higher than $\eta_{o,max}$ ($\tau_i \tilde{=} 1.0$) in the symmetric case.

4.1.3 Comparison to Schumann's Model

Because of the complexity of the model for heat regenerators, the closed methods in evaluating regenerator performance and efficiency have only been used for some simple models so far. The simplest model

was proposed by Schumann (25) who assumed infinite thermal conductivity of the solids in the direction perpendicular to the flow and zero in the direction of flow. Only the heat transfer resistance of the boundary layer was considered. For cocurrent operation Schumann's model is:

1. Heating period, $0 < \tau_1 < \tau_h$

$$-\frac{\partial t_g}{\partial \xi_1} = t_g - t_s \qquad \text{with:} \quad \tau_1 = 0,\ t_s = f_1(\xi_1)$$

$$\frac{\partial t_s}{\partial \tau_1} = t_g - t_s \qquad \xi_1 = 0,\ t_g = 1$$

2. Cooling period, $0 < \tau_2 < \tau_c$

$$-\frac{\partial t_g}{\partial \xi_2} = t_g - t_s \qquad \text{with:} \quad \tau_2 = 0,\ t_s = f_2(\xi_2)$$

$$\frac{\partial t_s}{\partial \tau_2} = t_g - t_s \qquad \xi_2 = 0,\ t_g = 0$$

where

$$\xi' = \frac{z}{L}, \quad \tau_1' = \theta \Big/ \frac{\rho_s C_{ps}(1-\epsilon)V}{\dot{m}_h C_{ph}} = \frac{\theta}{\mu_h}, \quad St_1 = \frac{hA}{\dot{m}_h C_{ph}},$$

$$\tau_2' = \theta \Big/ \frac{\rho_s C_{ps}(1-\epsilon)V}{\dot{m}_c C_{pc}} = \frac{\theta}{\mu_c}, \quad St_2 = \frac{hA}{\dot{m}_c C_{pc}},$$

$$\xi_1 = \xi'(St_1),\ \tau_1 = \tau_1'(St_1);\quad \xi_2 = \xi'(St_2),\ \tau_2 = \tau_2'(St_2)$$

and $f_1(\xi_1)$ and $f_2(\xi_2)$ are the solid temperature profiles at the end of cooling and heating periods, respectively.

The variance of this model can readily be found from Equation 3.1.3. Now only film resistance need to be considered, so that:

$$\sigma_h^2 = 2\,\mu_h^2\,\left(\frac{1}{St_1}\right) \text{ for the heating period and}$$

$$\sigma_c^2 = 2\,\mu_c^2\,\left(\frac{1}{St_2}\right) \text{ for the cooling period.}$$

Hausen (6) solved the above model by semianalytical methods and the results were checked later by Iliffe (9) and Nahavandi and Weinstein (22) who applied numerical integration techniques to solve the pair of Nusselt's (21) integral equations with the reversal conditions of solid temperatures. Our results obtained from the approximate solutions for the cocurrent case match theirs quite well, always within 5%. Of course our method which relies on the principle of superposition and an approximate expression for the impulse response is much simpler than their numerical solution method of a pair of integral equations. In addition our method establishes that the efficiency is primarily a function of $1/\sigma_D^2$ and τ_i. Thus our method can be applied to any model once we can calculate its variance.

However, as mentioned earlier, the way of applying the principle of superposition to the case of countercurrent flow, which is more efficient than cocurrent operation, escapes us at present. Thus we are forced to solve the countercurrent case by closed methods. Here we are going to construct a model based on n-tanks in series and consider just Schumann's type of model in each tank. This can then be used for large

n as an approximation to the packed bed regenerator and enable us to solve the equations for the closed method explicitly instead of having to solve a pair of integral equations.

4.2 FINITE ELEMENT APPROACH TO THE SCHUMANN MODEL OF HEAT REGENERATORS - n-STAGED FLUIDIZED BEDS MODEL

Fluidized beds of fine particles are characterized by good mixing of solids. Thus we may take the solids to be uniform in temperature at any time. Also since the unsteady term of gas phase energy equation can be neglected due to the small heat capacity of gas compared to the solids, the flow pattern of gas is much less important than the state of mixing of solids. So we can make the following assumption to simplify the model:

- Batch well mixed solids/well mixed gas

If we connect the fluidized beds in series, we have the n-staged fluidized bed model, as sketched below:

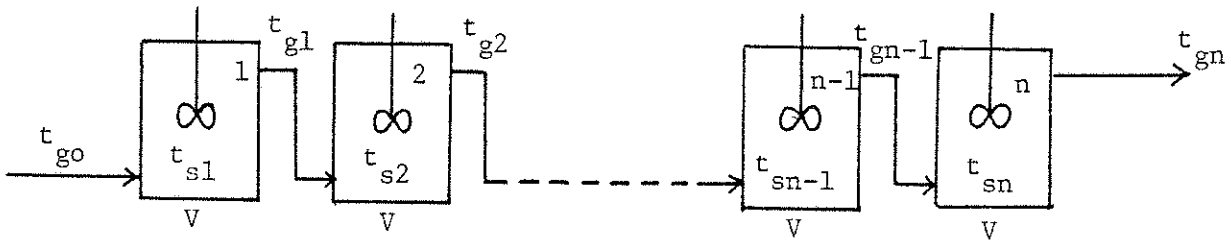

Figure 4.4

n-Staged Fluidized Beds Regenerators
——— Cocurrent Operation

Either single pass or periodic operations can be considered.

For single pass operation we have the following mathematical model for each element m based on the above assumption:

gas: $$0 = (t_{g\,m-1} - t_{g\,m}) - \beta\,(t_{gm} - t_{sm}) \quad ; \quad m = 1, 2, \cdots, n \qquad 4.2.1$$

solids: $$\frac{dt_{sm}}{d\tau} = \beta\,(t_{gm} - t_{sm}) \quad ; \quad m = 1, 2, \cdots, n \qquad 4.2.2$$

$$\tau = 0 \;,\; t_{sm} = t_{sm}^{o} \quad ; \quad m = 1, 2, \cdots, n \qquad 4.2.3a$$

$$m = 1 \;,\; t_{go} = H(\tau) \qquad 4.2.3b$$

and the dimensionless groups are:

$$\tau = \theta \Big/ \left[\frac{\rho_s C_{ps}(1-\epsilon)V}{\dot{m}_g C_{pg}}\right] = \theta/\mu \;, \qquad St = \frac{hAi}{\dot{m}_g C_{pg}} = \beta\,(\text{individual}) \qquad 4.2.4$$

where V is the volume of a single tank and μ is the thermal mean residence time for a single tank.

Equations 4.2.1 to 4.2.3 represent a realistic model of n fluidized beds in series. The main departure from an ideal regenerator is caused by the backmixing of solids, a secondary effect comes from the gas-solids heat transfer resistance which is typically quite small in fluidized beds. It is assumed that particles are small and of high conductivity.

The above model also represents a discrete approximation to the packed bed regenerator if n is sufficiently large. Although only

gas-solid resistance is considered, as in the Schumann model, we know that the addition of the intraparticle conduction resistance can readily be added.

After taking the Laplace transformation, we get:

$$\bar{t}_{gm} = \left[\frac{1}{1+\beta}\left(\frac{s+\beta}{s+\lambda}\right)\right]^m \bar{t}_{go} + \sum_{i=1}^{m} \frac{\lambda}{s+\lambda}\left[\frac{1}{1+\beta}\left(\frac{s+\beta}{s+\lambda}\right)\right]^{m-i} t_{si}^{o} \qquad 4.2.5$$

$$m = 1, 2, \cdots, n$$

$$\bar{t}_{sm} = \frac{1}{(s+\lambda)} t_{sm}^{o} + \frac{\beta}{(1+\beta)^m}\frac{(s+\beta)^{m+1}}{(s+\lambda)^m}\bar{t}_{go} + \beta^2 \sum_{i=1}^{m+1} \frac{(s+\beta)^{m+1-i}}{(1+\beta)^{m+1-i}} \frac{1}{(s+\lambda)^{m+1-i}} t_{si}^{o} \qquad 4.2.6$$

$$m = 1, 2, \cdots, n$$

where $\lambda = \frac{\beta}{1+\beta}$

The impulse response $E(\tau)$ can be found when $t_{go} = \delta(\tau)$ and $t_{so}^{o} = 0$ so that the Laplace transformation of $E(\tau)$, $\bar{E}(s)$, is:

$$\bar{E}(s) = \bar{t}_{gn}(s) = \left[\frac{1}{1+\beta}\left(\frac{s+\beta}{s+\lambda}\right)\right]^n \qquad 4.2.7$$

After expanding $\bar{E}(s)$ into power series of s and from the definition of the moments, the mean and variance can be expressed as:

$$\mu_1 = n \qquad 4.2.8$$

and

$$\sigma^2 = \frac{2n}{\beta} + n \qquad 4.2.9$$

If we define the dimensionless time, $\tau^{(T)}$, based on the total mean residence time, then we have:

$$\tau^{(T)} = \frac{\tau}{n} \qquad 4.2.10$$

$$\bar{E}^{(T)}(s) = \left[\frac{1}{1+\beta}\left(\frac{s/n+\beta}{s/n+\lambda}\right)\right]^n \qquad 4.2.11$$

and

$$\mu_1^{(T)} = 1 \qquad 4.2.12$$

$$\sigma^{2(T)} = \frac{2}{n\beta} + \frac{1}{n} = \frac{\sigma^2}{n^2} \qquad 4.2.13$$

The dimensionless variance is:

$$\sigma_D^2 = \frac{2}{n\beta} + \frac{1}{n} \qquad 4.2.14a$$

or

$$\sigma_D^2 = \frac{2}{\beta_{total}} + \frac{1}{n} = \sigma_{D,fh}^2 + \frac{1}{n} \qquad 4.2.14b$$

where β is the Stanton number of the individual bed as defined in equation 4.2.4, and

$n\beta = \beta_{total} = h \sum_{i=1}^{n} A_i / \dot{m}_g C_{pg}$; $\sigma_{D,fh}^2$ is the contribution to the variance due to film heat transfer resistances and 1/n is the contribution due to effective backmixing of n-well mixed tanks.

Rearranging Equation 4.2.14, we get:

$$\beta = \frac{2}{\sigma_D^2 n - 1} = \frac{2\left(\frac{1}{\sigma_D^2}\right)}{n - \left(\frac{1}{\sigma_D^2}\right)} \qquad 4.2.15$$

and

$$\lambda = \frac{\beta}{1+\beta} = \frac{2}{\sigma_D^2 n + 1} \qquad 4.2.16$$

We have one limiting case here. When $\beta >> 1$, the film heat transfer resistance is very small, $\sigma_{D,fh}^2 \to 0$ and $\sigma_D^2 \to 1/n$, $\lambda \to 1$. For all the other cases, $\sigma_{D,fh}^2 \geq 0$ and $\sigma_D^2 \geq 1/n$ or $1/\sigma_D^2 \leq n$ is the limitation to the dimensionless variance in n-staged fluidized beds regenerators.

The exit gas temperature (m = n) can be found from the inverse Laplace transformation of Equation 4.2.5:

$$t_{gn}(\tau) = \frac{1}{(1+\beta)^n}\left\{t_{go}(\tau) + \sum_{K=1}^{n} \frac{\beta^{2K}}{(1+\beta)^K}\binom{n}{K}\int_0^{\tau} \frac{\theta^{K-1}}{(K-1)!} e^{-\lambda\theta} t_{go}(\tau-\theta)\,d\theta\right\}$$

$$+ \lambda \sum_{i=1}^{n} \frac{t_{si}^{o}}{(1+\beta)^{n-i}} \sum_{K=0}^{n-i} \frac{\beta^{2K}}{(1+\beta)^K}\binom{n-i}{K} \frac{\tau^K}{K!} e^{-\lambda\tau} \qquad 4.2.17$$

The step response is obtained when $t_{go} = 1$ and $t_{si}^{o} = 0$:

$$U(\tau) = \frac{1}{(1+\beta)^n}\left\{1 + \sum_{K=1}^{n} \frac{\beta^{2K}}{(1+\beta)^K}\binom{n}{K}\int_0^{\tau} \frac{\theta^{K-1}}{(K-1)!} e^{-\lambda\theta}\,d\theta\right\} \qquad 4.2.18$$

After integration, we get:

$$U(\tau) = 1 - \frac{1}{(1+\beta)^n} e^{-\lambda\tau} \sum_{K=1}^{n} \binom{n}{K} \beta^K e_{K-1}(\lambda\tau) \qquad 4.2.19$$

where

$$e_K(\tau) = \sum_{j=0}^{K} \frac{\tau^j}{j!} \quad \text{and} \quad e_0(\tau) = 1\,,\ e_K(0) = 1$$

The dimensionless form of thermal efficiency for single pass operation is:

$$\eta_s(\tau_i) = \frac{1}{\tau_i}\int_0^{\tau_i}[1-U(\tau)]\,d\tau \qquad 2.2.7$$

here $\tau_i = \theta_i \Big/ \left[\frac{P_s\, C_{ps}\,(1-\varepsilon)\, V_{single}}{\dot{m}_g\, C_{pg}}\right]$ is the dimensionless switching time based on single volume of a tank. If we choose the dimensionless switching time based on total volume, $\tau_i^{(T)}$, then $\tau_i^{(T)} = \tau_i/n$. After integration, we have the simple expression for $\eta_s(\tau_i)$:

$$\eta_s(\tau_i) = \frac{1}{\tau_i}\gamma(\tau_i) \qquad 4.2.20$$

where

$$\gamma(\tau_i) = n\left[1 - \frac{e^{-\lambda\tau_i}}{n\beta(1+\beta)^{n-1}}\sum_{k=1}^{n}\binom{n}{k}\beta^k \sum_{j=0}^{k-1}\frac{e_j(\lambda\tau_i)}{}\right] \qquad 4.2.21$$

For the limiting case $\beta >> 1$, $\gamma(\tau_i)$ can be expressed as:

$$\gamma(\tau_i) = n\left[1 - \frac{e^{-\tau_i}}{n}\sum_{j=0}^{n-1} e_j(\tau_i)\right] \qquad 4.2.22$$

For periodic operation we will consider cocurrent flow case here and leave the countercurrent flow case for the next chapter. The mathematical model for cocurrent operation is:

(1) Heating period, $0 < \tau < \tau_h$

gas: $$0 = (t_{gm-1} - t_{gm}) - \beta_h(t_{gm} - t_{sm}) \qquad 4.2.23$$

solids: $$\frac{dt_{sm}}{d\tau} = \beta_h(t_{gm} - t_{sm}) \qquad 4.2.24$$

$$\tau = 0, \quad t_{sm} = t_{sm}^{(I)} \qquad 4.2.25a$$

$$m = 1, \quad t_{g0} = H(\tau) \qquad 4.2.25b$$

where

$$\tau=\frac{\theta}{\mu_h}\ ,\quad \beta_h=St_1=\frac{hAi}{\dot{m}_h C_{ph}} \qquad 4.2.26$$

(2) Cooling period, $0 < \tau' < \tau_c$

gas: $$0=(t_{gm-1}-t_{gm})-\beta_c(t_{gm}-t_{sm}) \qquad 4.2.27$$

solids: $$\frac{dt_{sm}}{d\tau'}=\beta_c(t_{gm}-t_{sm}) \qquad 4.2.28$$

$$\tau'=0,\ t_{sm}=t_{sm}^{(II)} \qquad 4.2.29a$$

$$m=1,\ t_{g0}=0 \qquad 4.2.29b$$

where

$$\tau'=\frac{\theta}{\mu_c}\ ,\quad \beta_c=St_2=\frac{hAi}{\dot{m}_c C_{pc}} \qquad 4.2.30$$

with the reversal conditions:

(1) Heating period: $t_{sm}(\tau_h) = t_{sm}^{(II)}$ $\quad m = 1,2,\ldots n$ $\qquad 4.2.31$

(2) Cooling period: $t_{sm}(\tau_c) = t_{sm}^{(I)}$ $\quad m = 1,2,\ldots n$ $\qquad 4.2.32$

For symmetric regenerators we have the symmetry of solid temperature profiles from Equation 2.2.10a:

$$t_{sm}^{(II)} = 1 - t_{sm}^{(I)} \qquad 4.2.33$$

The exit gas temperature for the heating period, from Equation 4.2.17 and 4.2.19, is:

$$t_{gn}(\tau)=1-e^{-\lambda_h\tau}\left\{\frac{1}{(1+\beta_h)^n}\sum_{K=1}^{n}\binom{n}{K}\beta_h^K e_{K-1}(\lambda_h\tau)-\lambda_h\sum_{i=1}^{n}\frac{1}{(1+\beta_h)^{n-i}}\sum_{K=0}^{n-i}\lambda_h^K\beta_h^K\binom{n-i}{K}\frac{\tau^K}{K!}t_{si}^{(I)}\right\} \qquad 4.2.34$$

The solid temperature profile during the heating period can be found from the inverse Laplace transformation of Equation 4.2.6:

$$t_{sm}(\tau)=1+e^{-\lambda_h\tau}\left\{t_{sm}^{(I)}+\lambda_h^2\sum_{i=1}^{m-1}\frac{1}{(1+\beta_h)^{m-i}}\sum_{k=0}^{m-1-i}\binom{m-1-i}{k}\lambda_h^k\beta_h^k\frac{\tau^{k+1}}{(k+1)!}t_{si}^{(I)}\right.$$

$$\left.-\frac{1}{(1+\beta_h)^{m-1}}\sum_{k=0}^{m-1}\binom{m-1}{k}\beta_h^k e_k(\lambda_h\tau)\right\}\qquad m=1,2,\cdots,n \qquad 4.2.35$$

The exit gas temperature for the cooling period when t_{go} = 0 is:

$$t_{gn}(\tau')=\lambda_c\sum_{i=1}^{n}\frac{1}{(1+\beta_c)^{n-i}}\sum_{k=0}^{n-i}\lambda_c^k\beta_c^k\binom{n-i}{k}\frac{\tau'^k e^{-\lambda_c\tau'}}{k!}t_{si}^{(II)} \qquad 4.2.36$$

The solid temperature profile during the cooling period can be expressed as:

$$t_{sm}(\tau')=e^{-\lambda_c\tau'}\left\{t_{sm}^{(II)}+\lambda_c^2\sum_{i=1}^{m-1}\frac{1}{(1+\beta_c)^{m-i}}\sum_{k=0}^{m-1-i}\binom{m-1-i}{k}\lambda_c^k\beta_c^k\frac{\tau'^{k+1}}{(k+1)!}t_{si}^{(II)}\right\} \qquad 4.2.37$$

$$m=1,2,\cdots,n$$

4.2.1 Principle of Superposition for n-Staged Fluidized Beds Model

(a) Equal Product of Mass Flow Rate and Specific Heat - Symmetric Regenerators

The dimensionless input in cocurrent operation is:

$$t_{go}(\tau)=t_{in}(\tau)=\sum_{j=0}^{\infty}\left[H(\tau-2j\tau_i)-H(\tau-(2j+1)\tau_i)\right] \qquad 4.1.2b$$

For symmetric regenerators, we have $\tau_h = \tau_c = \tau_i$.

The dimensionless output by appling the superposition principle is:

$$t_{gn}(\tau)=t_{ex}(\tau)=\sum_{j=0}^{\infty}\left[U(\tau-2j\tau_i)H(\tau-2j\tau_i)-U(\tau-(2j+1)\tau_i)H(\tau-(2j+1)\tau_i)\right] \qquad 4.1.3b$$

Here $u(\tau)$ is the step response to either heating or cooling period and is expressed in equation 4.2.19.

The dimensionless form of the thermal efficiency for the heating period is then:

$$\eta_h(\tau_i) = \frac{1}{\tau_i} \int_{2L\tau_i}^{(2L+1)\tau_i} [t_{go}(\tau) - t_{gn}(\tau)] d\tau \qquad 4.1.4b$$

where L is the number large enough so that stationary state is reached. After several manipulations (see Appendix D), we get:

$$\eta_h(\tau_i) = \frac{1}{\tau_i} \left\{ \gamma(\tau_i) - \sum_{i=1}^{L} [2\gamma(2i\tau_i) - \gamma((2i+1)\tau_i) - \gamma((2i-1)\tau_i)] \right\} \qquad 4.2.38$$

where $\gamma(\tau_i)$ is defined by Equation 4.2.21 and 4.2.22.

The results of the thermal efficiency as a function of $1/\sigma_D^2$ are shown in Figure 4.5 and are almost the same as those from the approximate solutions, Figure 4.2, except for the cases $1/\sigma_D^2 < 5.0$ (short regenerators) where the maximal deviation is about 20%.

Again, L is determined from the convergence criterion in the summation. L is large for small $1/\sigma_D^2$ values and short switching times but is small for large $1/\sigma_D^2$ values and long switching times.

The variations between these two methods for small $1/\sigma_D^2$ cases can be caused by the following reasons:

1. The errors in the approximate solution which neglects the effect of the skewness of the impulse response curve on efficiency. However, the skewness may be important for short regenerators.
2. The deviation of the n-staged fluidized bed model from the real continuous packed bed heat regenerator model.

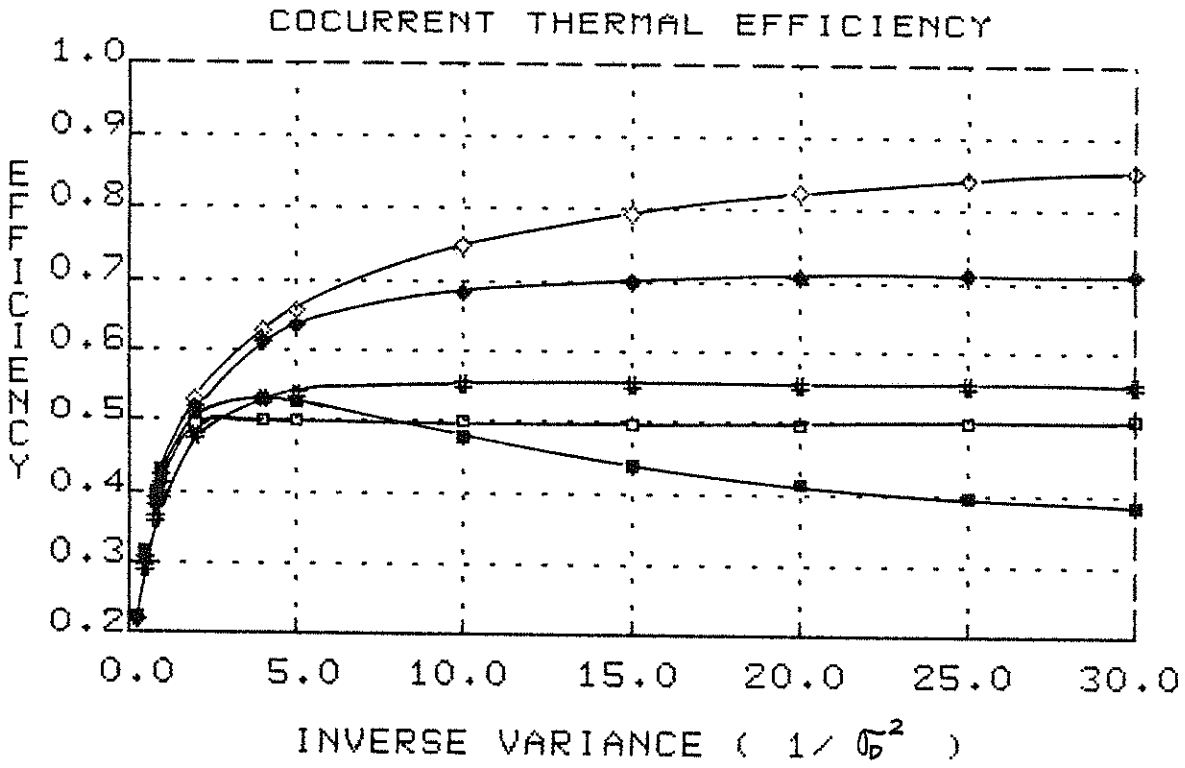

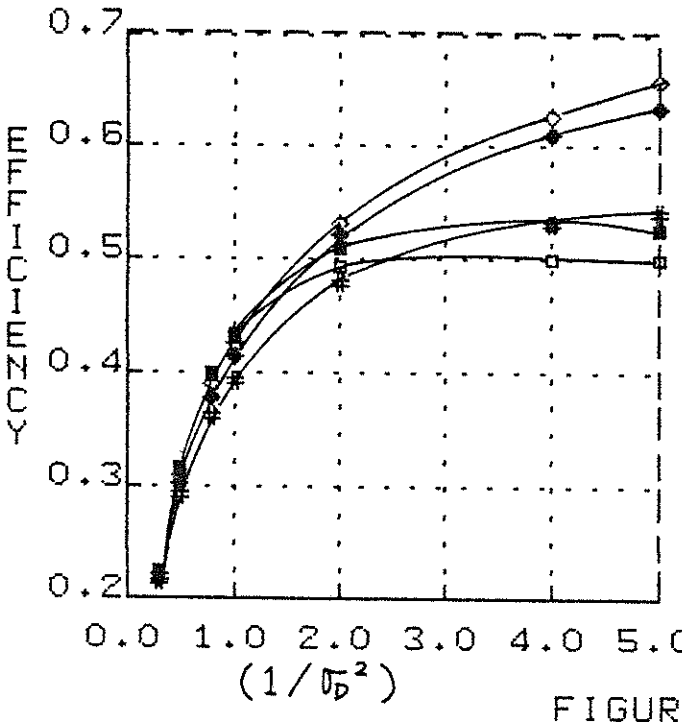

$\tau_h = \tau_c = \tau_i$

□	:	0.2
■	:	0.6
◇	:	1.0
◆	:	1.4
#	:	1.8

FIGURE 4.5

THERMAL EFFICIENCIES OF COCURRENT OPERATION
——30-STAGES FLUIDIZED BED APPROACH
USING THE PRINCIPLE OF SUPERPOSITION .
SYMMETRIC CASE

(b) Unequal Product of Mass Flow Rate and Specific Heat - Unbalanced Regenerators

As mentioned before the dimensionless input for "unequal product of $\dot{m}C_p$" cases is:

$$t_{in}(\tau)=\sum_{j=0}^{\infty}\left[H(\tau-j\tau_p)-H(\tau-j\tau_p-\tau_h)\right] \qquad 4.1.1b$$

and the dimensionless output is then:

$$t_{ex}(\tau)=\sum_{j=0}^{\infty}\left[u_h(\tau-j\tau_p)H(\tau-j\tau_p)-u_c(\tau-j\tau_p-\tau_h)H(\tau-j\tau_p-\tau_h)\right] \qquad 4.1.7$$

where $\tau_p = \tau_h + \tau_c = \tau_h\ (1 + \mu_h/\mu_c) = \tau_c\ (1 + \mu_c/\mu_h)$ and $u_h(\tau)$ and $u_c(\tau)$ are the step response for the heating and cooling periods, respectively. From Equation 4.2.19, we have:

$$u_h(\tau)=1-\frac{1}{(1+\beta_h)^n}e^{-\lambda_h\tau}\sum_{K=1}^{n}\binom{n}{K}\beta_h^K e_{K-1}(\lambda_h\tau) \qquad 4.2.39$$

$$u_c(\tau)=1-\frac{1}{(1+\beta_c)^n}e^{-\lambda_c\tau}\sum_{K=1}^{n}\binom{n}{K}\beta_c^K e_{K-1}(\lambda_c\tau) \qquad 4.2.40$$

The thermal efficiency of the heating period is defined as:

$$\eta_h(\tau_h)=\frac{1}{\tau_h}\int_{L\tau_p}^{L\tau_p+\tau_h}\left[t_{in}(\tau)-t_{ex}(\tau)\right]d\tau \qquad 4.1.8$$

After similar manipulations as before (see Appendix E), we get:

$$\eta_h(\tau_h)=\frac{1}{\tau_h}\left\{\gamma_h(\tau_h)-\sum_{i=1}^{L}\left[\gamma_h(i\tau_p)+\gamma_c(i\tau_p)-\gamma_h(i\tau_p+\tau_h)-\gamma_c(i\tau_p-\tau_h)\right]\right\} \qquad 4.2.41$$

where

$$\gamma_h(\tau_h)=n\left[1-\frac{e^{-\lambda_h\tau_h}}{n\beta_h(1+\beta_h)^{n-1}}\sum_{K=1}^{n}\binom{n}{K}\beta_h^K\sum_{j=0}^{K-1}e_j(\lambda_h\tau_h)\right] \qquad 4.2.42$$

$$\gamma_c(\tau_c)=n\left[1-\frac{e^{-\lambda_c\tau_c}}{n\beta_c(1+\beta_c)^{n-1}}\sum_{K=1}^{n}\binom{n}{K}\beta_c^K\sum_{j=0}^{K-1}e_j(\lambda_c\tau_c)\right] \qquad 4.2.43$$

and for the limiting cases $\beta_h >> 1$ and $\beta_c >> 1$.

$$\gamma_h(\tau_h) = n\left[1 - \frac{e^{-\tau_h}}{n}\sum_{j=0}^{n-1} e_j(\tau_h)\right] \qquad 4.2.44$$

$$\gamma_c(\tau_c) = n\left[1 - \frac{e^{-\tau_c}}{n}\sum_{j=0}^{n-1} e_j(\tau_c)\right] \qquad 4.2.45$$

The dimensionless inverse variance of the cooling period ($1/\sigma_{D,c}^2$) can be calculated from Equation 4.2.15 once we choose the dimensionless inverse variance of the heating period ($1/\sigma_{D,h}^2$) and the ratio of mass flow rates (or μ_h/μ_c). The correspondence of $1/\sigma_{D,h}^2$ and $1/\sigma_{D,c}^2$ for the case of 30-stages is the same as given in Table 4.1a and Table 4.1b for $\mu_h/\mu_c = 0.5$ and $\mu_h/\mu_c = 2.0$, respectively.

The results of the overall thermal efficiency η_o as a function of $1/\sigma_{D,h}^2$ for different switching times are shown in Figure 4.6a and 4.6b for $\mu_h/\mu_c = 0.5$ and $\mu_h/\mu_c = 2.0$, respectively. Except for very short regenerators ($1/\sigma_{D,h}^2 < 5.0$) results are almost the same for both methods with maximum deviation not exceeding 1%. The maximal deviation for small $1/\sigma_D^2$ cases is about 10% for both $\mu_h/\mu_c = 0.5$ and $\mu_h/\mu_c = 2.0$ cases.

4.2.2 Closed Methods for the n-staged Fluidized Beds Model

(a) Equal Product of Mass Flow Rate and Specific Heat - Symmetric Regenerators

For the symmetric case we can take the advantage of the symmetry of solid temperature profiles as described before, Equation 4.2.33. The solid temperature profile at the end of heating period ($\tau = \tau_i$), from Equation 4.2.35, is:

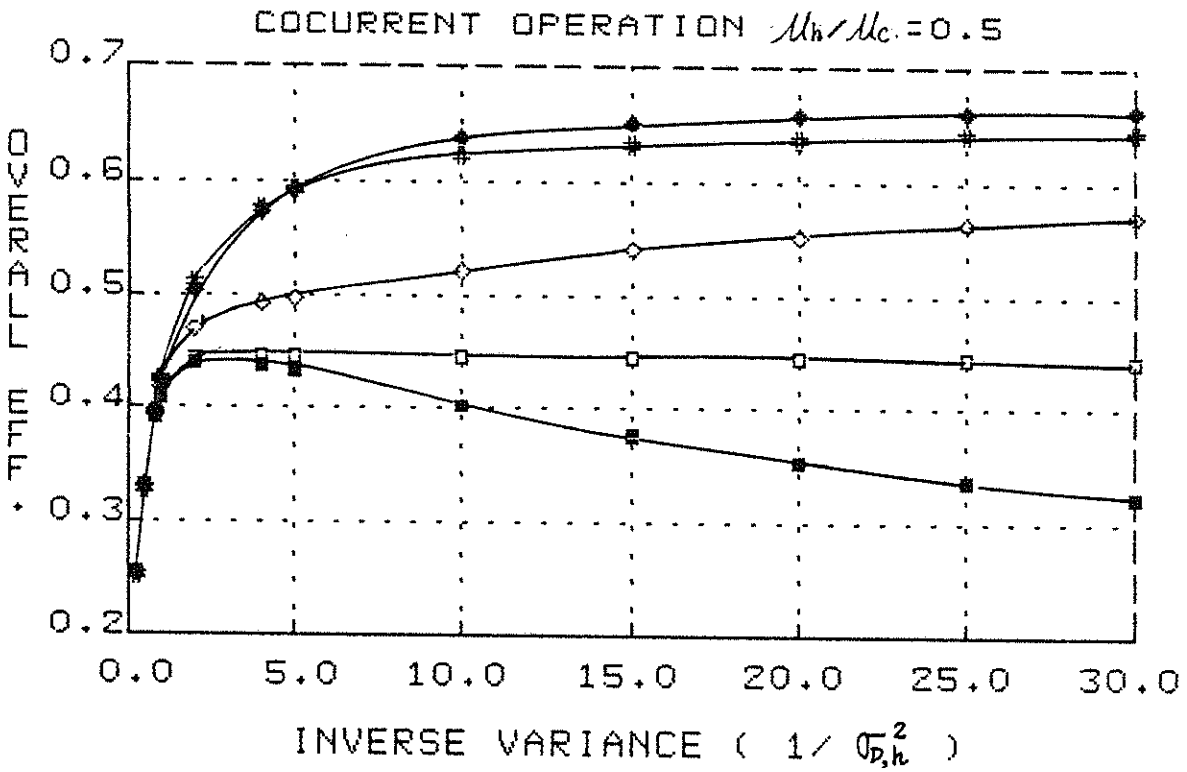

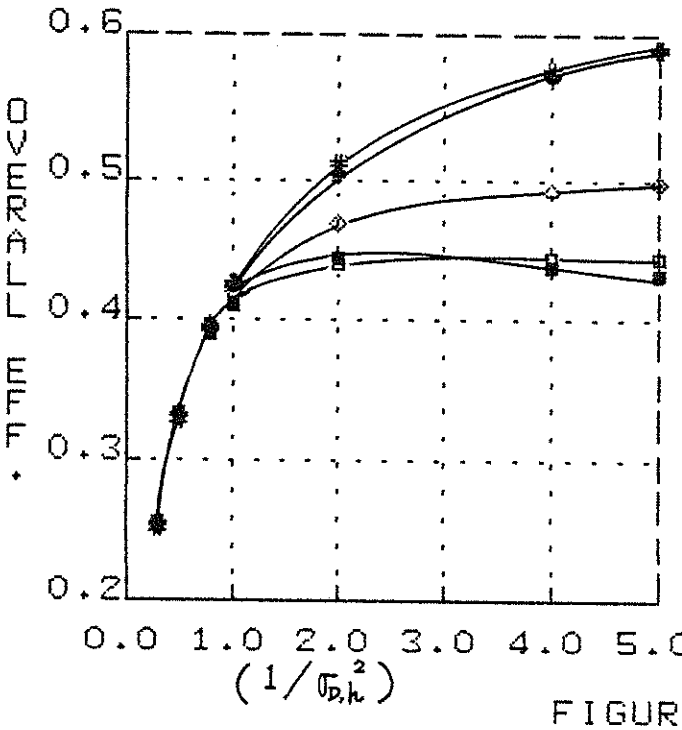

	τ_h	τ_c
□ :	0.2	0.1
■ :	0.6	0.3
◇ :	1.0	0.5
◆ :	1.4	0.7
✱ :	1.8	0.9

FIGURE 4.6a

THERMAL EFFICIENCIES OF COCURRENT OPERATION
——30-STAGES FLUIDIZED BED APPROACH
USING THE PRINCIPLE OF SUPERPOSITION ,
UNBALANCED CASE ($M_h/M_c=0.5$)

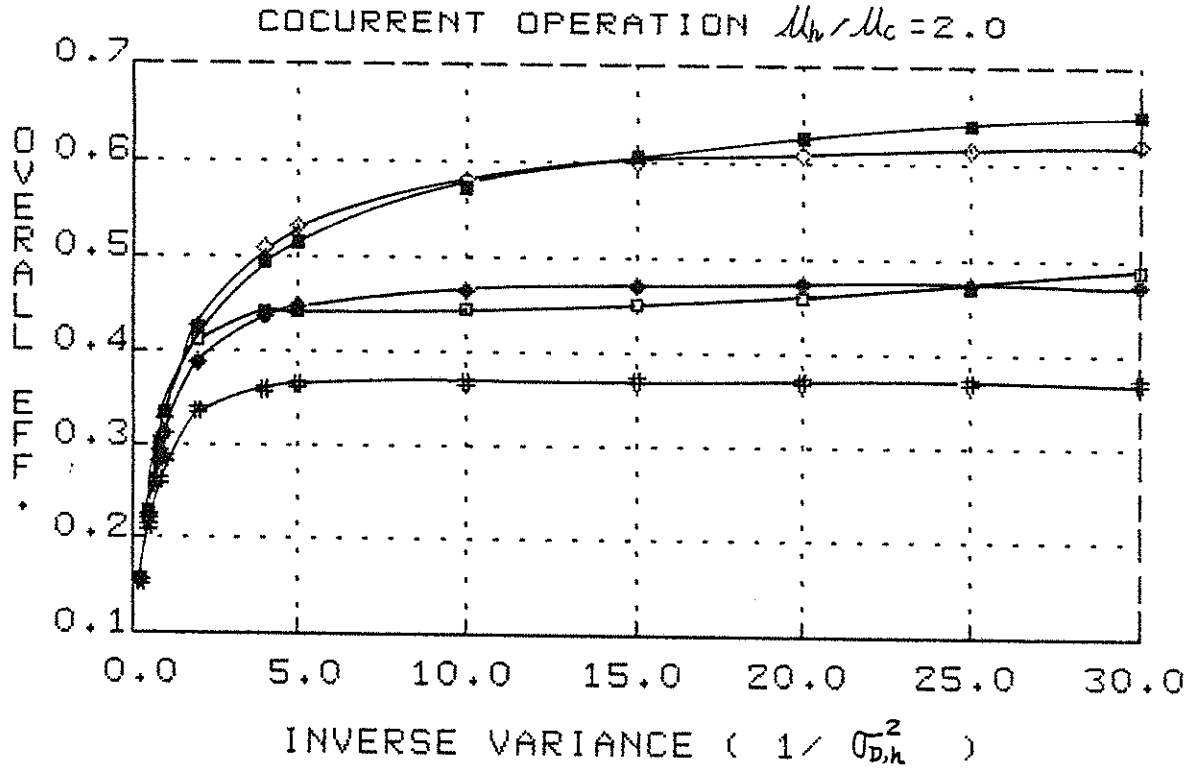

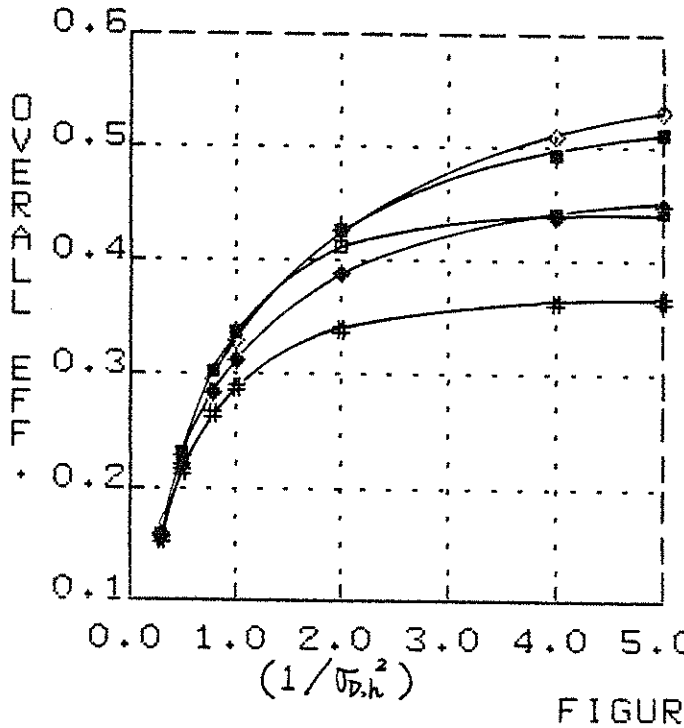

	τ_h , τ_c
□ :	0.2 , 0.4
■ :	0.6 , 1.2
◇ :	1.0 , 2.0
◆ :	1.4 , 2.8
# :	1.8 , 3.6

FIGURE 4.6b

THERMAL EFFICIENCIES OF COCURRENT OPERATION
——30-STAGES FLUIDIZED BED APPROACH
USING THE PRINCIPLE OF SUPERPOSITION ,
UNBALANCED CASE ($\mu_h/\mu_c = 2.0$)

$$t_{sm}(\tau_i) = 1 + e^{-\lambda\tau_i}\left\{t_{sm}^{(I)} + \lambda^2 \sum_{i=1}^{m-1} \frac{1}{(1+\beta)^{m-1-i}} \sum_{K=0}^{m-1-i} \binom{m-1-i}{K} \lambda^K \beta^K \frac{\tau_i^{K+1}}{(K+1)!} t_{si}^{(I)} \right.$$

$$\left. - \frac{1}{(1+\beta)^{m-1}} \sum_{K=0}^{m-1} \binom{m-1}{K} \beta^K e_K(\lambda\tau_i)\right\} \qquad m = 1, 2, \cdots, n \qquad 4.2.46$$

The reversal condition, Equations 4.2.31, and the property of symmetry, Equation 4.2.33, tells us:

$$t_{sm}^{(II)} = t_{sm}(\tau_i) = 1 - t_{sm}^{(I)}$$

$$= 1 + e^{-\lambda\tau_i}\left\{t_{sm}^{(I)} + \lambda^2 \sum_{i=1}^{m-1} \frac{1}{(1+\beta)^{m-1-i}} \sum_{K=0}^{m-1-i} \binom{m-1-i}{K} \lambda^K \beta^K \frac{\tau_i^{K+1}}{(K+1)!} t_{si}^{(I)} \right.$$

$$\left. - \frac{1}{(1+\beta)^{m-1}} \sum_{K=0}^{m-1} \binom{m-1}{K} \beta^K e_K(\lambda\tau_i)\right\} \qquad m = 1, 2, \cdots, n \qquad 4.2.47$$

Rearranging into matrix form, we have:

$$\begin{bmatrix} (1+e^{\lambda\tau_i}) & & & \\ \lambda^2\tau_i & & 0 & \\ (m=3) & & & \\ (m=n) & \cdots\cdots & (m=3)\ \lambda^2\tau_i & (1+e^{\lambda\tau_i}) \end{bmatrix} \begin{bmatrix} t_{s1}^{(I)} \\ t_{s2}^{(I)} \\ \vdots \\ t_{sn}^{(I)} \end{bmatrix} = \begin{bmatrix} (m=1) \\ (m=2) \\ \vdots \\ (m=n) \end{bmatrix}$$

$$\lambda^2 \frac{1}{(1+\beta)^{m-2}} \sum_{K=0}^{m-2} \binom{m-2}{K} \lambda^K \beta^K \frac{\tau_i^{K+1}}{(K+1)!} \qquad \frac{1}{(1+\beta)^{m-1}} \sum_{K=0}^{m-1} \binom{m-1}{K} \beta^K e_K(\lambda\tau_i) \qquad 4.2.48$$

Using forward substitution, we can readily solve for the solid temperature profiles, $t_{sm}^{(I)}$ and $t_{sm}^{(II)}$ (m:1~n).

The dimensionless form of the thermal efficiency of the heating period is given as:

$$\eta_h(\tau_i)=\frac{1}{\tau_i}\int_0^{\tau_i}[1-t_{gn}(\tau)]d\tau \qquad 2.2.7$$

where $t_{gn}(\tau)$ is the exit temperature as expressed in Equation 4.2.34. After integration, we get:

$$\eta_h(\tau_i)=\frac{1}{\tau_i}\gamma(\tau_i)+\frac{1}{\tau_i}\sum_{i=1}^{n}\frac{t_{si}^{(I)}}{(1+\beta)^{n-i}}\sum_{K=0}^{n-i}\binom{n-i}{K}\beta^K e^{-\lambda\tau_i}e_K(\lambda\tau_i)$$

$$-\frac{1}{\tau_i}\sum_{i=1}^{n}t_{si}^{(I)} \qquad 4.2.49$$

where $t_{si}^{(I)}$ (i:1~n) can be solved from Equation 4.2.48 and $\gamma(\tau_i)$ is defined in Equation 4.2.21.

For the limiting case $\beta >> 1$ Equation 4.2.48 can be changed to:

$$\begin{bmatrix} (He^{\tau_i}) & & & \\ \tau_i & & 0 & \\ (m=3) & & & \\ (m=n)- & ---- & (m=3)\ \tau_i & (He^{\tau_i}) \end{bmatrix}\begin{bmatrix} t_{s1}^{(I)} \\ t_{s2}^{(I)} \\ \\ t_{sn}^{(I)} \end{bmatrix}=\begin{bmatrix} (m=1) \\ (m=2) \\ \\ (m=n) \end{bmatrix}$$

$$\frac{\tau_i^{m-1}}{(m-1)!} \qquad e_{m-1}(\tau_i) \qquad 4.2.50$$

and

$$\eta_h(\tau_i) = \frac{1}{\tau_i}\gamma(\tau_i) + \frac{1}{\tau_i}\sum_{i=1}^{n} t_{si}^{(I)} e^{-\tau_i} e_{n-i}(\tau_i) - \frac{1}{\tau_i}\sum_{i=1}^{n} t_{si}^{(I)} \qquad 4.2.51$$

where $\gamma(\tau_i)$ is defined in Equation 4.2.22.

The results for the solid temperature profiles for different values of $1/\sigma_D^2$ for different switching times are shown in Figure 4.7. Here we have a pair of profiles for each $1/\sigma_D^2$ case : one is the profile before the heating period, the other after the heating period. The profile before the heating period can be identified always at the utmost left position of Figure 4.7 as the lower one of the two. The two profiles are clearly symmetric w.r.t. the central line.

The exit gas temperature profiles and the thermal efficiencies can be readily calculated from Equation 4.2.34 and Equation 4.2.49, respectively, once we find the solid temperature profile before the heating period, and the results are shown in Figure 4.8 and 4.9, respectively. It can be seen that the average temperature for different switching times goes down first until $\tau_i \simeq 1.0$ and then rises again. This is the reason why we have the highest efficiency at $\tau_i \simeq 1.0$.

Needless to say, both the method of superposition and the closed method generate the same answer for thermal efficiency within 1%.

(b) Unequal Product of Mass Flow Rate and Specific Heat - Unbalanced Regenerators

For the asymmetric case it is necessary to solve for the solid temperature profiles at the beginning and at the end of the heating

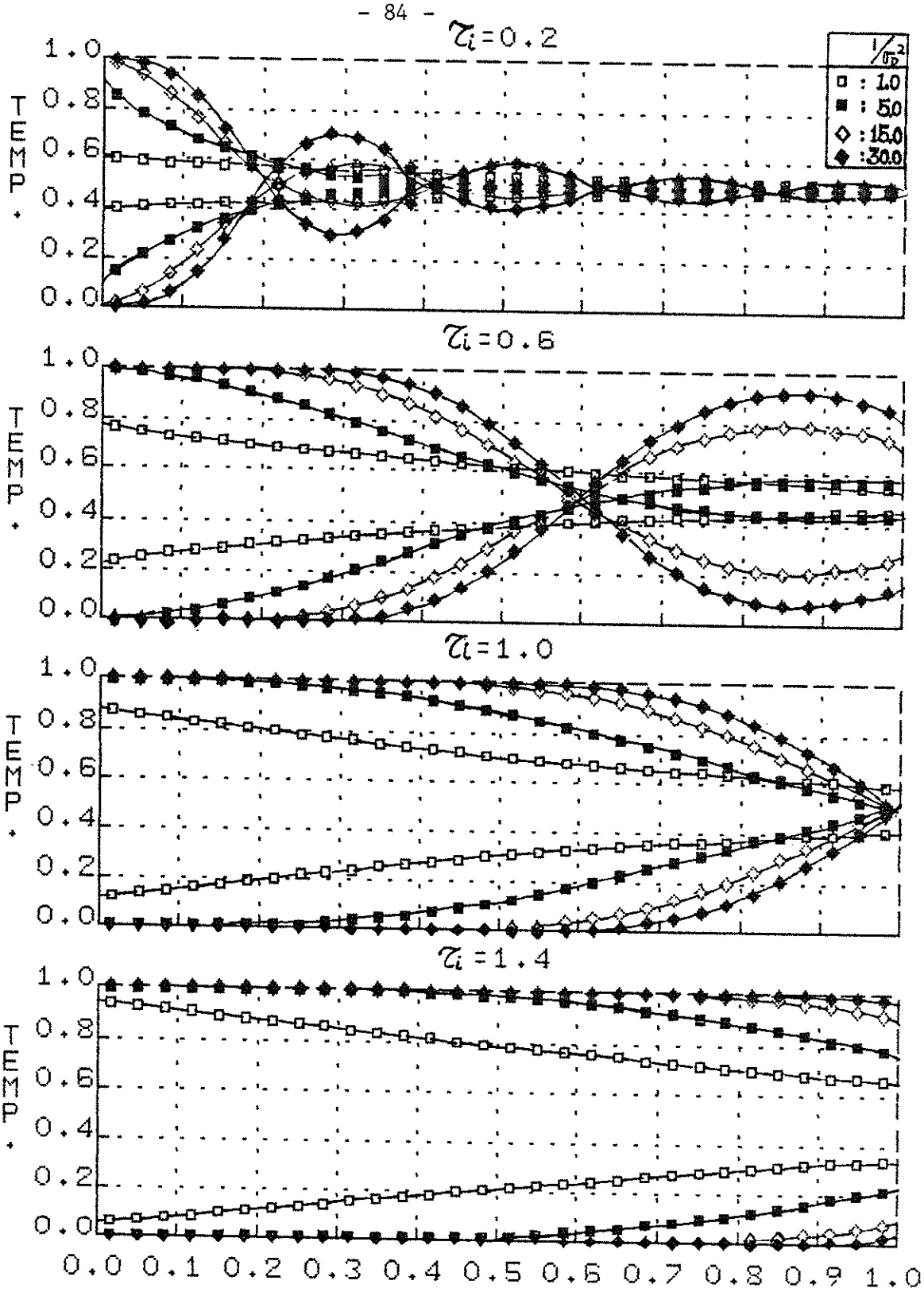

FIGURE 4.7

SOLID TEMPERATURE PROFILES OF COCURRENT OPERATION
——SYMMETRIC CASE

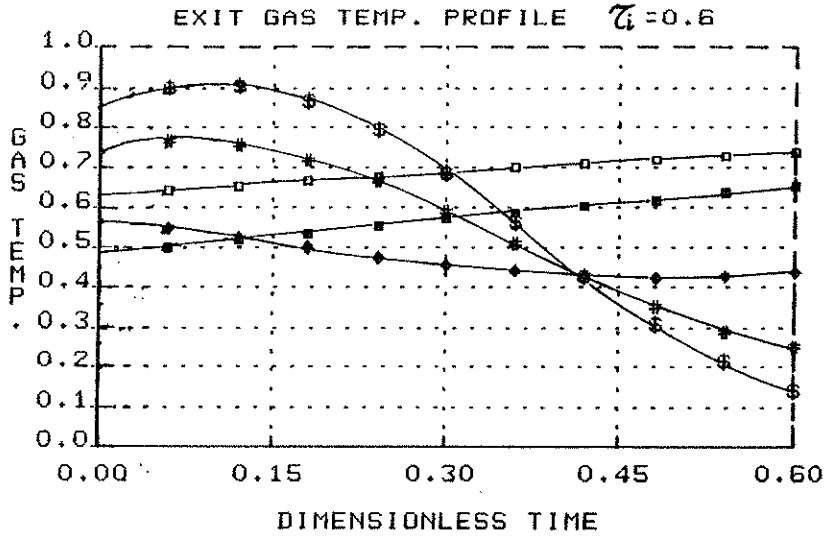

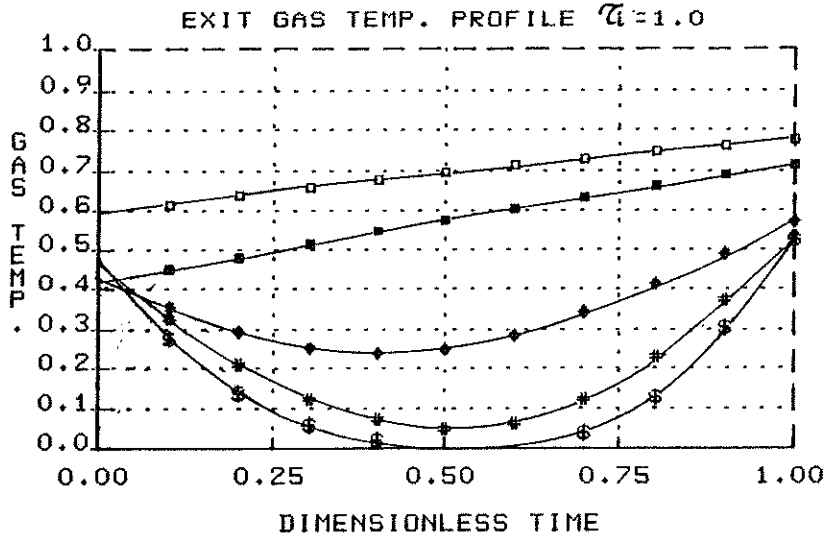

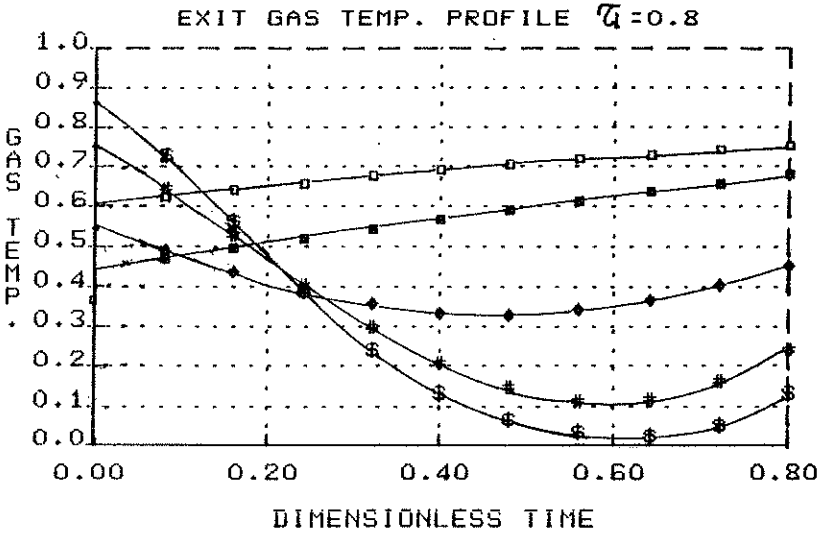

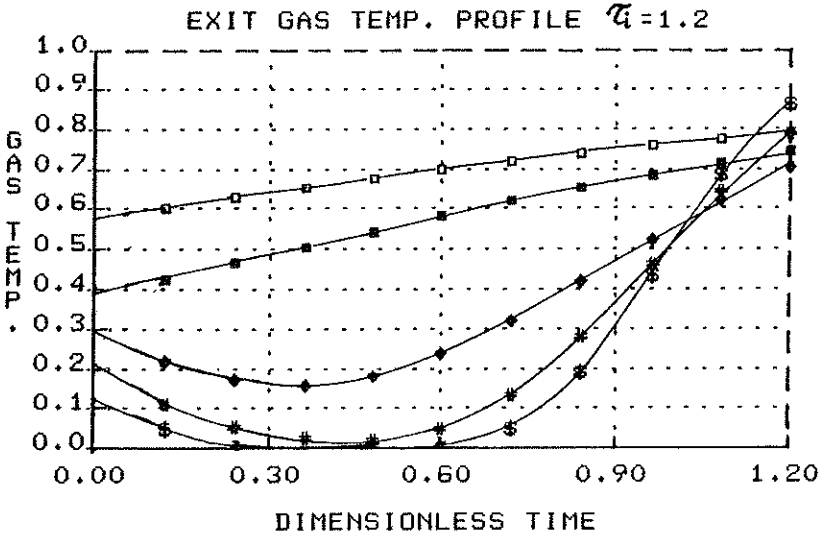

$1/\tau_p^2$: □—0.5 ♦—5.0 $—30.0
■—1.0 #—15.0

FIGURE 4.8a

EXIT GAS TEMP. PROFILES OF COCURRENT OPERATION (HEATING PERIOD) —SYMMETRIC CASE

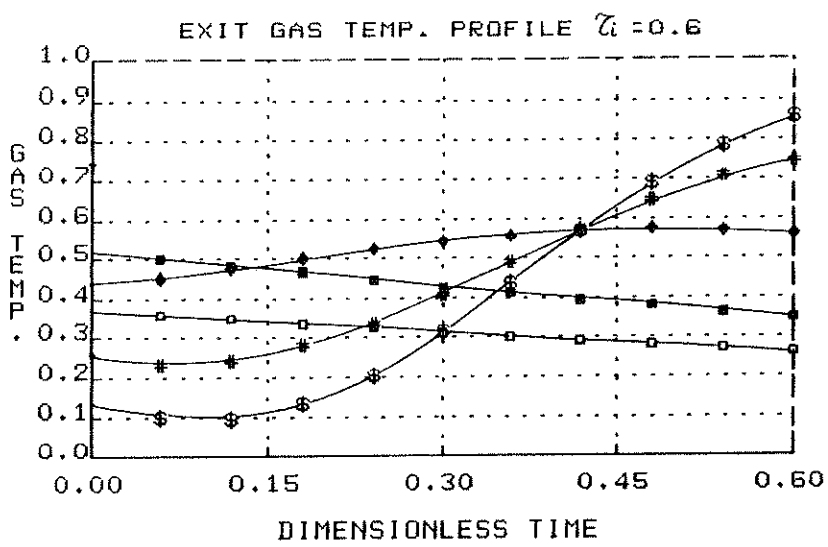

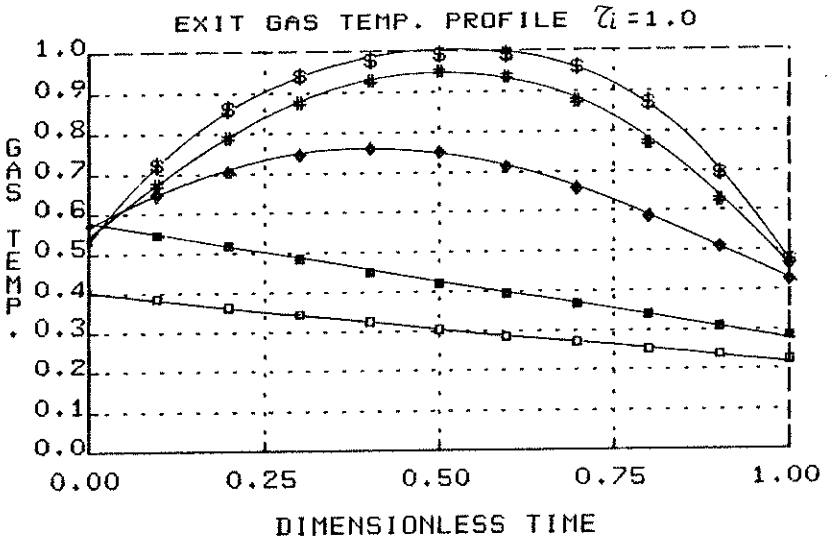

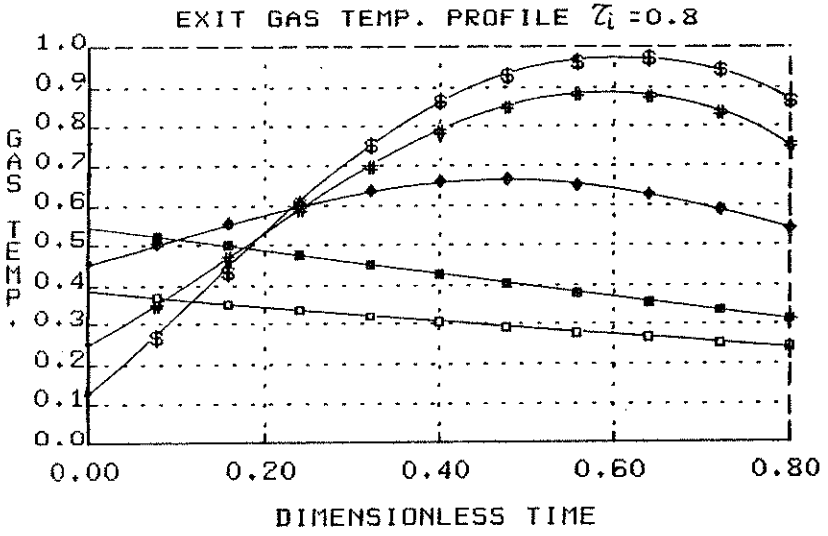

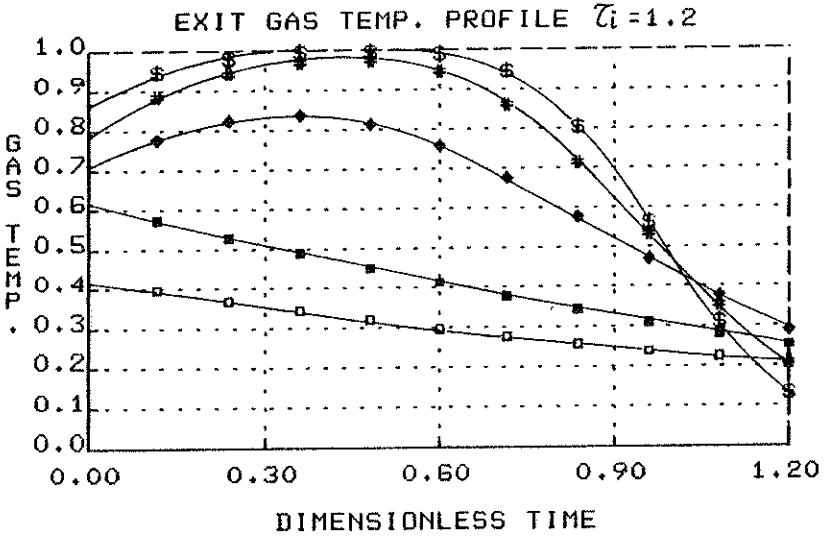

$1/\beta_b^2$: □ — 0.5 ♦ — 5.0 $ — 30.0
■ — 1.0 # — 15.0

FIGURE 4.8 b

EXIT GAS TEMP. PROFILES OF COCURRENT OPERATION (COOLING PERIOD) —— SYMMETRIC CASE

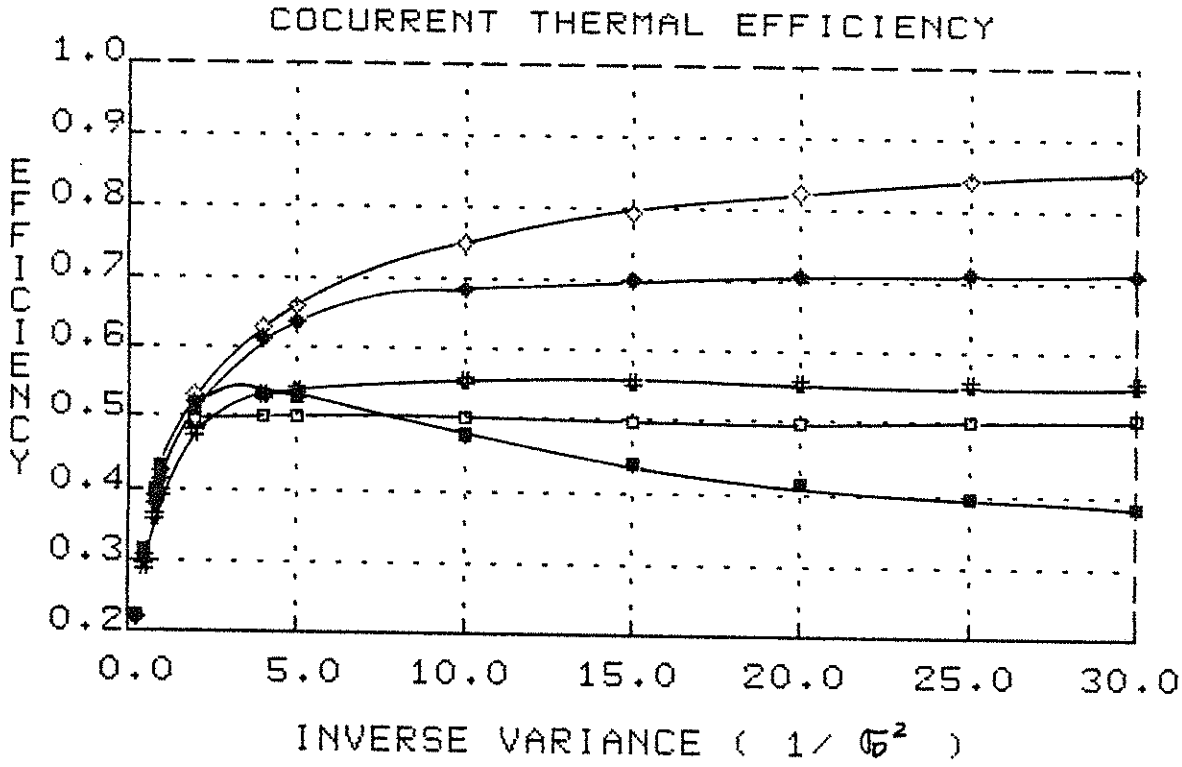

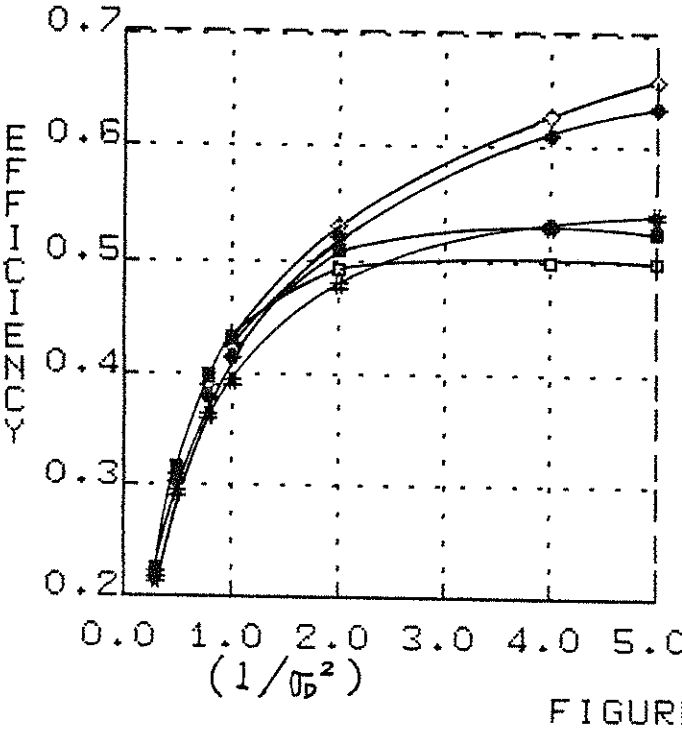

$\tau_h = \tau_c = \tau_i$

- □ : 0.2
- ■ : 0.6
- ◇ : 1.0
- ◆ : 1.4
- # : 1.8

FIGURE 4.9

THERMAL EFFICIENCIES OF COCURRENT OPERATION
——30-STAGES FLUIDIZED BED APPROACH
USING THE CLOSED METHOD ,
SYMMETRIC CASE

period, $t_{sm}^{(I)}$ and $t_{sm}^{(II)}$, without the symmetric property. From the solid temperature profile at the end of heating period, Equation 4.2.35, and the reversal condition, Equation 4.2.31, we get:

$$t_{sm}^{(II)} = t_{sm}(\tau_h) = 1 + e^{-\lambda_h \tau_h}\left\{ t_{sm}^{(I)} + \lambda_h^2 \sum_{i=1}^{m-1} \frac{1}{(1+\beta_h)^{m-i}} \sum_{K=0}^{m-1-i} \binom{m-1-i}{K} \lambda_h^K \beta_h^K \frac{\tau_h^{K+1}}{(K+1)!} t_{si}^{(I)} \right.$$

$$\left. - \frac{1}{(1+\beta_h)^{m-1}} \sum_{K=0}^{m-1} \binom{m-1}{K} \beta_h^K e_K(\lambda_h \tau_h) \right\} \qquad m = 1, 2, ---, n \qquad 4.2.52$$

For the limiting case $\beta_h >> 1$

$$t_{sm}^{(II)} = t_{sm}(\tau_h) = 1 + e^{-\tau_h}\left\{ t_{sm}^{(I)} + \sum_{i=1}^{m-1} \frac{\tau_h^{m-i}}{(m-i)!} t_{si}^{(I)} - e_{m-1}(\tau_h) \right\}$$

$$m = 1, 2, ---, n \qquad 4.2.53$$

The solid temperature profile at the end of the cooling period, $\tau' = \tau_c$ in Equation 4.2.37, and the reversal condition, Equation 4.2.32, tell us:

$$t_{sm}^{(I)} = t_{sm}(\tau_c) = e^{-\lambda_c \tau_c}\left\{ t_{sm}^{(II)} + \lambda_c^2 \sum_{i=1}^{m-1} \frac{1}{(1+\beta_c)^{m-i}} \sum_{K=0}^{m-1-i} \binom{m-1-i}{K} \lambda_c^K \beta_e^K \frac{\tau_c^{K+1}}{(K+1)!} t_{si}^{(II)} \right\}$$

$$m = 1, 2, ---, n \qquad 4.2.54$$

here $\tau_c = \theta_i / \mu_c = \tau_h \left(\frac{\mu_h}{\mu_c}\right)$.

For the limiting case $\beta_c >> 1$:

$$t_{sm}^{(I)} = t_{sm}(\tau_c) = e^{-\tau_c}\left\{t_{sm}^{(II)} + \sum_{i=1}^{m-1} \frac{\tau_c^{m-i}}{(m-i)!} t_{si}^{(II)}\right\}$$

$$m = 1, 2, \cdots, n \qquad 4.2.55$$

So we can solve for $t_{sm}^{(I)}$ and $t_{sm}^{(II)}$ from Equations 4.2.52 to 4.2.55 by either successive substitution or using some methods of acceleration.

The thermal efficiency can then be found from:

$$\eta_h(\tau_h) = \frac{1}{\tau_h}\gamma(\tau_h) + \frac{1}{\tau_h}\sum_{i=1}^{n} \frac{t_{si}^{(I)}}{(1+\beta_h)^{n-i}} \sum_{k=0}^{n-i} \binom{n-i}{k} \beta_h^k e^{-\lambda_h \tau_h} e_k(\lambda_h \tau_h)$$

$$- \frac{1}{\tau_h}\sum_{i=1}^{n} t_{si}^{(I)} \qquad 4.2.56$$

For the limiting case $\beta_h >> 1$:

$$\eta_h(\tau_h) = \frac{1}{\tau_h}\gamma(\tau_h) + \frac{1}{\tau_h}\sum_{i=1}^{n} t_{si}^{(I)} e^{-\tau_h} e_{n-i}(\tau_h) - \frac{1}{\tau_h}\sum_{i=1}^{n} t_{si}^{(I)} \qquad 4.2.57$$

The results of the solid temperature profiles and the thermal efficiencies are shown in Figures 4.10, 4.11 and Figures 4.12, 4.13 for the cases of $\mu_h/\mu_c = 0.5$ and $\mu_h/\mu_c = 2.0$, respectively. It can be seen that the solid temperature profiles are no longer symmetric with respect to the central line and the results are just the same (within 1%) as those obtained from the method of superposition.

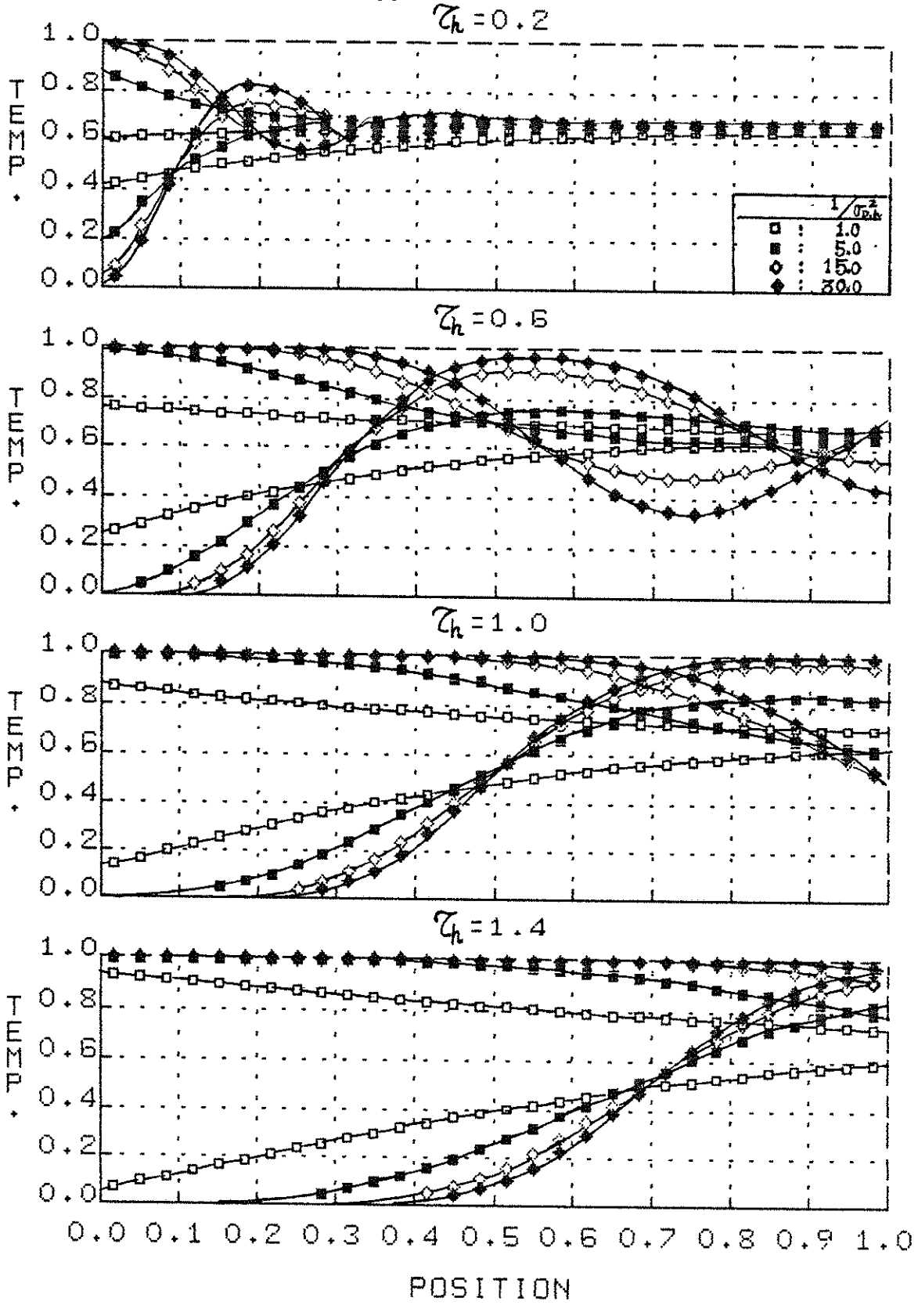

FIGURE 4.10

SOLID TEMPERATURE PROFILES OF COCURRENT OPERATION
——UNBALANCED CASE (M_h/M_c = 0.5)

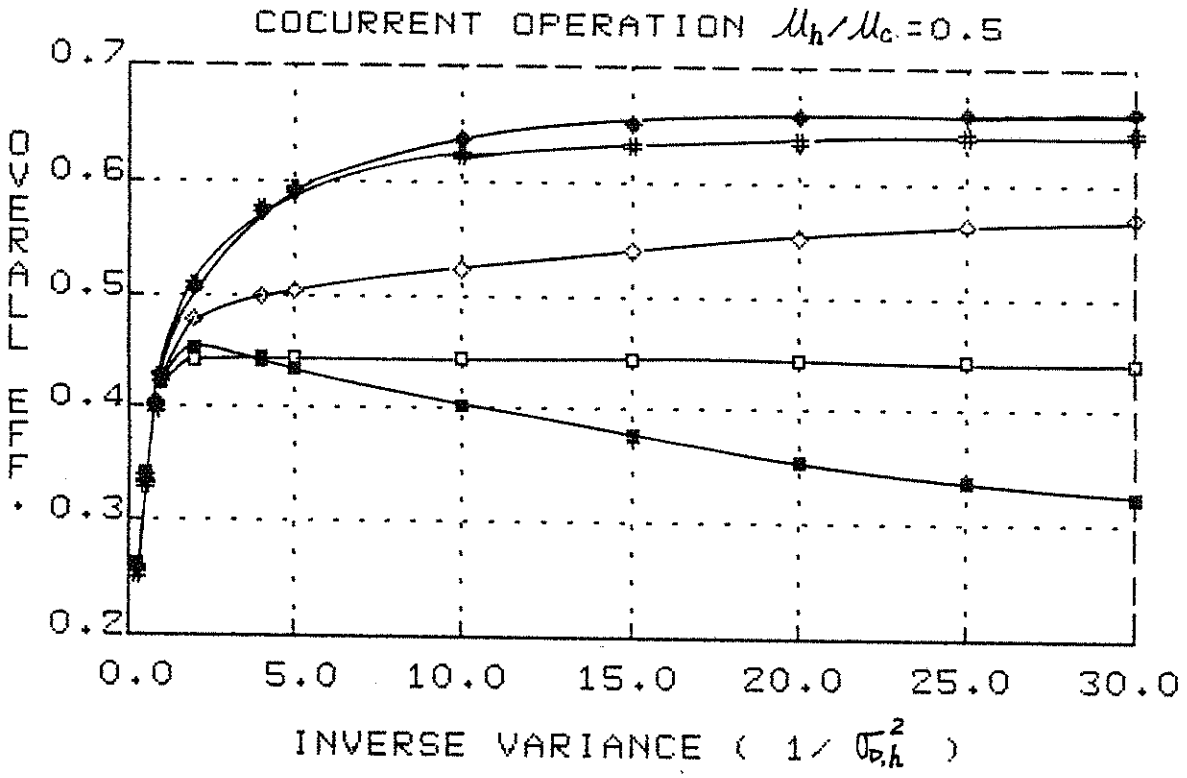

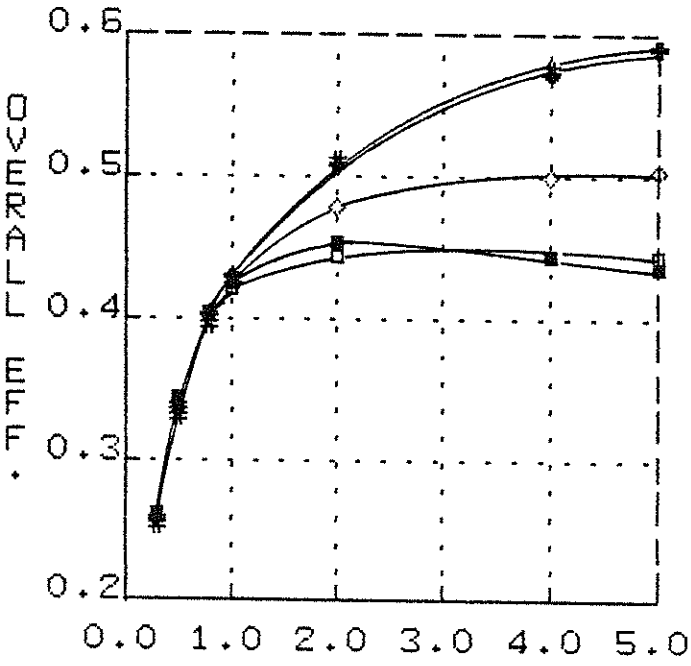

	τ_h	τ_c
□ :	0.2	0.1
■ :	0.6	0.3
◇ :	1.0	0.5
◆ :	1.4	0.7
# :	1.8	0.9

FIGURE 4.11

THERMAL EFFICIENCHES OF COCURRENT OPERATION
——30-STAGES FLUIDIZED BED APPROACH
USING THE CLOSED METHOD ,
UNBALANCED CASE ($M_h/M_c=0.5$)

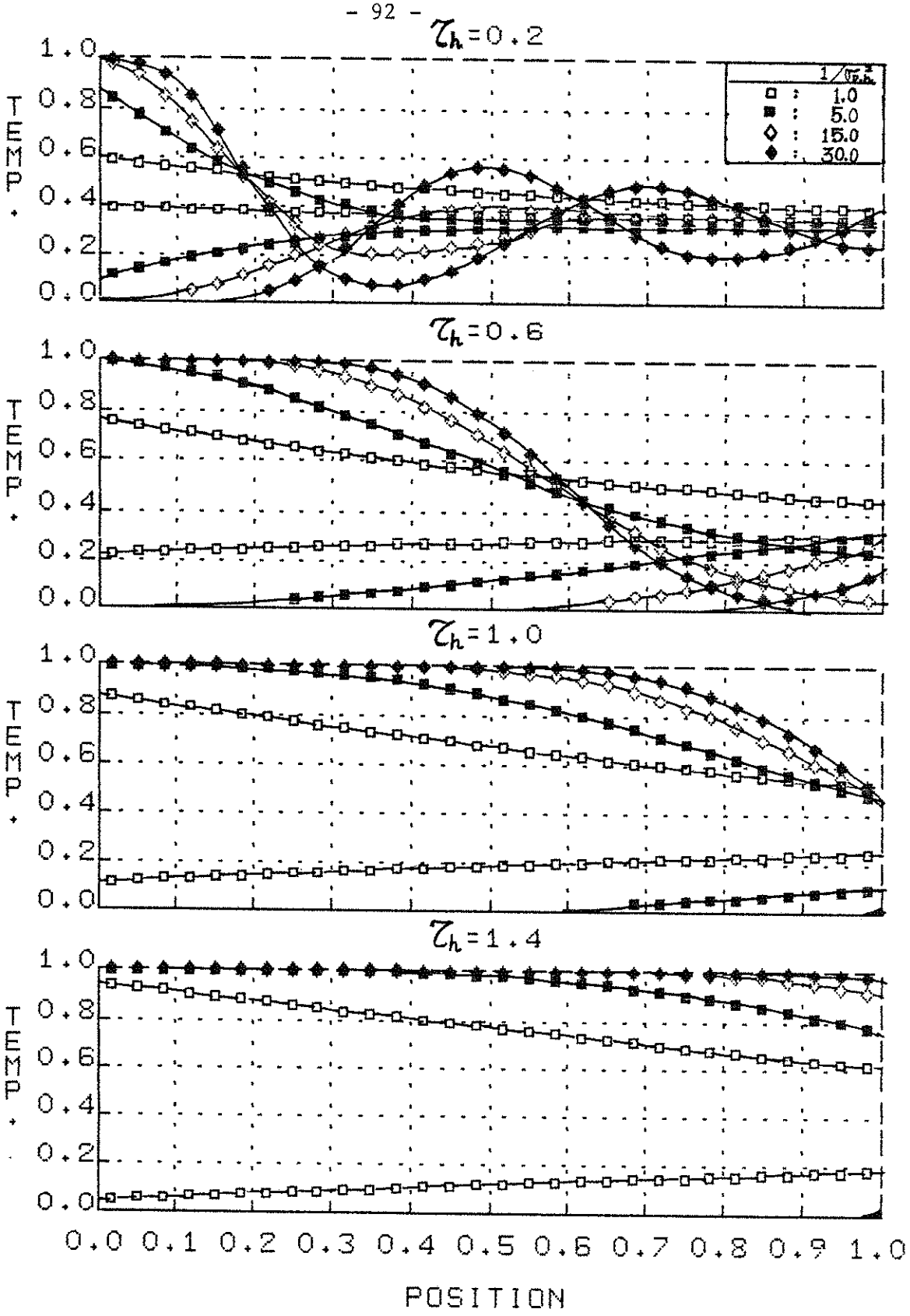

FIGURE 4.12

SOLID TEMPERATURE PROFILES OF COCURRENT OPERATION
——UNBALANCED CASE ($M_h/M_c = 2.0$)

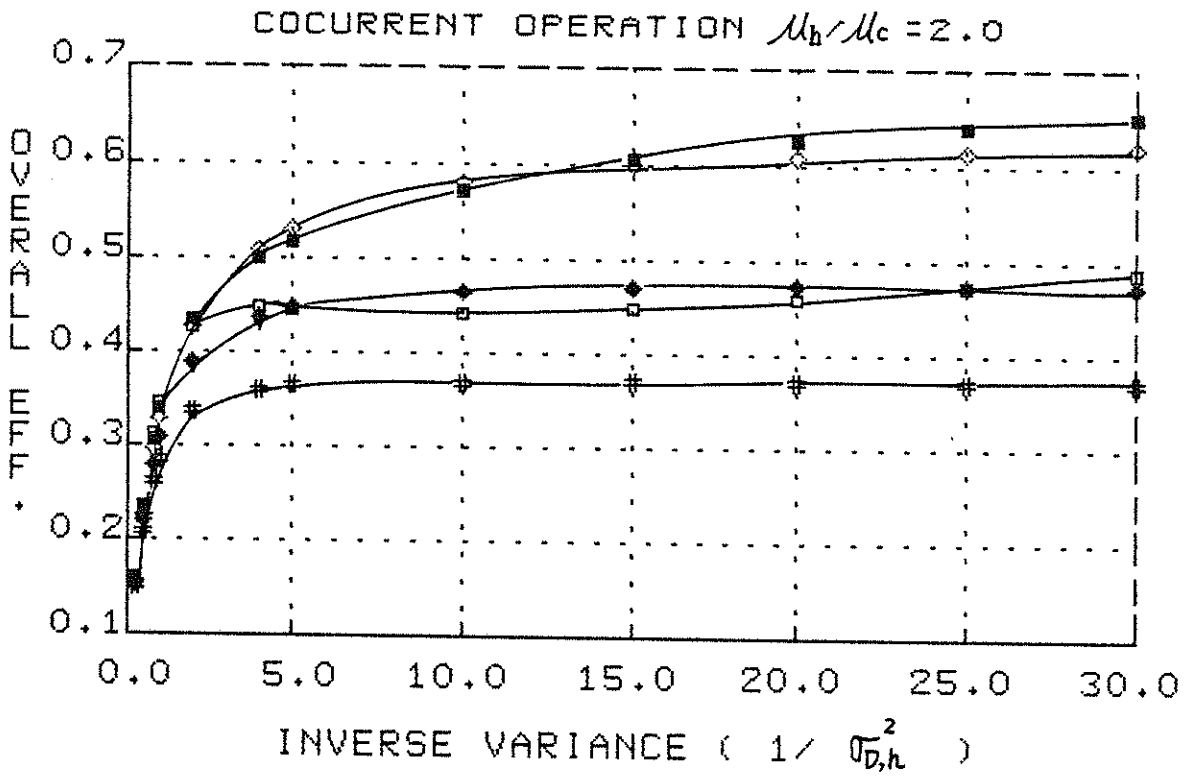

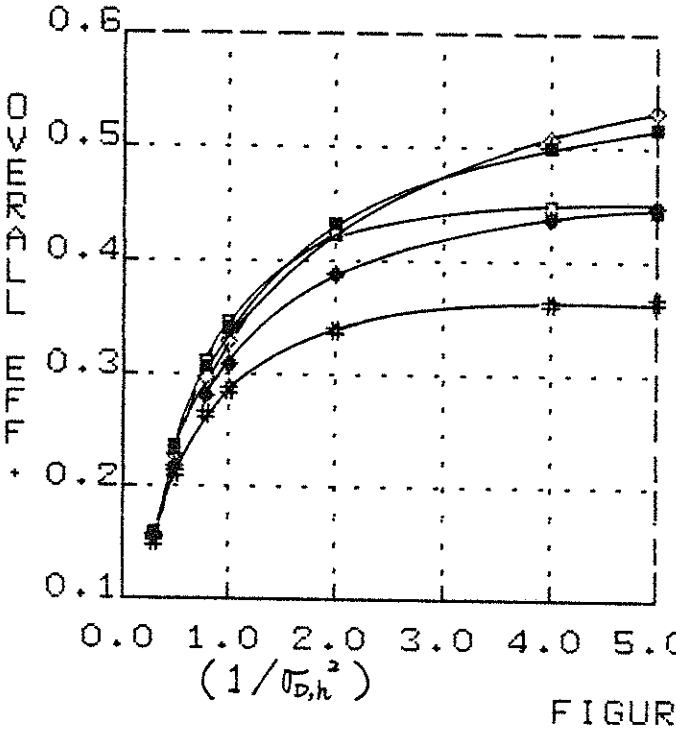

	τ_h	τ_c
□ :	0.2	0.4
■ :	0.6	1.2
◇ :	1.0	2.0
◆ :	1.4	2.8
# :	1.8	3.6

FIGURE 4.13

THERMAL EFFICIENCIES OF COCURRENT OPERATION
——30-STAGES FLUIDIZED BED APPROACH
USING THE CLOSED METHOD ,
UNBALANCED CASE ($M_h/M_c = 2.0$)

5. COUNTERCURRENT OPERATION

Based on the comparisons from last chapter, we feel confident that the n-staged fluidized beds model is a good approximation to the Schumann model. We would like to use this model to calculate the regenerator performance in countercurrent operation which we are unable to obtain in terms of the variance of the impulse response based on the principle of superposition.

For countercurrent flow the operation proceeds as sketched below:

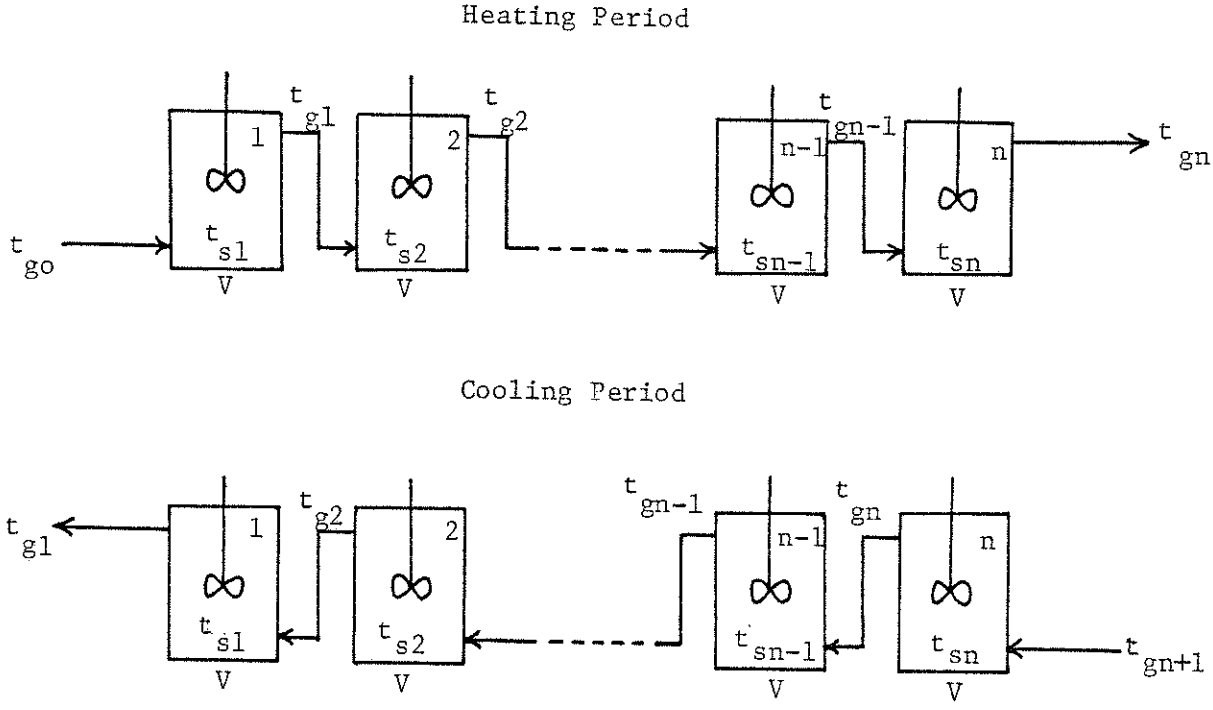

Figure 5.1 n-Staged Fluidized Beds Regenerators

—— Countercurrent Operation

The mathematical model for countercurrent operation is:

(1) Heating period, $0 < \tau < \tau_h$:

gas: $$0 = (t_{gm-1} - t_{gm}) - \beta_h (t_{gm} - t_{sm}) \qquad 4.2.23$$

solids: $$\frac{dt_{sm}}{d\tau} = \beta_h (t_{gm} - t_{sm}) \qquad 4.2.24$$

$$\tau = 0 \,, \quad t_{sm} = t_{sm}^{(I)} \quad ; \quad m = 1 \,, \quad t_{g_0} = H(\tau) \qquad 4.2.25a \;\; 4.2.26b$$

where $$\tau = \frac{\theta}{\mu_h} \,, \quad \beta_h = St_1 = \frac{hA_i}{\dot{m}_h C_{ph}} \qquad 4.2.26$$

(2) Cooling period, $0 < \tau' < \tau_c$:

gas: $$0 = (t_{gm+1} - t_{gm}) - \beta_c (t_{gm} - t_{sm}) \qquad 5.0.1$$

solids: $$\frac{dt_{sm}}{d\tau'} = \beta_c (t_{gm} - t_{sm}) \qquad 5.0.2$$

$$\tau' = 0 \,, \quad t_{sm} = t_{sm}^{(II)} \quad ; \quad m = n \,, \quad t_{gm+1} = 0 \qquad 5.0.3a \;\; 5.0.3b$$

where $$\tau' = \frac{\theta}{\mu_c} \,, \quad \beta_c = St_2 = \frac{hA_i}{\dot{m}_c C_{pc}} \qquad 5.0.4$$

with reversal conditions:

(1) Heating period: $t_{sm}(\tau_h) = t_{sm}^{(II)}$ $\quad m = 1,2,\ldots,n$ $\qquad 4.2.31$

(2) Cooling period: $t_{sm}(\tau_c) = t_{sm}^{(I)}$ $\quad m = 1,2,\ldots,n$ $\qquad 4.2.32$

For symmetric regenerators we have the symmetry of solid temperature profiles from Equation 2.2.10b:

$$t_{sm}^{(II)} = 1 - t_{s(n-m+1)}^{(I)} \qquad 5.0.5$$

The exit gas temperature during the heating period is still given by the same formal equation in terms of solid temperature as in cocurrent operation:

$$t_{gn}(\tau) = 1 - e^{-\lambda_h \tau}\left\{\frac{1}{(1+\beta_h)^n}\sum_{K=1}^{n}\binom{n}{K}\beta_h^K e_{K-1}(\lambda_h\tau) - \lambda_h \sum_{i=1}^{n}\frac{1}{(1+\beta_h)^{n-i}}\sum_{K=0}^{n-i}\lambda_h^K \beta_h^K \binom{n-i}{K}\frac{\tau^K}{K!}\, t_{si}^{(I)}\right\} \qquad 4.2.34$$

The solid temperature profile during the heating period is also analogous to the equation for the cocurrent case:

$$t_{sm}(\tau) = 1 + e^{-\lambda_h \tau}\left\{t_{sm}^{(I)} + \lambda_h^2 \sum_{i=1}^{m-1}\frac{1}{(1+\beta_h)^{m+1-i}}\sum_{K=0}^{m-1-i}\binom{m-1-i}{K}\lambda_h^K \beta_h^K \frac{\tau^{K+1}}{(K+1)!}\, t_{si}^{(I)}\right.$$

$$\left. - \frac{1}{(1+\beta_h)^{m-1}}\sum_{K=0}^{m-1}\binom{m-1}{K}\beta_h^K e_K(\lambda_h\tau)\right\} \qquad m = 1, 2, \cdots, n \qquad 4.2.35$$

For the cooling period the Laplace transformation of Equations 5.0.1 to 5.0.3 is:

$$\bar{t}_{g(n-m+1)} = \left[\frac{1}{1+\beta_c}\left(\frac{s+\beta_c}{s+\lambda_c}\right)\right]^m \cancel{\bar{t}_{g\,n+1}}^{\,0} + \sum_{i=1}^{m}\frac{\lambda_c}{s+\lambda_c}\left[\frac{1}{1+\beta_c}\left(\frac{s+\beta_c}{s+\lambda_c}\right)\right]^{m-i} t_{s(n-i+1)}^{(II)} \qquad 5.0.6$$

and

$$m = 1, 2, \cdots, n$$

$$\bar{t}_{s(n-m+1)} = \frac{1}{(s+\lambda_c)}\, t_{s(n-m+1)}^{(II)} + \frac{\beta_c}{(1+\beta_c)^m}\frac{(s+\beta_c)^{m-1}}{(s+\lambda_c)^m}\cancel{\bar{t}_{g\,n+1}}^{\,0}$$

$$+ \beta_c^2 \sum_{i=1}^{m-1}\frac{(s+\beta_c)^{m-i}}{(1+\beta_c)^{m+1-i}}\frac{1}{(s+\lambda_c)^{m+1-i}}\, t_{s(n-i+1)}^{(II)} \qquad m = 1, 2, \cdots, n \qquad 5.0.7$$

The exit gas temperature during the cooling period is:

$$t_{g1}(\tau') = \lambda_c \sum_{i=1}^{n}\frac{1}{(1+\beta_c)^{n-i}}\sum_{K=0}^{n-i}\lambda_c^K \beta_c^K \binom{n-i}{K}\frac{\tau'^K e^{-\lambda_c \tau'}}{K!}\, t_{s(n-i+1)}^{(II)} \qquad 5.0.8$$

and the solid temperature profile during the cooling period is:

$$t_{s_{(n-m+1)}}(\tau') = e^{-\lambda_c \tau'}\left\{ t^{(II)}_{s_{(n-m+1)}} + \lambda_c^2 \sum_{i=1}^{m-1} \frac{1}{(1+\beta_c)^{m-i}} \sum_{k=0}^{m-1-i} \binom{m-1-i}{k} \lambda_c^k \beta_c^k \frac{\tau'^{k+1}}{(k+1)!}\, t^{(II)}_{s_{(n-i+1)}} \right\} \qquad 5.0.9$$

$$m = 1, 2, \cdots, n$$

5.1 EQUAL PRODUCT OF MASS FLOW RATE AND SPECIFIC HEAT — SYMMETRIC REGENERATORS

The solid temperature profile at the end of the heating period ($\tau = \tau_1$), from Equation 4.2.35, is still the same:

$$t_{sm}(\tau_i) = 1 + e^{-\lambda \tau_i}\left\{ t^{(I)}_{sm} + \lambda^2 \sum_{i=1}^{m-1} \frac{1}{(1+\beta)^{m-i}} \sum_{k=0}^{m-1-i} \binom{m-1-i}{k} \lambda^k \beta^k \frac{\tau_i^{k+1}}{(k+1)!}\, t^{(I)}_{si} - \frac{1}{(1+\beta)^{m-1}} \sum_{k=0}^{m-1} \binom{m-1}{k} \beta^k e_k(\lambda \tau_i) \right\} \qquad m = 1, 2, \cdots, n \qquad 4.2.46$$

The reversal condition, Equation 4.2.31, and the property of symmetry, Equation 5.0.5, tell us:

$$t^{(II)}_{sm} = t_{sm}(\tau_i) = 1 - t^{(I)}_{s_{(n-m+1)}}$$

$$= 1 + e^{-\lambda \tau_i}\left\{ t^{(I)}_{sm} + \lambda^2 \sum_{i=1}^{m-1} \frac{1}{(1+\beta)^{m-i}} \sum_{k=0}^{m-1-i} \binom{m-1-i}{k} \lambda^k \beta^k \frac{\tau_i^{k+1}}{(k+1)!}\, t^{(I)}_{si} - \frac{1}{(1+\beta)^{m-1}} \sum_{k=0}^{m-1} \binom{m-1}{k} \beta^k e_k(\lambda \tau_i) \right\} \qquad 5.1.1$$

Rearranging into matrix form, we have:

$$\begin{bmatrix} 1 & 0 & e^{\lambda \tau_i} \\ \lambda^2 \tau_i & & \\ (m=3) & & \\ \vdots & & \\ (m=n) & \cdots\cdots & (m=3)\ \ \lambda^2 \tau_i\ \ 1 \end{bmatrix} \begin{bmatrix} t^{(I)}_{s1} \\ t^{(I)}_{s2} \\ \vdots \\ t^{(I)}_{sn} \end{bmatrix} = \begin{bmatrix} (m=1) \\ (m=2) \\ \vdots \\ (m=n) \end{bmatrix} \qquad 5.1.2$$

$$\lambda^2 \frac{1}{(1+\beta)^{m-2}} \sum_{k=0}^{m-2} \binom{m-2}{k} \lambda^k \beta^k \frac{\tau_i^{k+1}}{(k+1)!} \qquad \frac{1}{(1+\beta)^{m-1}} \sum_{k=0}^{m-1} \binom{m-1}{k} \beta^k e_k(\lambda \tau_i)$$

We can solve for the solid temperature profile, $t_{sm}^{(I)}$ (m:1~n), using Gaussian elimination.

The thermal efficiency of the heating period is the same formula as in the cocurrent case:

$$\eta_h(\tau_i) = \frac{1}{\tau_i}\gamma(\tau_i) + \frac{1}{\tau_i}\sum_{i=1}^{n}\frac{t_{si}^{(I)}}{(1+\beta)^{n-i}}\sum_{K=0}^{n-i}\binom{n-i}{K}\beta^K e^{-\lambda\tau_i} e_K(\lambda\tau_i) - \frac{1}{\tau_i}\sum_{i=1}^{n} t_{si}^{(I)} \qquad 4.2.49$$

For the limiting case $\beta >> 1$, Equation 5.1.2 will be simplified to:

$$\begin{bmatrix} 1 & & & & \\ \tau_i & 1 & & 0 & \\ (m=3) & & \ddots & & e^{\tau_i} \\ & e^{\tau_i} & & \ddots & \\ (m=n) & \cdots\cdots & (m=3) & \tau_i & 1 \end{bmatrix} \begin{bmatrix} t_{s1}^{(I)} \\ t_{s2}^{(I)} \\ \vdots \\ t_{sn}^{(I)} \end{bmatrix} = \begin{bmatrix} (m=1) \\ (m=2) \\ \vdots \\ (m=n) \end{bmatrix} \qquad 5.1.3$$

$$\frac{\tau_i^{m-1}}{(m-1)!} \qquad e_{m-1}(\tau_i)$$

and the thermal efficiency is:

$$\eta_h(\tau_i) = \frac{1}{\tau_i}\gamma(\tau_i) + \frac{1}{\tau_i}\sum_{i=1}^{n} t_{si}^{(I)} e^{-\tau_i} e_{n-i}(\tau_i) - \frac{1}{\tau_i}\sum_{i=1}^{n} t_{si}^{(I)} \qquad 4.2.51$$

The results of the solid temperature profile for different values of $1/\sigma_D^2$ for different switching times are shown in Figure 5.2. It can be seen that the profile after the heating period is always higher than the profile before the heating period and both are symmetric with respect to the diagonal line.

The results for exit gas temperature profiles and the thermal efficiencies are shown in Figures 5.3 and 5.4, respectively. The

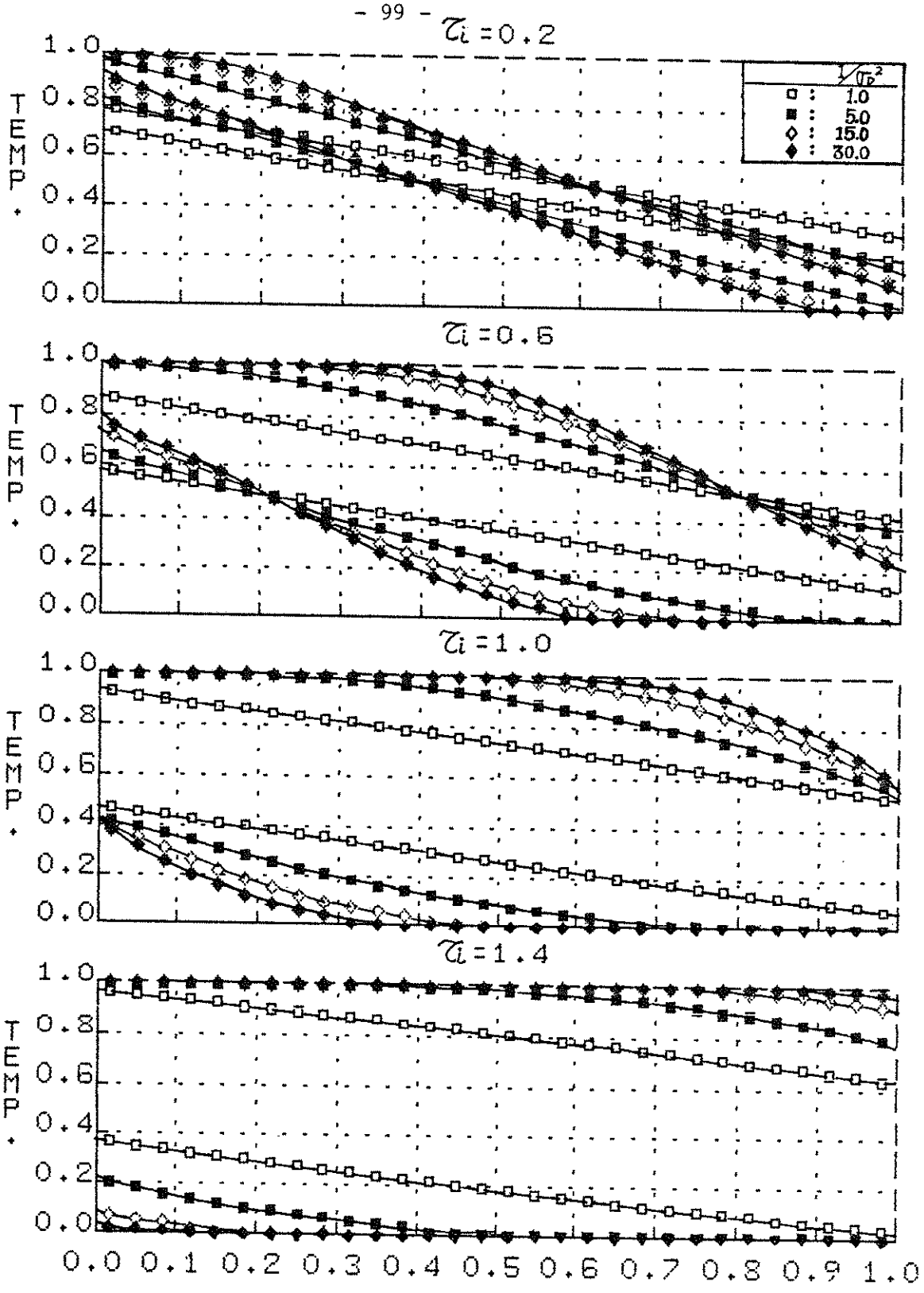

FIGURE 5.2

SOLID TEMP. PROFILES OF COUNTERCURRENT OPERATION
——SYMMETRIC CASE

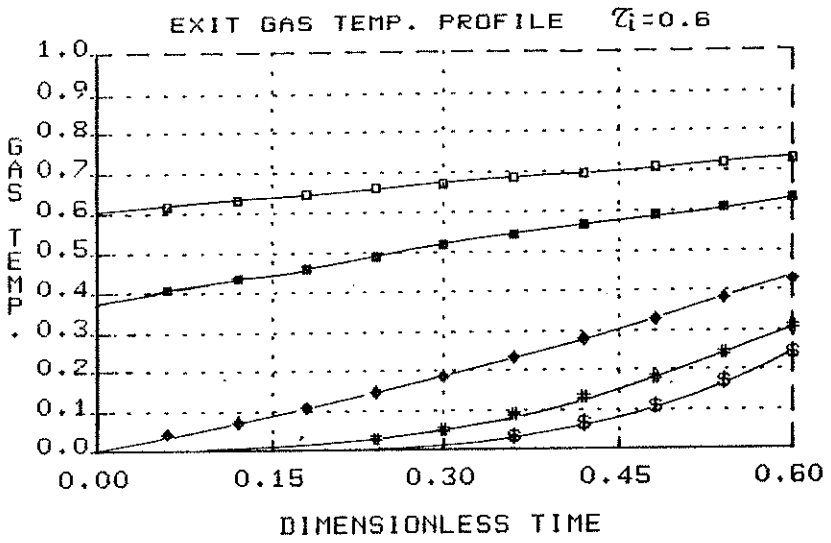

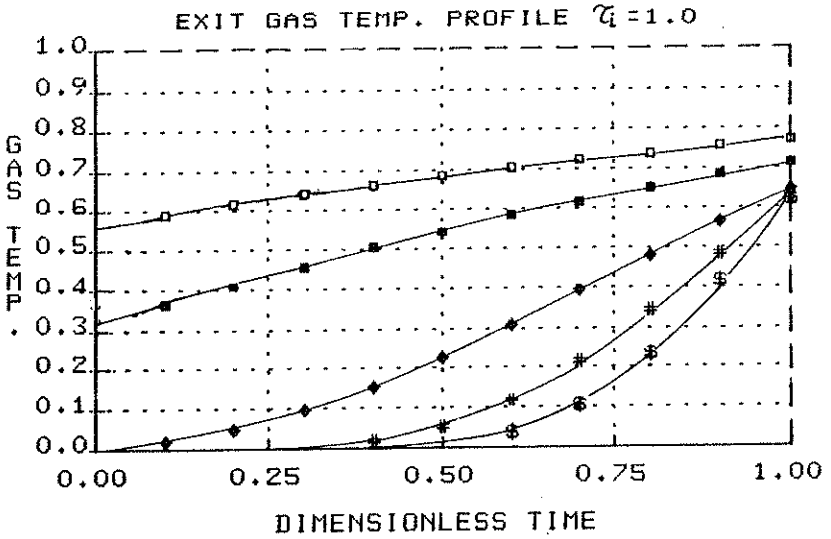

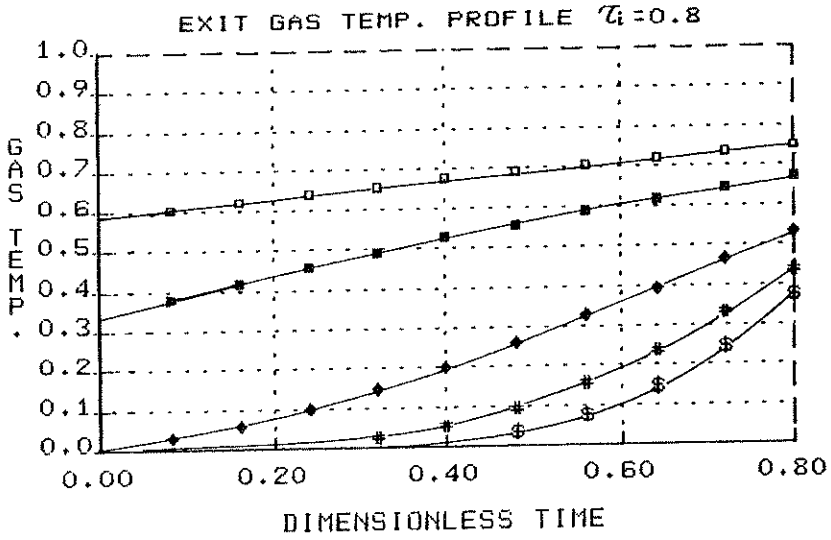

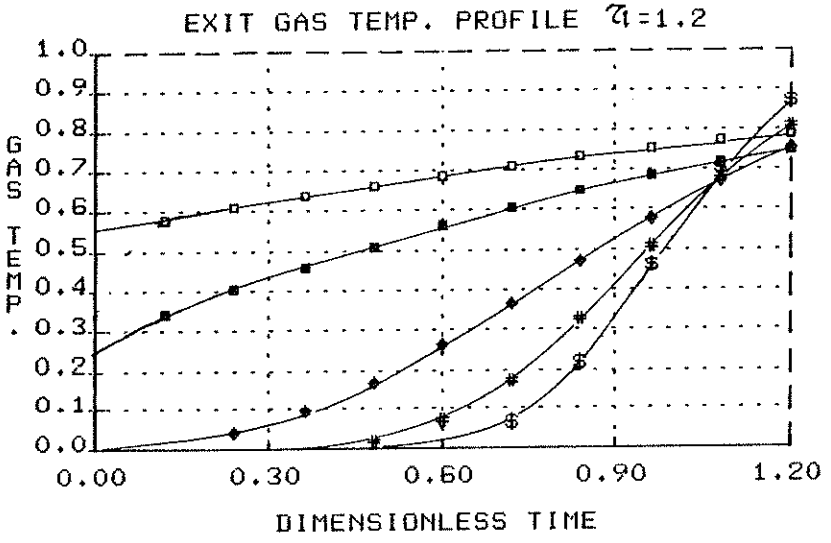

$1/\mathbb{D}_D^2$: □ — 0.5 ♦ — 5.0 $ — 30.0
■ — 1.0 # — 15.0

FIGURE 5.3a

EXIT GAS TEMP. PROFILES OF COUNTERCURRENT OPERATION
(HEATING PERIOD) ——— SYMMETRIC CASE

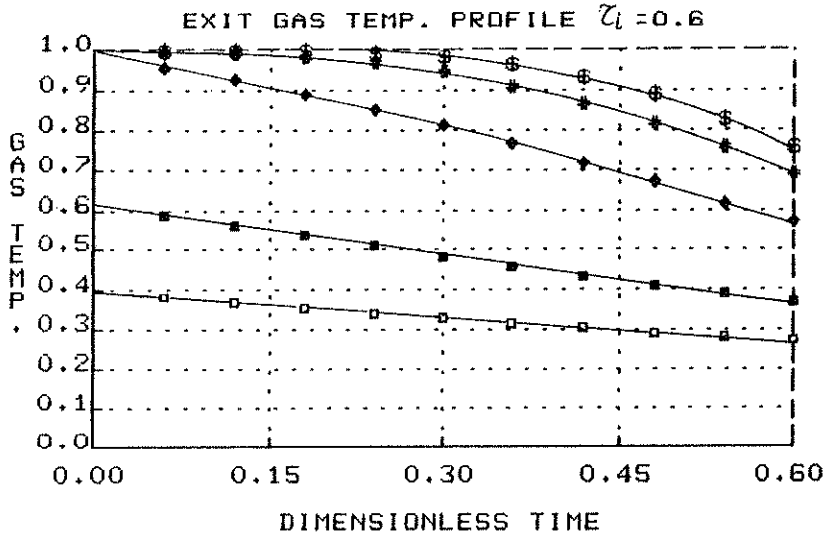

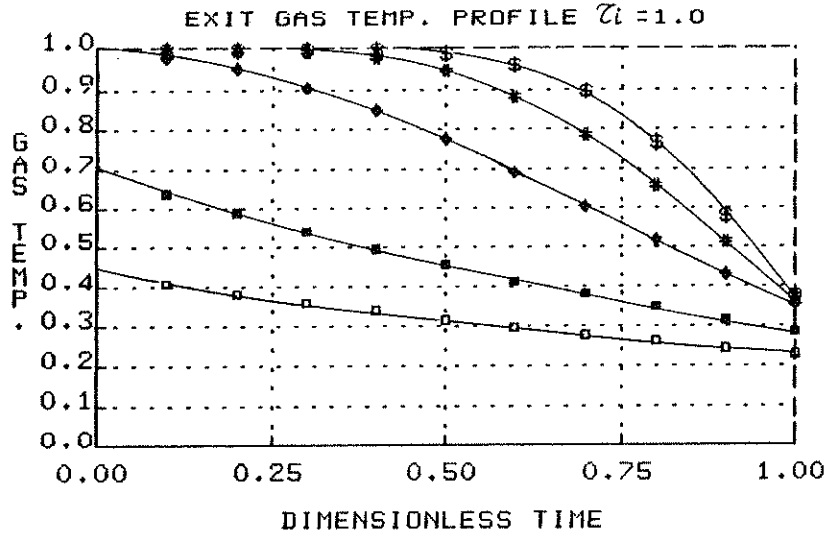

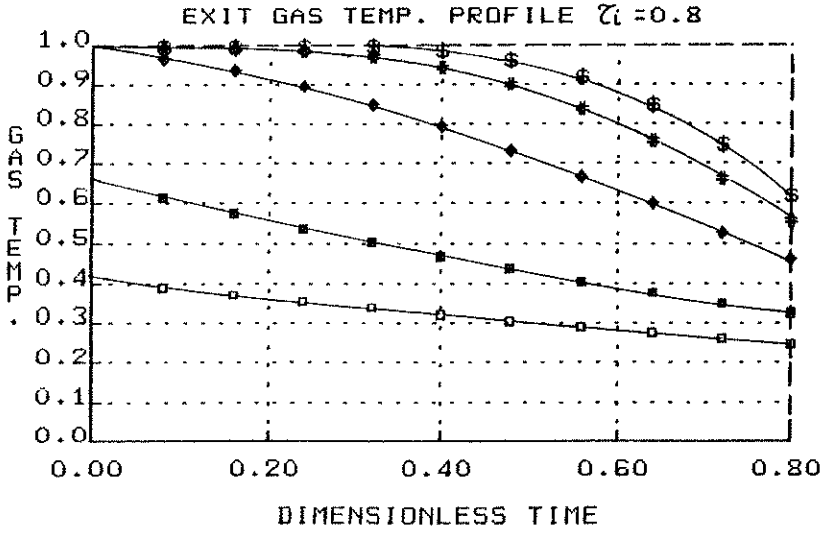

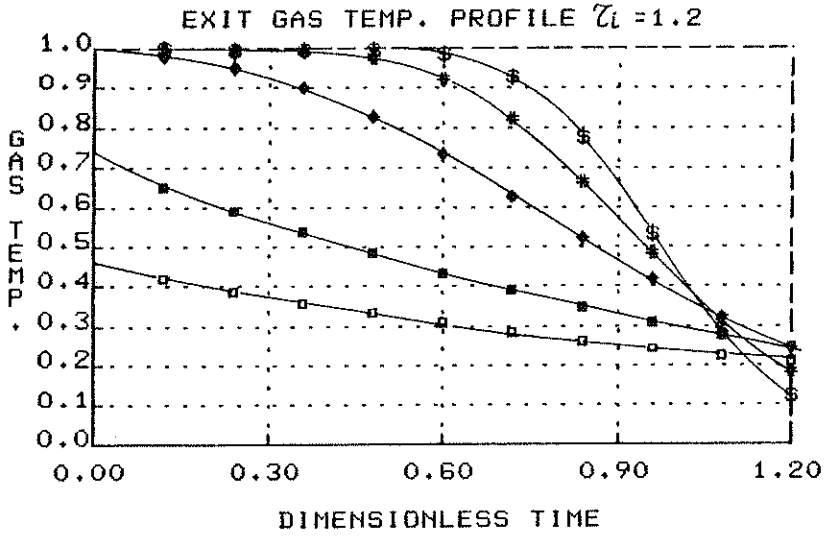

$1/\theta_D^2$: □ — 0.5 ♦ — 5.0 $ — 30.0
■ — 1.0 # — 15.0

FIGURE 5.3 **b**

EXIT GAS TEMP.PROFILE OF COUNTERCURRENT OPERATION
(**COOLING PERIOD**) ——— SYMMETRIC CASE

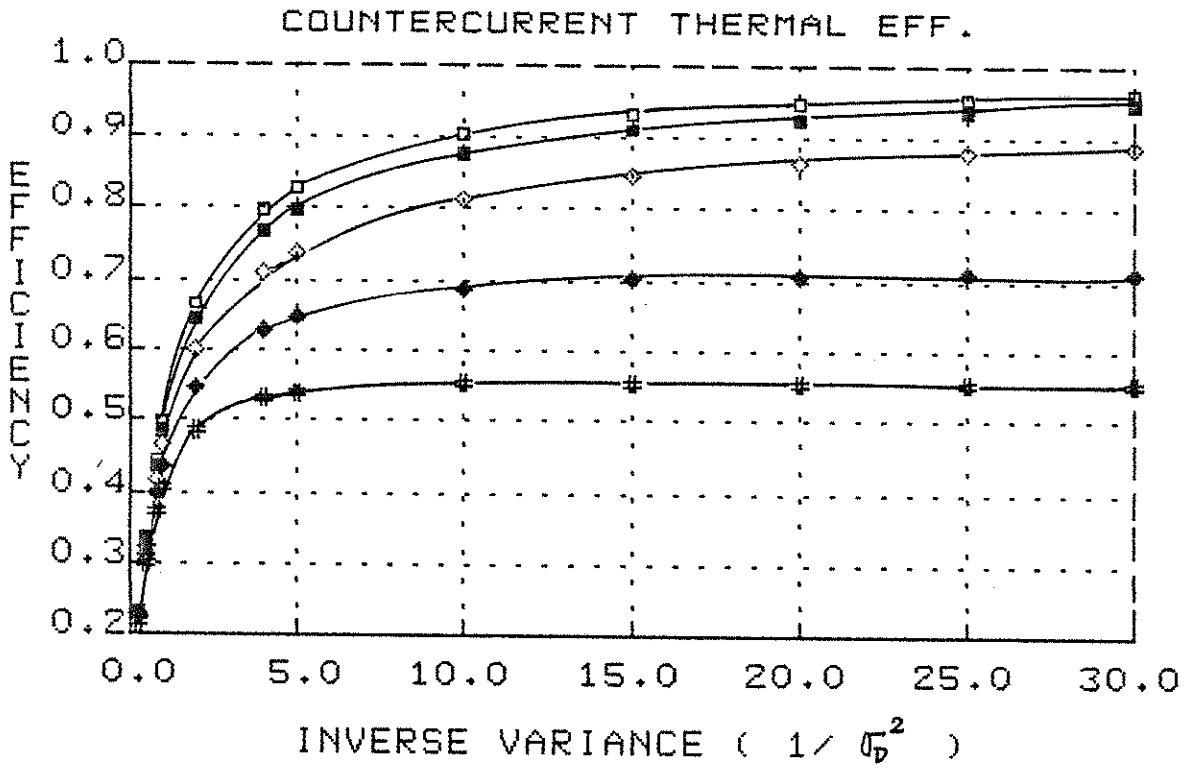

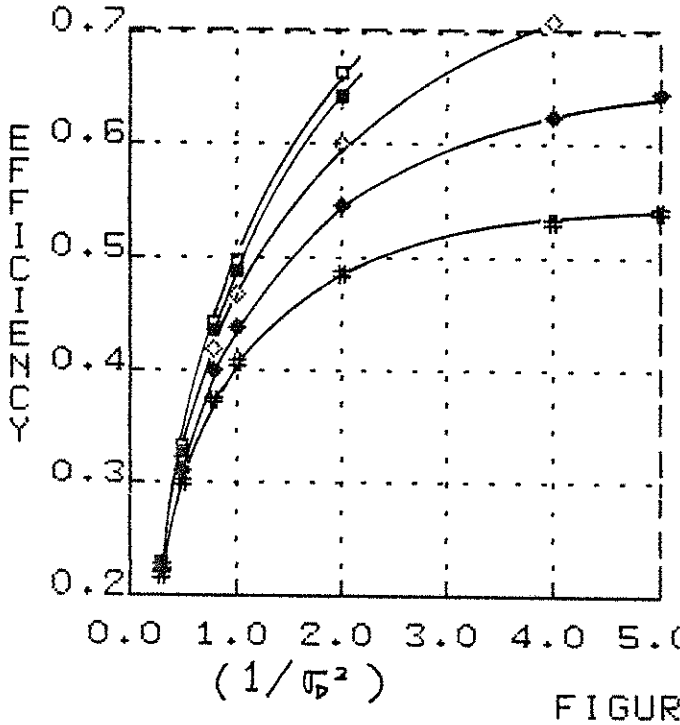

$\tau_h = \tau_c = \tau_i$

□ : 0.2
■ : 0.6
◇ : 1.0
◆ : 1.4
: 1.8

FIGURE 5.4

THERMAL EFF. OF COUNTERCURRENT OPERATION
——30-STAGES FLUIDIZED BED APPROACH
USING THE CLOSED METHOD ,
SYMMETRIC CASE

average gas temperature for different switching times always increases with increasing τ_i and this is the reason why the thermal efficiency increases with decreasing τ_i. Indeed, based on the analogy with a countercurrent flow recuperator, as argued by Jakob (10), one should get the thermal efficiency for infinitely small switching time:

$$\eta_{reg}(0) = \frac{\Lambda}{\Lambda+2} = \frac{St}{St+2} = \frac{(1/\sigma_D^2)}{(1/\sigma_D^2)+1} \qquad 5.1.4$$

where Schumann's model is considered and $\sigma_D^2 = 2\left(\frac{1}{St}\right)$. The thermal efficiency at $\tau_i = 0.2$ is almost as large as $\eta_{reg}(0)$ within 1%.

Again, our results, based on the same parameters: the reduced length $\Lambda = St = 2(1/\sigma_D^2)$ and the reduced period $\pi = \Lambda \cdot \tau_i$, are in agreement with those of Hausen (6) and Nusselt (21) as presented by Jakob (10) within 1% for $1/\sigma_D^2 > 5.0$ (long regenerators) and with 5% for $1/\sigma_D^2 \leq 5.0$.

It can be seen that for long switching times ($\tau_i \geq 1.4$), the thermal efficiencies for both cocurrent and countercurrent operations are almost the same with maximum deviation not exceeding 1%. For short switching times ($\tau_i < 1.4$) countercurrent operations always have the higher efficiency.

5.2 UNEQUAL PRODUCT OF MASS FLOW RATE AND SPECIFIC HEAT - UNBALANCED REGENERATORS

From the solid temperature profile at the end of the heating period, Equation 4.2.35, and the reversal condition, Equation 4.2.31, we have:

$$t_{sm}^{(II)} = t_{sm}(\tau_h) = 1 + e^{-\lambda_h \tau_h}\left\{ t_{sm}^{(I)} + \lambda_h^2 \sum_{i=1}^{m-1} \frac{1}{(1+\beta_h)^{m-i}} \sum_{k=0}^{m-1-i} \binom{m-1-i}{k} \lambda_h^k \beta_h^k \frac{\tau_h^{k+1}}{(k+1)!} + t_{si}^{(I)} \right.$$
$$\left. - \frac{1}{(1+\beta_h)^{m-1}} \sum_{k=0}^{m-1} \binom{m-1}{k} \beta_h^k e_k(\lambda_h \tau_h) \right\} \qquad m = 1, 2, \cdots, n \qquad 4.2.52$$

and for the same limiting case $\beta_h >> 1$:

$$t_{sm}^{(II)} = t_{sm}(\tau_h) = 1 + e^{-\tau_h}\left\{t_{sm}^{(I)} + \sum_{i=1}^{m-1}\frac{\tau_h^{m-i}}{(m-i)!}t_{si}^{(I)} - e_{m-1}(\tau_h)\right\} \qquad 4.2.53$$

$m = 1, 2, \cdots, n$

Also from the solid temperature profile at the end of the cooling period, $\tau' = \tau_c$ in Equation 5.0.9, and the reversal condition, Equation 4.2.32, we get:

$$t_{s_{(n-m+1)}}^{(I)} = t_{s_{(n-m+1)}}(\tau_c) = e^{-\lambda_c\tau_c}\left\{t_{s_{(n-m+1)}}^{(II)} + \lambda_c^2\sum_{i=1}^{m-1}\frac{1}{(1+\beta_c)^{m-i}}\sum_{k=0}^{m-i}\binom{m-1-i}{k}\lambda_c^k\beta_c^k\frac{\tau_c^{k+1}}{(k+1)!}t_{s_{(n-i+1)}}^{(II)}\right\} \qquad 5.2.1$$

and for the limiting case $\beta_h >> 1$:

$$t_{s_{(n-m+1)}}^{(I)} = t_{s_{(n-m+1)}}(\tau_c) = e^{-\lambda_c\tau_c}\left\{t_{s_{(n-m+1)}}^{(II)} + \sum_{i=1}^{m-1}\frac{\tau_c^{m-i}}{(m-i)!}t_{s_{(n-i+1)}}^{(II)}\right\} \qquad 5.2.2$$

We can also solve for $t_{sm}^{(I)}$ and $t_{sm}^{(II)}$ from Equations 4.2.52 and 5.2.1 by either successive substitution or by some methods of acceleration.

The thermal efficiency can be found from:

$$\eta_h(\tau_h) = \frac{1}{\tau_h}\gamma(\tau_h) + \frac{1}{\tau_h}\sum_{i=1}^{n}\frac{t_{si}^{(I)}}{(1+\beta_h)^{n-i}}\sum_{k=0}^{n-i}\binom{n-i}{k}\beta_h^k e^{-\lambda_h\tau_h}e_k(\lambda_h\tau_h) - \frac{1}{\tau_h}\sum_{i=1}^{n}t_{si}^{(I)} \qquad 4.2.56$$

and for the limiting case $\beta >> 1$

$$\eta_h(\tau_h) = \frac{1}{\tau_h}\gamma(\tau_h) + \frac{1}{\tau_h}\sum_{i=1}^{n}t_{si}^{(I)}e^{-\tau_h}e_{n-i}(\tau_h) - \frac{1}{\tau_h}\sum_{i=1}^{n}t_{si}^{(I)} \qquad 4.2.57$$

The results of the solid temperature profiles and the thermal efficiencies are shown in Figures 5.5, 5.6 and Figures 5.7, 5.8 for the cases of $\mu_h/\mu_c = 0.5$ and $\mu_h/\mu_c = 2.0$, respectively. It can also be

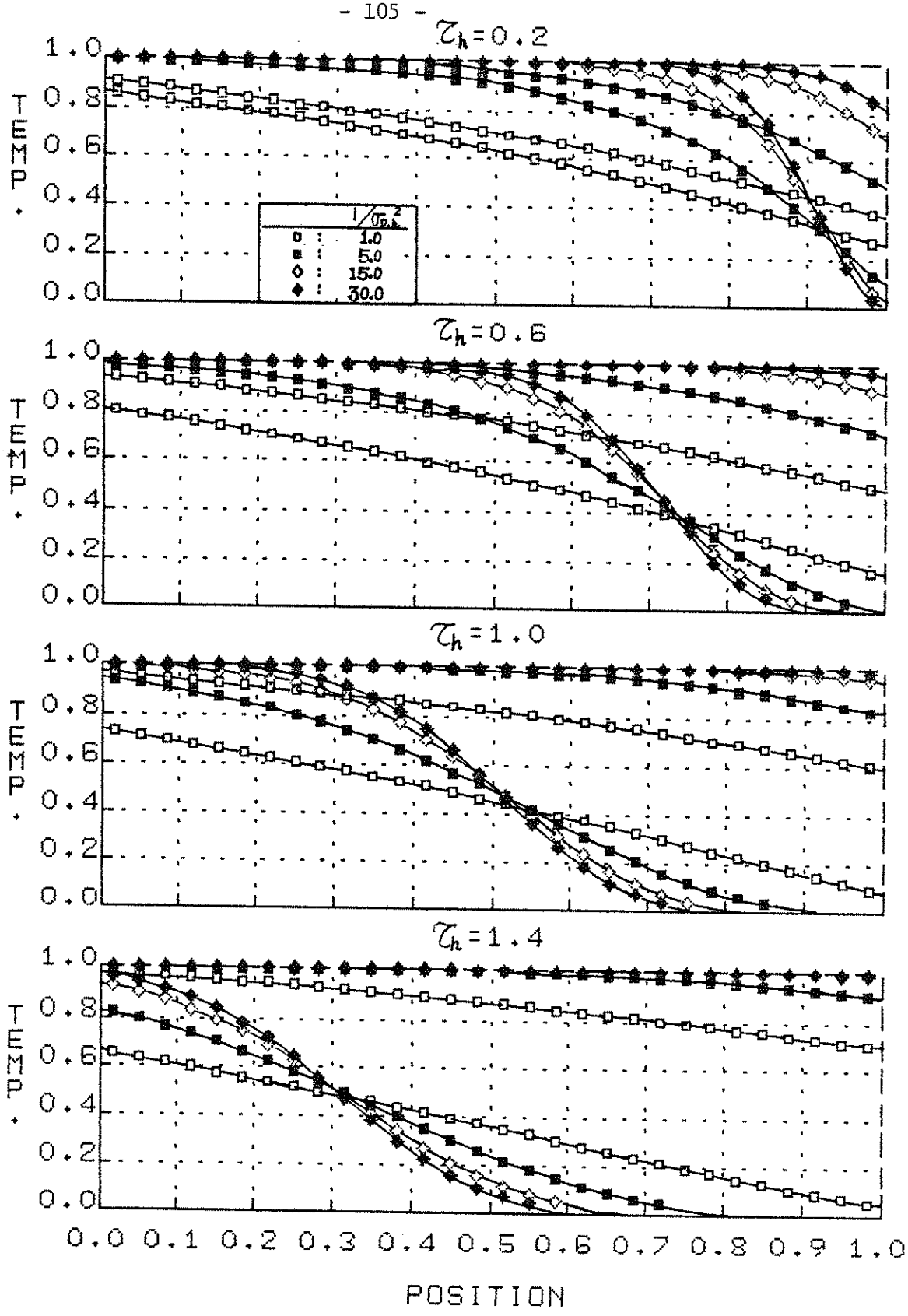

FIGURE 5.5

SOLID TEMP. PROFILES OF COUNTERCURRENT OPERATION
——UNBALANCED CASE ($M_h/M_c = 0.5$)

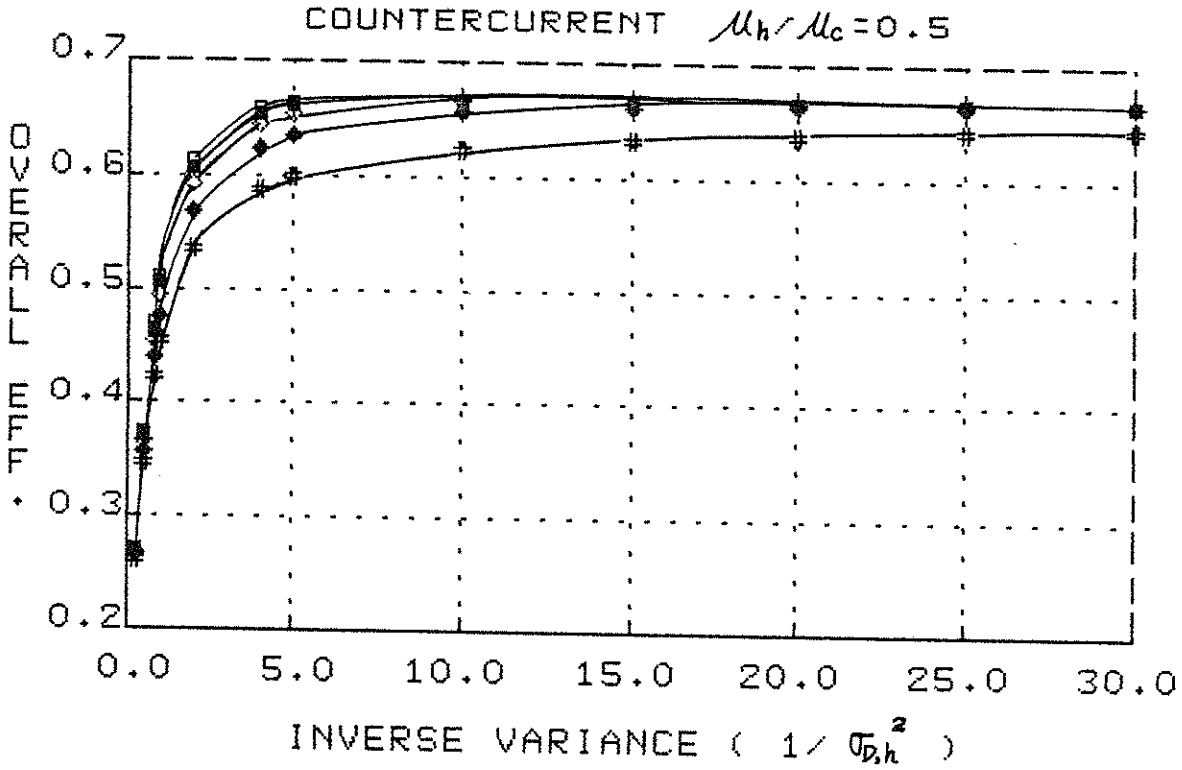

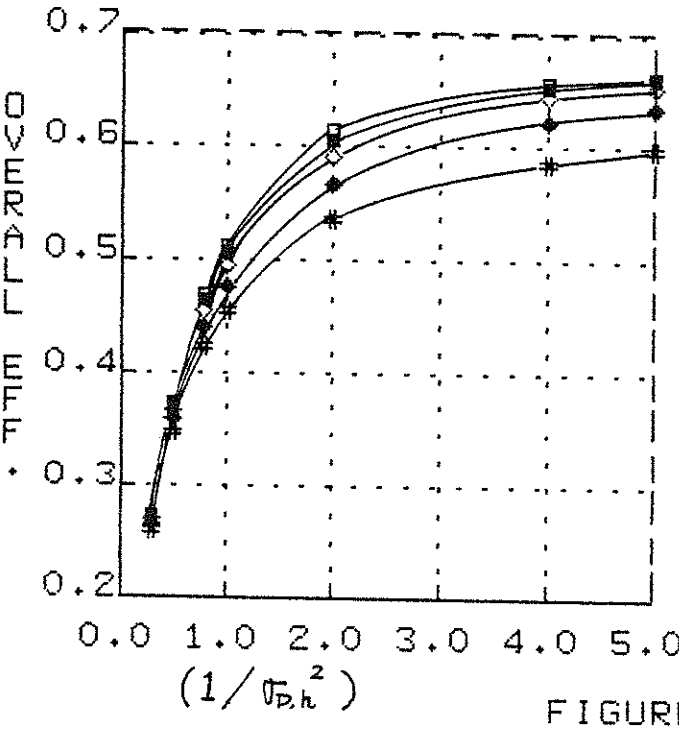

	τ_h	τ_c
□ :	0.2	0.1
■ :	0.6	0.3
◇ :	1.0	0.5
◆ :	1.4	0.7
# :	1.8	0.9

FIGURE 5.6

THERMAL EFF. OF COUNTERCURRENT OPERATION
——30-STAGES FLUIDIZED BED APPROACH
USING THE CLOSED METHOD .
UNBALANCED CASE ($M_h/M_c=0.5$)

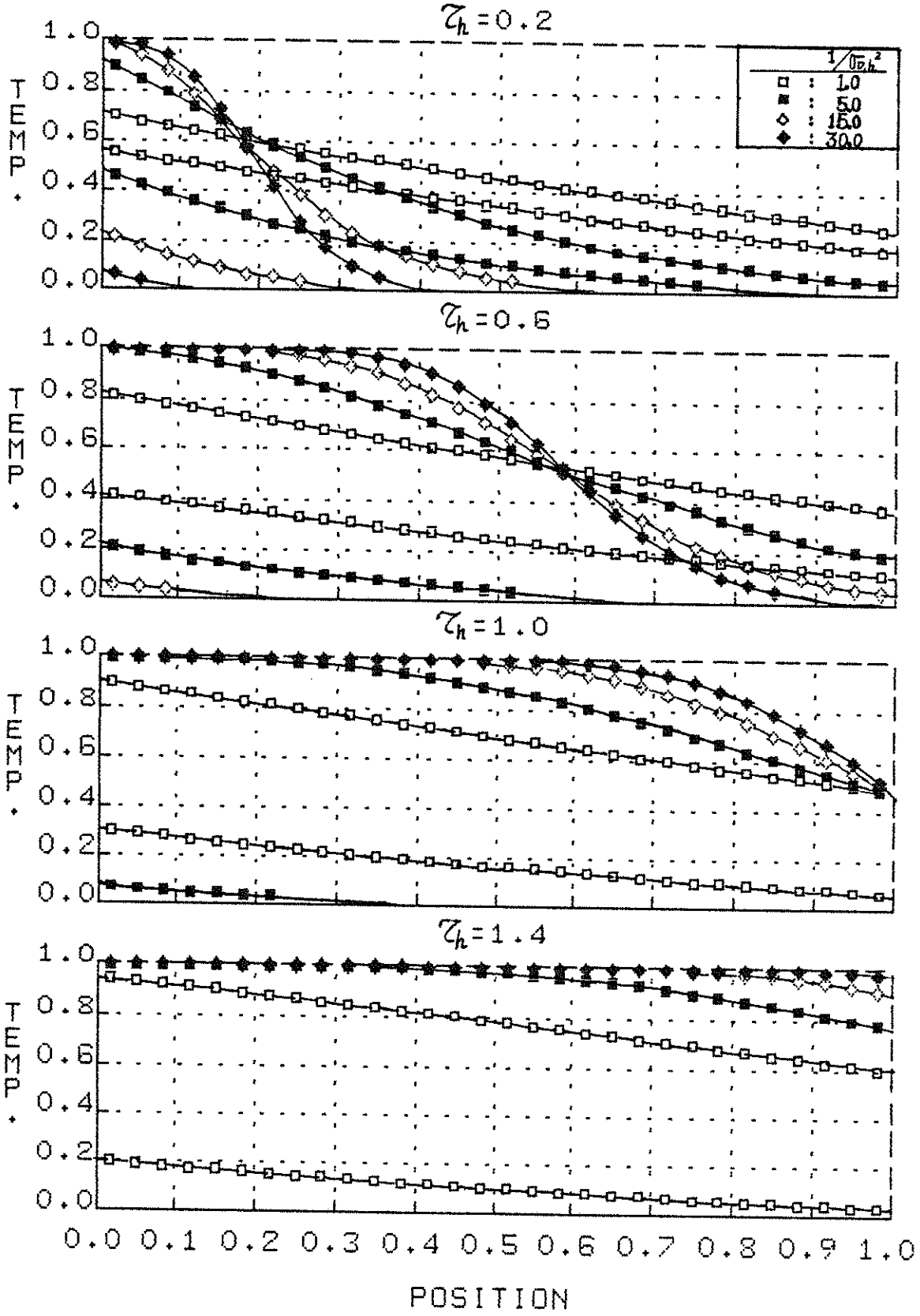

FIGURE 5.7

SOLID TEMP. PROFILES OF COUNTERCURRENT OPERATION
——UNBALANCED CASE ($M_h/M_c = 2.0$)

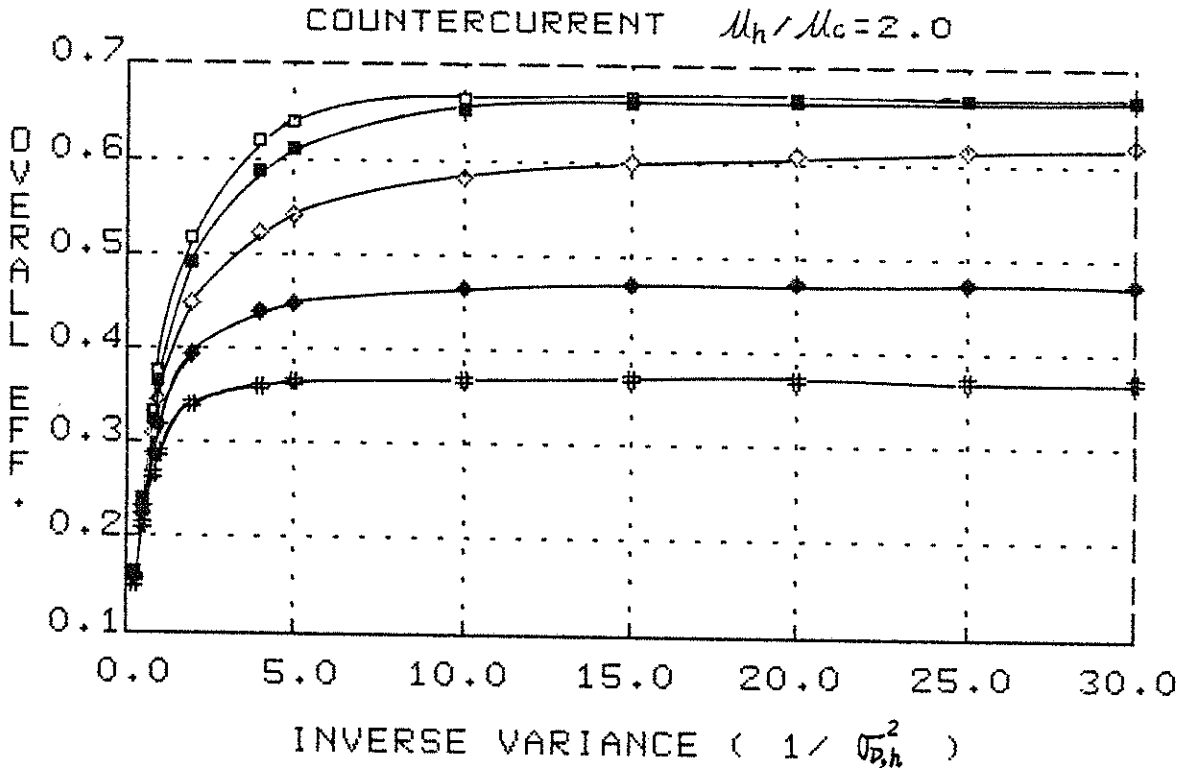

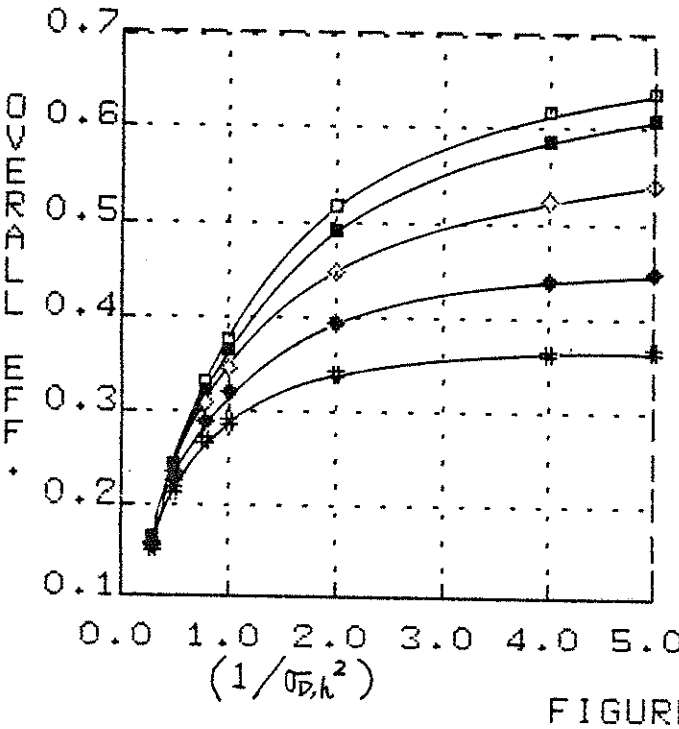

	τ_h	τ_c
□ :	0.2	0.4
■ :	0.6	1.2
◇ :	1.0	2.0
◆ :	1.4	2.8
# :	1.8	3.6

FIGURE 5.8

THERMAL EFF. OF COUNTERCURRENT OPERATION
——30-STAGES FLUIDIZED BED APPROACH
USING THE CLOSED METHOD ,
UNBALANCED CASE ($M_h/M_c=2.0$)

seen that the solid temperature profiles are no longer symmetric with respect to the dragonal line. The solids temperature after the heating period is always higher than the one before the heating period. The thermal efficiency always increases with decreasing τ_h (or τ_c) and is higher than the one for cocurrent operation. Only for long switching times ($\tau_h \geq 1.7$ for $\mu_h/\mu_c = 0.5$ and $\tau_h \geq 1.0$ for $\mu_h/\mu_c = 2.0$), the results from both operations are almost the same (with maximum deviations not exceeding 1%).

6. DISUCSSION OF MAJOR FINDINGS

6.1 COMPARISON TO THE RESULTS OF JAKOB AND SCHMIDT AND WILLMOTT

We showed that one can get the regenerator efficiency for any model for cocurrent flow by using the principle of superpostion and an approximate solution expressed in terms of the variance of the impulse response. The results are shown in Figure 4.2 for the symmetric case and Figure 4.3 for the unbalanced case. We also developed a model consisting of n-staged fluidized beds which can be used for large n as an approximation to the packed bed regenerator. This allows us to apply both open and closed methods in solving the regenerator performance for cocurrent operation and the results are shown in Figure 4.5 (open method), Figure 4.9 (closed method) for the symmetric case and in Figure 4.6 (open method), Figures 4.11, 4.13 (closed method) for the unbalanced case. The results from these two approaches are both in agreement with those of Hausen (6) and Nusselt (21) as presented by Jakob (10) for $1/\sigma_D^2 > 5.0$ (long regenerators). In contrast other authors needed complex computational schemes just for solving the Schumann's model. Our approach based on the superposition principle is much simpler, faster and of sufficient accuracy.

For countercurrent operation only the closed method using the n-staged fluidized beds is considered. The results are shown in Figure 5.4 for the symmetric case and Figures 5.6, 5.8 for the unbalanced case. Again for $1/\sigma_D^2 > 5.0$, the results are in agreement with those not only from the Schumann's model (25) but also from more complex models as presented by Schmidt and Willmott (28) where longitudinal or latitudinal solid conduction are also considered.

The good agreement between these different models establishes that the regenerator performance for $1/\sigma_D^2 > 5.0$ is primarily a function of $1/\sigma_D^2$ and τ_i only, i.e. all models that have the same variance and same switching time would give the same result for long regenerators. This tells us that the skewness (shape) of the curve of the impulse response is not important for long regenerators. We can then represent the approximate solutions of impulse response by truncating the Laguerre series after the leading term and use only the mean and the variance of the curve. However, for short regenerators the skewness of the curve may become important, the approximate solutions cannot account for it completely, and for increased accuracy we may need to solve each model individually. Even for short regenerators the approximate method developed here gives an estimate for efficiency with better than 20% accuracy.

6.2 COMPARISON TO LEVENSPIEL'S METHOD

Levenspiel (19) suggests some simple, useful formulas and charts for evaluation of thermal efficiencies of heat regenerators in periodic operations. The basic premise is that the solids temperature distribution at the end of the heating or cooling period can be represented by the symmetric s-shaped distribution which is the integral of the normal distribution. The dimensionless variance of this distribution is equal to the one for the impulse response of the gas, however, this assertion has not been proven yet.

Our results for solids temperature distribution in Figure 4.7 for symmetric cocurrent operations, Figures 4.10 and 4.12 for unbalanced cocurrent operations, Figure 5.2 for symmetric countercurrent operations,

Figures 5.5 and 5.7 for unbalanced countercurrent operations show that the symmetric s-shaped curves can only be formed for the long regenerators ($1/\sigma_D^2 > 5.0$) in the following cases:

(*i*) Symmetric cocurrent operations at $\tau_i > 0.7$.

(*ii*) Unbalanced cocurrent operations at $\tau_h > 0.7$ and $\tau_c > 0.7$. Both cases are symmetric w.r.t. the position of the dimensionless switching time (regard the whole length of regenerators as μ_h or μ_c).

(*iii*) Symmetric countercurrent operations at $\tau_i > 0.7$. This case is symmetric w.r.t. the central point between the dimensionless switching time and the end point of regenerators for $\tau_i < 1.0$ and w.r.t. the exact position of the dimensionless switching time for $\tau_i \geq 1.0$. But for the case of unbalanced countercurrent operations, only one of the solids temperature distribution is s-shaped symmetric w.r.t. τ_h or τ_c.

We have tested Levenspiel's formulas for cocurrent operation and found them, for the above cases, to be quite close to numerical results for efficiency often within a couple of percent. However, his formula for the countercurrent case is not that accurate and we find deviations up to 25%.

Instead of tedious evaluation Levenspiel's method gives us a quick, simple way to calcualte a very complex problem. However, the formulas for calculating the thermal efficiency for countercurrent operations based on the solids temperature distribution need modification.

6.3 THE CONTRIBUTIONS OF VARIOUS HEAT TRANSFER RESISTANCES AND ERROR ANALYSIS

For a model of packed bed regenerators that treats the solids as a discrete medium and assume spherical particles, the variance, from Equations 3.1.3 and 3.1.4, is:

$$\sigma_D^2 = 2\left\{\frac{1}{5}\frac{Bi_\rho}{St_\rho} + \frac{1}{St_\rho} + \frac{1}{Pe_{gz}}\right\}$$

and

$$Pe_{gz} = \frac{LG_gC_{pg}}{Ke_{gz}}$$

$$St_\rho = \frac{h_\rho a_s L}{G_gC_{pg}} \quad , \quad a_s = \frac{3(1-\epsilon)}{\Pi_{\rho o}} \quad \text{for spherical particles}$$

$$Bi_\rho = \frac{h_\rho \Pi_{\rho o}}{K_\rho} = \frac{h_\rho (3L_\rho)}{K_\rho} \quad , \quad L_\rho = \frac{\Pi_{\rho o}}{3} \quad \text{for spherical particles}$$

Drawing on the analogy between heat, mass and momentum transfer we can write

$$Pe,_h = Pe,_m$$

Dispersion theory for fluid flow plus experiment results with gas, see Levenspiel (17), gives:

$$Pe,_m = \frac{u_o L}{D\epsilon} = \left(\frac{u_o d_p}{D\epsilon}\right)\frac{L}{d_p} = \left(\frac{u d_p}{D}\right)\frac{L}{d_p} = 2\frac{L}{d_p} = \frac{L}{\Pi_{\rho o}} \qquad 6.3.1$$

when

$$Re,_p = d_p u_o \rho_g / \mu > 10$$

Replacing,

$$\sigma_D^2 = \frac{2}{5}\frac{G_gC_{pg}\Pi_{\rho o}}{K_\rho a_s L} + \frac{2G_gC_{pg}}{h_\rho a_s L} + \frac{2\Pi_{\rho o}}{L}$$

$$= \frac{1}{30(1-\epsilon)}\frac{G_gC_{pg}d_p^2}{K_\rho L} + \frac{1}{3(1-\epsilon)}\frac{G_gC_{pg}d_p}{h_\rho L} + \frac{d_p}{L} \qquad 6.3.2$$

$$= \sigma_D^2{}_{\substack{\text{particle}\\\text{conduction}}} + \sigma_D^2{}_{\substack{\text{film}\\\text{resistance}}} + \sigma_D^2{}_{\substack{\text{gas}\\\text{dispersion}}}$$

Equation 6.3.2 will tell us which term dominates and is the main cause for the lowering of thermal efficiency. Then we can predict how changes in system geometry (particle size, regenerator length and diameter) or heat transfer parameters (K_s, K_g, h, etc.) will affect the relative heat transfer resistances, and thus change the thermal efficiency. For example:

Consider a pair of regenerators 60 m high and 4 m in diameter filled with uniformly sized and close to spherical basaltic beach stones to be used to transfer heat from hot waste gases leaving a process to cold incoming air.

Data:

For the solid: $d_p = 0.08$ m $\qquad K_\rho = 0.5$ W m^{-1} K^{-1}

$\rho_s = 2280$ kg m^{-3} $\qquad C_{ps} = 1000$ J kg^{-1} K^{-1}

For both hot and cold gas take the properties of air at 20°C:

$\mu = 1.8 \times 10^{-5}$ kg m^{-1} s^{-1} $\qquad K_g = 0.026$ W m^{-1} K^{-1}

$\rho_g = 1.2$ kg m^{-3} $\qquad C_{pg} = 1013$ J kg^{-1} K^{-1}

In the regenerator:

$\varepsilon = 0.4$ $\qquad G_g = u_g \rho_g = 3.6$ kg m^{-2} s^{-1}

(or $u_g \simeq 3$ m s^{-1})

1. Solution

(*i*) Find h_ρ

$$Re = \frac{d_p u_g \rho_g}{\mu} = \frac{d_p G_g}{\mu} = \frac{(0.08)(3.6)}{1.8 \times 10^{-5}} = 1.6 \times 10^4 > 10$$

$$Pr = \frac{C_{pg} \mu}{K_g} = \frac{(1013)(1.8 \times 10^{-5})}{0.026} = 0.70$$

Replacing in one of the recommended correlation

$$\frac{h_\rho d_p}{K_g} = 2 + 1.8\ Re^{1/2}\ Pr^{1/3}$$

then give $h_\rho = 66.35\ W\ m^{-2}\ K^{-1}$

(*ii*) Find contribution of the various resistances

$$\sigma_D^2 = \frac{1}{30\ (1-0.4)} \frac{(3.6)(1013)(0.08)^2}{(0.5)(60)} + \frac{1}{3(1-0.4)} \frac{(3.6)(1013)(0.08)}{(66.35)\ (60)} + \frac{0.08}{60}$$

$$= \underset{(51\%)}{0.0432} + \underset{(48\%)}{0.0407} + \underset{(1\%)}{0.0013} = 0.0852$$

or $1/\sigma_D^2 = 11.737$

(*iii*) Find the single pass efficiency from(Figure 3.2)

$$\eta_s = 0.887 \text{ at } \tau_i = 1.0$$

2. Effects of ± 30% variations in heat transfer parameters (K_g, K_s, h, etc.) on $1/\sigma_D^2$ and η_s: See Table 6.1.

The effects on $1/\sigma_D^2$ and η_s caused from the variations in K_ρ and h_ρ are more significant than the variations in K_g. All errors in η_s are within ±2% in this example. Because the performance curve is getting smoother in large $1/\sigma_D^2$ values, so the errors will be reduced for long regenerators. Similar analysis can be performed for the errors in η_o of cocurrent and countercurrent operations.

We can see that the solid film resistance is not the only one dominating factor in our example. Actually, for small particles of highly conductive solids film resistances may well dominate; however, for large particles of poorly conducting solids conduction into those solids may become the major factor.

Table 6.1

Errors in $1/\sigma_D^2$ and η_s with ±30% Variations in Heat Transfer Parameters

	σ_D^2 particle conduction	σ_D^2 film resistance	σ_D^2 gas dispersion	σ_D^2	$1/\sigma_D^2$	$\eta_{s_{\tau_i = 1.0}}$	Error
K_g = 0.0338 (30%)	55%	43%	2%	0.0786	12.723	0.891	0.45%
K_g = 0.0182 (-30%)	45%	54%	1%	0.0962	10.395	0.876	-1.24%
K_ρ = 0.65 (30%)	44%	54%	2%	0.0752	13.298	0.896	1.01%
K_ρ = 0.35 (-30%)	59%	39%	2%	0.1037	9.643	0.870	-1.92%
h_ρ = 86.255 (30%)	57%	41%	2%	0.0758	13.193	0.895	0.90%
h_ρ = 46.445 (-30%)	42%	57%	1%	0.1026	9.747	0.872	-1.69%

percentage of total σ_D^2

The contribution of axial dispersion for flow is usually negligible in most situations. But it can become a significant factor for very slow flow of gases.

6.4 DESIGN OPTIMIZATION

1. The results show that the optimal efficiency for the countercurrent case, which occurs at infinitesimally short switching time, is always higher than the optimal efficiency of the cocurrent case, which is obtained approximately at the switching time equal to the thermal mean residence time. When the same switching time is used in both operations countercurrent flow gives higher efficiency than cocurrent flow. Under these conditions, however, the two operations approach the same efficiency when the switching time is long enough such as $\tau_i \geq 1.4$ for the symmetric case, and $\tau_h \geq 1.7$ ($\mu_h/\mu_c = 0.5$) or $\tau_h \geq 1.1$ ($\mu_h/\mu_c = 2.0$) for the unbalanced case.
2. For countercurrent operations the longer the exchanger (the larger $1/\sigma_D^2$) the higher will be its efficiency, with a limiting value given by the ideal regenerators, while for some cases in cocurrent operation the thermal efficiency decreases with increasing $1/\sigma_D^2$.
3. The maximum overall efficiencies of ideal regenerators from Figure 2.5 show that the best operation is at $\mu_h/\mu_c = 1.0$, i.e. equal product of mass flow rate and specific heat, for both cocurrent and countercurrent operations.
4. The optimal switching time required to get the maximum overall thermal efficiency of real regenerators is:

   (*i*) symmetric case ($\mu_h/\mu_c = 1.0$):

—— cocurrent operations: $\tau_i \cong 1.0$

—— countercurrent operations: $\tau_i \to 0$

(*ii*) unbalanced case:

—— cocurrent operations: τ_h as shown in Figure 6.1

—— countercurrent operations: $\tau_h \to 0$

Real regenerators at all values of the variance, σ_D^2, have highest efficiency at $\mu_h/\mu_c = 1$. This maximum efficiency approaches that of ideal regenerators at large $1/\sigma_D^2$ as evident from Figure 6.1. The optimal switching time for cocurrent operations is a little higher than μ_h at $\mu_h/\mu_c = 1.0$ and will approach to μ_h when the regenerators are long enough. At $\tau_i = 1$ countercurrent flow is somewhat better than cocurrent at a given $1/\sigma_D^2$ but the difference never exceeds 10% and it becomes lower at higher values of $1/\sigma_D^2$.

The ratio $\dfrac{\eta_{reg}(\tau_i=0) - \eta_{reg}(\tau_i=1.0)}{\eta_{reg}(\tau_i=1.0)}$ for countercurrent flow is always lower than 15%. Hence, using $\tau_i \to 0$ may be quite an impractical way to raise efficiency.

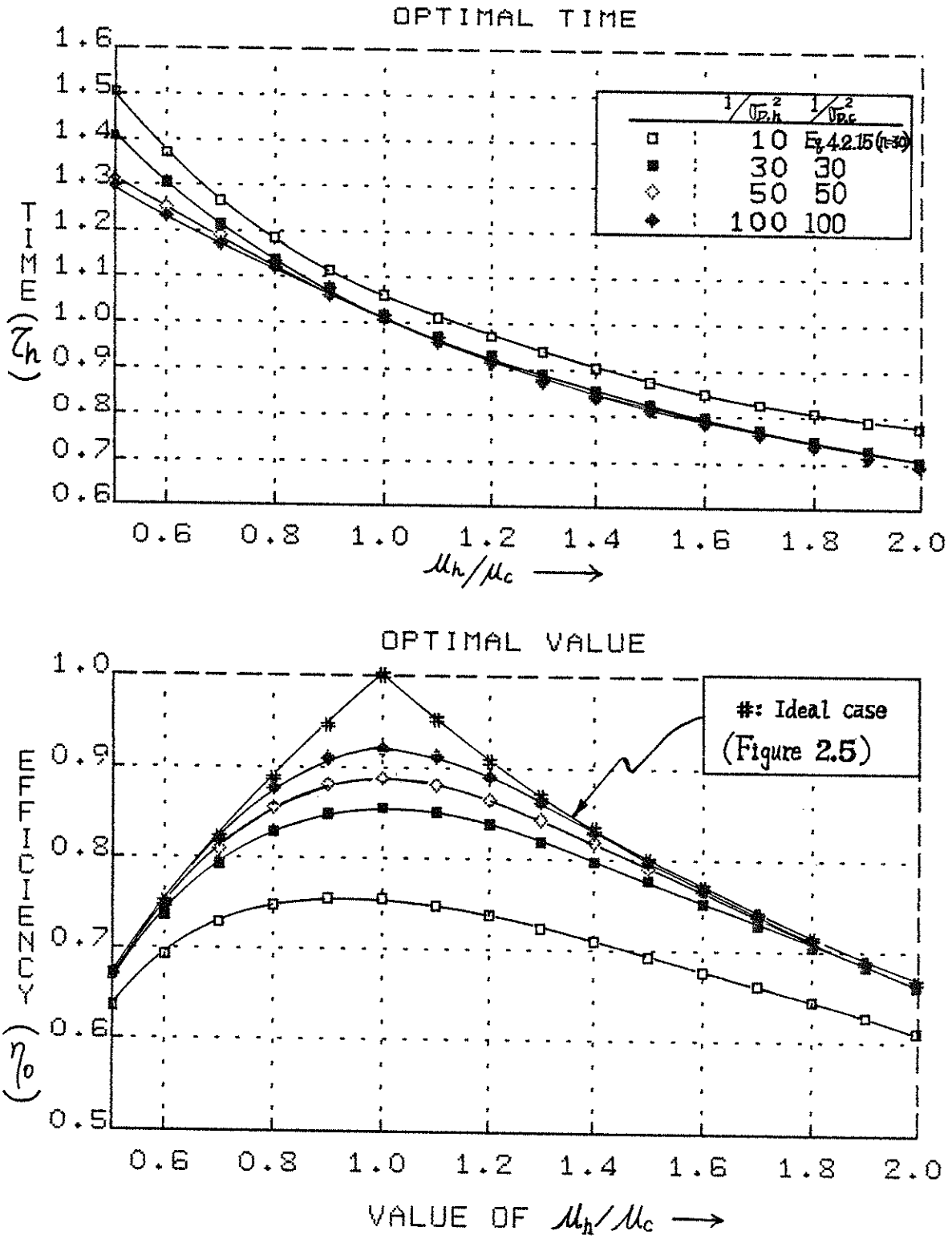

FIGURE 6.1 OPTIMAL SWITCHING TIME AND MAXIMUM EFFICIENCIES FOR COCURRENT OPERATIONS

7. CONCLUSIONS

The new method using the approximate solutions in terms of the variance of the impulse response and the principle of superposition gives us an easy, fast way for calculation of the regenerator performance in cocurrent operation. Compared with other studies from the literature the results tell us that the regenerator performance for long regenerators ($1/\sigma_D^2 > 5.0$) is primarily a function of $1/\sigma_D^2$ and switching time conditions only. This allows us to calculate the regenerator performance in cocurrent operation by using this method for any complex model when the variance is available. For short regenerators the results can still be used with maximum deviation not exceeding 20% or we need to consider the actual model in order to find the exact performance.

The closed method using the n-staged fluidized beds model enables us to calculate the regenerator performance in countercurrent flow which we are unable to obtain from the above method. This model can be used for large n as an approximation to fixed solids regenerators. The model is especially useful for representation of actual staged fluidized beds used for situations when gases carry a considerable amount of particulates.

For packed bed regenerator models that treat the solids as a discrete medium the variance is additive for various heat transfer resistance. We find that the solids film resistance is not the only factor in determining regenerator efficiency. The solids conduction redistance may become the major factor for large particles or the

contribution of axial dispersion can become a significant factor for slow flow of gases. We can predict how changes in system geometry and heat transfer parameters affect the relative heat transfer resistance and change the thermal efficiency. Generally, the smaller the variance (large $1/\sigma_D^2$) the higher will be its efficiency.

Countercurrent operation is more efficient than cocurrent operation. However, only for some cases cocurrent operation is preferred from constructional or operational considerations. The thermal efficiency for countercurrent operation always increases with decreasing switching time and is at a maximum at infinitely fast switching ($\tau_i \to 0$) for both symmetric and unbalanced regenerators.

Results show that the optimal operation is always at $\mu_h/\mu_c = 1.0$ (i.e. symmetric regenerators) for both cocurrent and countercurrent operations. In this case, we should set the switching time always around the thermal mean residence time ($\tau_i \simeq 1.0$) in cocurrent operation to get the maximal thermal efficiency. For countercurrent case optimal operation is at $\tau_i \to 0$ but the difference in efficiency is never more than 15% of the efficiency at $\tau_i = 1.0$. Hence, using thermal mean residence time as switching time is best from the practical standpoint.

In case of operations at $\mu_h/\mu_c \neq 1.0$ (i.e. unbalanced regenerators) the optimal switching times to get the maximal overall thermal efficiency in cocurrent operation are given in Figure 6.1 with different μ_h/μ_c values. One should always keep in mind that the maximal thermal efficiency can reach at most the value of ideal regenerators which is readily found from Figure 2.1.

8. NOMENCLATURE

Symbol	Definition	Unit
a_s	external particle surface area per unit volume of packed bed regenerator, $(1+\nu)/R$ for Model IA and $(1-\varepsilon)(1+\nu)/r_{\rho o}$ for Model IB.	(m^{-1})
Bi_{es}	Biot number for heat losses between solids and surroundings, $h_e L/K_{esz}$ for model IA.	
Bi_{wg}	Biot number for heat losses between the gas and the wall, $h_{wg} R/K_{egr}$ for Model IA.	
Bi_{ws}	Biot number for heat losses between solids and the wall, $h_{ws} R/K_{esr}$ for Model IA.	
Bi_ρ	Biot number for heat losses between the gas and solid particles, $h_\rho r_{\rho o}/K_\rho$ for model IB.	
Bi_s'	Biot number for heat losses between the plates and surroundings, $h_e L/K_{sz}'$ for model IIA.	
Bi'	Biot number for heat losses between the gas and the plate, hR_ρ/K_{esx}' for model IIB.	
C_{pg}	Specific heat of gas stream	(J/Kg^oK)
C_{pc}	Specific heat of cold gas stream	(J/Kg^oK)
C_{ph}	Specific heat of hot gas stream	(J/Kg^oK)
C_{ps}	Specific heat of solids	(J/Kg^oK)
d_p	Diameter of spherical particles, $2r_{\rho o}$	(m)
d_c	Smallest height of the rectangular channel, $2r_c$	(m)
$E(\theta)$	Impulse response; Equations 3.1.2 and 3.2.4.	
$E(\tau)$	Impulse response based on dimensionless time.	

8. NOMENCLATURE
(Continued)

Symbol	Definition	Unit
$\bar{E}(s), \bar{E}^{(T)}(s)$	Laplace transformation of dimensionless impulse response for n-staged fluidized bed model; Equation 4.2.7 based on the thermal mean residence time of a single volume or Equation 4.2.11 based on the total thermal mean residence time.	
$erf(\theta)$	Error function.	
$erfc(\theta)$	Complementary error function, $1-erf(\theta)$.	
$e_K(\tau)$	Special summation function, $\sum_{j=0}^{K} \tau^j/j!$	
G_g	Mass rate of gas flow per unit area, $\rho_g u_g$.	(Kgm^2/s)
$H(\theta)$	Heaviside unit step function.	
h	Heat transfer coefficient.	$(W/m^{2o}K)$
h_e	Heat transfer coefficient for film between solids and surroundings, Model IA.	$(W/m^{2o}K)$
h_{wg}	Heat transfer coefficient for film between the gas and the wall, Model IA .	$(W/m^{2o}K)$
h_{ws}	Heat transfer coefficient for film between solids and the wall, Model IA.	$(W/m^{2o}K)$
h_ρ	Heat transfer coefficient for film between the gas and solid particles, Model IB.	$(W/m^{2o}K)$
K_{egz}, K_{esz}	Effective thermal conductivity of the gas and solids respectively in the axial direction, Models IA and IB.	(W/m K)
K_{egr}, K_{esr}	Effective thermal conductivity of the gas and solids respectively in the radial direction, Models IA and IB.	(W/m K)
K_ρ	Thermal conductivity of the solid particle, Model IB.	(W/m K)

8. NOMENCLATURE
(Continued)

Symbol	Definition	Unit
K_{gz}', K_{sz}'	Thermal conductivity of the gas and plates respectively in the direction of flow, Models IIA and IIB.	(W/m K)
K_{gx}', K_{sx}'	Thermal conductivity of the gas and plates respectively in the direction perpendicular to the flow, Models IIA and IIB.	(W/m K)
K_{esx}'	Effective thermal conductivity of plates in the direction perpendicular to the flow, Model IIB.	(W/m K)
K_{egz}'	Effective thermal conductivity of the gas in the direction of flow, Model IIB.	(W/m K)
L	Length of heat regenerator.	(m)
ℓ	Dimensionless length, L/R.	
M_s	Total mass of solids.	(Kg)
$\dot{m}_c$	Mass flow rate of cold gas stream.	(Kg/s)
$\dot{m}_h$	Mass flow rate of hot gas stream.	(Kg/s)
P(a;x)	Incomplete gamma function.	
$\mathcal{P}(X^2/D)$	Chi-square probability distribution function.	
Pe_{gz}	Peclet number for the axial dispersion of the gas, $LG_g C_{pg}/K_{egz}$ for Models IA and IB.	
Pe_{gr}	Peclet number for the radial dispersion of the gas, $RG_g C_{pg}/K_{egr}$ for Models IA and IB.	
Pe_{sz}	Peclet number for the axial dispersion of the solid, $LG_g C_{pg}/K_{esz}$ for Model IA.	
Pe_{sr}	Peclet number for the radial dispersion of the solid, $RG_g C_{pg}/K_{esr}$ for Model IA.	

8. NOMENCLATURE
(Continued)

Symbol	Definition	Unit
Pe_{ρ}	Radial Peclet number in the solid particle, $r_{\rho o} G_g C_{pg} / K_{\rho}(1-\varepsilon)$ for Model IB.	
Pe_{gz}'	Peclet number for the heat conduction of the gas in the direction of flow, $LG_g C_{pg} / K_{gz}'$ for Model IIA.	
Pe_{gx}'	Peclet number for the heat conduction of the gas in the direction perpendicular to the flow. $r_c G_g C_{pg} / K_{gx}'$ for Model IIA.	
Pe_{sz}'	Peclet number for the heat conduction of plates in the direction of flow, $LG_g C_{pg} / K_{sz}'$ for Models IIA and IIB.	
Pe_{sx}'	Peclet number for the heat conduction of plates in the direction perpendicular to the flow, $R_{\rho} G_g C_{pg} / K_{sx}'$ for Models IIA and IIB.	
Pe_{go}'	Peclet number for the axial dispersion of the gas, $LG_g C_{pg} / K_{egz}'$ for Model IIB.	
$Q, (Q_h, Q_c)$	Heat actually exchanged, (for heating and cooling period).	(W)
$Q_{id}, (Q_{h,id}, Q_{c,id})$	Ideal amount of heat exchanged, (for heating and cooling period).	(W)
R	Radius of the regenerator's column.	(m)
r	Radial coordinate in the bed.	(m)
R_{ρ}	Half thickness of the plates around the rectangular channel.	(m)
r_c	Half height of the rectangular channel.	(m)
$r_{\rho o}$	Radius of the solid particles.	
r_{ρ}	Radial coordinate in solid particles	(m)
St	Stanton number, $h a_s L / C_g C_{pg}$ for Model IA.	

8. NOMENCLATURE
(Continued)

Symbol	Definition	Unit
St_ρ	Stanton number, $h_\rho a_s L/G_g C_{pg}$ for Model IB.	
St'	Stanton number, $h/G_g C_{pg}$ for Model IIB.	
T	Length unit in plate regenerators, $r_c + R_\rho$.	(m)
$T_g, (t_g)$	Gas temperature, (normalized $T_g - T_{go}/T_{gi} - T_{go}$).	(^oK)
$T_s, (t_s)$	Solid temperature, (normalized $T_s - T_{go}/T_{gi} - T_{go}$).	(^oK)
$T_w, (t_w)$	Wall temperature, (normalized $T_w - T_{go}/T_{gi} - T_{go}$).	(^oK)
$T_a, (t_a)$	Ambient temperature, (normalized $T_a - T_{go}/T_{gi} - T_{go}$).	(^oK)
$T_\rho, (t_\rho)$	Particle temperature, (normalized $T_\rho - T_{go}/T_{gi} - T_{go}$).	(^oK)
T_{go}	Initial gas temperature.	(^oK)
T_{gi}	Inlet gas temperature.	(^oK)
$T_{c,i}$, $T_{c,e}$	Inlet and exit temperature of cold gas.	(^oK)
$T_{h,i}$, $T_{h,e}$	Inlet and exit temperature of hot gas.	(^oK)
$t_{c,e}$	Normalized exit cold gas temperature, $T_{c,e} - T_{c,i}/T_{h,i} - T_{c,i}$.	

8. NOMENCLATURE
(Continued)

Symbol	Definition	Unit
$t_{h,e}$	Normalized exit hot gas temperature, $T_{h,e}-T_{c,i}/T_{h,i}-T_{c,i}$.	
$\bar{T}_{s,o}$, $\bar{T}_{s,f}$	Average solid temperature at the beginning and end of the heating period, respectively.	(^{o}K)
$t_{in}(\theta)$, $t_{in}(\tau)$	Periodic input of dimensionless gas temperature in the cocurrent operation based on dimensional and dimensionless time, respectively.	
$t_{ex}(\theta)$, $t_{ex}(\tau)$	Exit dimensionless gas temperature by applying the superposition principle in the cocurrent operation, based on dimensional and dimensionless time, respectively.	
$t_{gm}(\tau)$	Dimensionless gas temperature in n-staged fluidized bed model.	
$t_{sm}(\tau)$	Dimensionless solid temperature in n-staged fluidized bed model.	
$t_{sm}^{(I)}$, $t_{sm}^{(II)}$ t_{sm} (m=1,2,..,n)	Stationary state solid temperature profiles at the beginning and the end of the heating period, respectively.	
u_g	Gas velocity in packed bed regenerators.	(m/s)
$\bar{u}_g'$	Gas velocity in plate regenerators.	(m/s)
$u(\theta)$	Step response; Equations 3.1.10a and 3.2.5a for approximate solution, Equations 4.2.18 for n-staged fluidized bed model.	
$u(\theta)$	Step response based on dimensionless time.	
$u_h(\theta)$, $u_h(\tau)$	Step response for heating period.	
$u_c(\theta)$, $u_c(\tau)$	Step response for cooling period.	

8. NOMENCLATURE
(Continued)

Symbol	Definition	Unit
x	Coordinate of plate regenerators in the direction perpendicular to the flow.	
z	Axial coordinate of regenerators.	

Greek Symbols

Symbol	Definition	Unit
ξ	dimensionless axial coordinate of regenerators, z/L	
η	dimensionless radial coordinate of regenerators, r/R	
φ	dimensionless radial coordinate in solid particles, $r_\rho/r_{\rho o}$	
η'	dimensionless coordinate of plate regenerators in the direction perpendicular to the flow, x/T	
ψ	dimensionless group, $\varepsilon\rho_g C_{pg}/(1-\varepsilon)\rho_s C_{ps}$ for packed bed regenerators	
ψ'	dimensionless group, $\rho_g C_{pg}/\rho_s C_{ps}$ for plate regenerators	
ν	shape factor	
ε	voidage	
θ	coordinate of real time	(s)
θ_a	appearance time in packed bed regenerators, $\varepsilon L/u_g$	(s)
θ_a'	appearance time in plate regenerators, $L/\bar{u}_g'$	(s)
τ	dimensionless time coordinate for packed bed regenerators, $\psi\theta/\theta_a$	
τ'	dimensionless time coordinate for plate regenerators, $\psi'\theta/\theta_a'$	
μ, μ_i	mean of the exit gas temperature distribution for single pass operation and symmetric periodic operation, respectively	
μ_h	mean of the exit gas temperature impulse response for heating period	
μ_c	mean of the exit gas temperature impulse response for cooling period	

Greek Symbols
(continued)

Symbol	Definition	Unit
$\theta_i, (\tau_i)$	real switching time for single pass operation or symmetric periodic operation, (dimensionless θ_i/μ or θ_i/μ_i)	
$\theta_h, (\tau_h)$	real switching time for heating period, (dimensionless θ_h/μ_h)	
$\theta_c, (\tau_c)$	real switching time for cooling period, (dimensionless θ_c/μ_c)	
τ_p	dimensionless quantity, $\tau_h + \tau_c$	
σ^2	variance of the exit gas temperature distribution	
$\sigma_D{}^2$	dimensionless variance of the exit gas temperature distriubtion for single pass operation or symmetric periodic operation, σ^2/μ^2 or $\sigma^2/\mu_i{}^2$	
$\sigma_{D,h}{}^2$	dimensionless variance for heating period, $\sigma_h{}^2/\mu_h{}^2$	
$\sigma_{D,c}{}^2$	dimensionless variance for cooling period, $\sigma_c{}^2/\mu_c{}^2$	
η_{th}	definition of thermal efficiency of regenerators, Equation 2.2.6	
η_h	thermal efficiency for the heating period	
η_c	thermal efficiency for the cooling period	
η_s	thermal efficiency for single pass operation	
η_o	overall thermal efficiency, Equation 2.2.11	
β	Stanton number of the individual bed in the n-staged fluidized bed model, Equation 4.2.4	
β_h	Stanton number for the heating period	

Greek Symbols
(continued)

Symbol	Definition	Unit
β_c	Stanton number for the cooling period	
λ	dimensionless quantity, $\beta/1+\beta)$	
λ_h	dimensionless quantity, $\beta_h/(1+\beta_h)$	
λ_c	dimensionless quantity, $\beta_c/(1+\beta_c)$	
$\gamma(\tau_i),\gamma_h(\tau_i)$, $\gamma_c(\tau_i)$	special functions, Equations 4.2.21, 4.2.42 and 4.2.43, respectively	

9. REFERENCES

1. Anzelius, A., "Über Erwarmung Vermittels Durchströmender Medien," Z. Angew. Math. Mech., Vol. 6, 1926, p. 291.

2. Bahnke, G. D. and C. P. Howard, "The Effect of Longitudinal Heat Conduction on Periodic-Flow Heat Exchanger Performance," J. Eng. Power, April 1964, pp. 105-120.

3. Hausen, H., "Über die Theorie des Wärmeaustausches in Regeneratoren," Z. Angew. Math. Mech., Vol. 9, 1929, p. 173.

4. Hausen, H., "Über den Wärmeaustausch in Regeneratoren," Tech. Mech. Thermodynam., Vol. 1, 1930, p. 219.

5. Hausen, H., "Vervollständigte Berechnung des Wärmeaustausches in Regeneratoren," Z. Ver. Deutsch, Ing., Betheft Verftk No. 2, 1942, pp. 31-43.

6. Hausen, H., "Wärmeübertragung im Gegenstron, Gleichstron und Krenzstrom," Springer-verlag, Berlin, 1950.

7. Hulburt, H. M. and S. Katz, "Some Problems in Particle Technology: A Statistical Mechanical Formulation", Chem. Eng. Sci., 19 (1964) 555.

8. Handley, D. and P. J. Heggs, "The Effect of Thermal Conductivity of the Packing in Transient Heat Transfer in a Fixed Bed," Int. J. Heat Mass Transfer, Vol. 12, 1969, pp. 549-570.

9. Iliffe, C. E., "Thermal Analysis of Counterflow Regenerative Heat Exchanger," J. Inst. Mech. Eng., Vol. 159, (1948), pp. 363-372.

10. Jakob, L. M., Heat Transfer, Vol. II, Wiley, (1955).

11. Klinkenberg, A., "Heat Transfer in Cross-Flow Heat Exchangers and Packed Beds," Ind. Eng. Chem., Vol. 46, 1954, p. 2285.

12. Kubin, M., "Coll. Czech. Chem. Commun.," 30 (1964), 1104, 2900.

13. Kucera, E., "J. Chromatogr.," 19 (1965) 237.

14. Kardas, A., "On a Problem in the Theory of the Unidirectional Regenerator," Int. J. Heat Mass Transfer, Vol. 19, 1966, p. 567.

15. Kumar, M., "Periodic Response of a Parallel Flow, Solid Sensible Heat Thermal Storage Unit," M.S. thesis, Penn. State Univ., University Park, PA, 1978.

16. Larsen, F. W., "Rapid Calculations of Temperature in a Regenerative Heat Exchanger Having Arbitrary Initial Solid and Entering Fluid Temperatures," Int. J. Heat Mass Transfer, Vol. 10, 1967, p. 149.

9. REFERENCES
(Continued)

17. Levenspiel, O. J., Chemical Reaction Engineering, 2nd Edition, Wiley, (1972).

18. Levenspiel, O. J., The Chemical Reactor Omnibook, OSU Bookstore, (1979).

19. Levenspiel, O. J., personal communication.

20. Linek, F. and M. P. Dudukovič, "Representation of Breakthrough Curves for Fixed-Bed Adsorbers and Reactors Using Moments of Impulse Response," Chem. Eng. J., 23 (1982) 31-36.

21. Nusselt, W., "Die Theorie des Winderhitzers," Z. Ver. Deutsch Ing. Vol. 71, 1927, pp. 85-91.

22. Nahavandi, A. N. and A. S. Weinstein, "A Solution to the Periodic-Flow Regenerative Heat Exchanger Problem," Appl. Sci. Res., Vol. A10, (1961), pp. 335-348.

23. Roy, D. and G. Gidaspow, "Prediction of Nusselt Numbers for Regenerators with Fully Developed Velocity Profiles," AIChE/ASME Heat Transfer Conference, 1970.

24. Razavi, M. S., B. J. McCoy and R. G. Carbonell, "Moment Theory of Breakthrough Curves for Fixed-Bed Adsorbers and Reactors," Chem. Eng. J., 16, (1978) 211-222.

25. Schumann, T. E. W., "Heat Transfer: A Liquid Flowing Through a Porous Prism," J. Franklin Inst., Vol. 208, (1929).

26. Sagara, M., P. Schneider and J. M. Smith, "The Determination of Heat-Transfer Parameters for Flow in Packed Beds Using Pulse Testing and Chromatography Theory," Chem. Eng. J., (1), 47, (1970).

27. Schmidt, F. W. and J. Szego, "Transient Response of a Hollow Cylindrical-Cross-Section Solid Sensible Heat Storage Unit-Single Fluid," J. Heat Transfer, Trans. ASME, Vol. 100, 1978, p. 737.

28. Schmidt, F. W. and A. J. Willmott, Thermal Energy Storage and Regeneration, McGraw-Hill, 1981.

29. Willmott, A. J., "The Regenerative Heat Exchanger Computer Representation," Int. J. Heat Mass Transfer, Vol. 12, 1969, pp. 997-1014.

30. Willmott, A. J. and R. J. Thomas, "Analysis of the Long Contra-flow Regenerative Heat Exchanger," J. Inst. Math. Appl., Vol. 14, 1974, pp. 267-280.

10. ACKNOWLEDGEMENT

I would like to express my sincere gratitude to Professor M. P. Duduković for his invaluable guidance and encouragement during the pursuit of this work.

The financial support from the Industry and the Department of Chemical Engineering is also greatly appreciated.

I also wish to thank several persons for providing various forms of support. Ming-Der Lu, I. P. Wang and Yoshio Yamashita were all very helpful in several aspects of my work. Especially the Plot-Subroutine in DEC-20 system designed by Yoshio is greatly appreciated.

Finally I would like to thank my family, although they are far away in Taiwan, for providing moral support during my studies at Washington University.

11. APPENDICES

A. Single pass efficiency.

$$\eta_s(\theta_i) = \frac{1}{\theta_i}\int_0^{\theta_i}\left[1 - P\left(\frac{\mu^2}{\sigma^2}; \frac{\mu}{\sigma^2}\theta\right)\right] d\theta$$

and

$$P\left(\frac{\mu^2}{\sigma^2}; \frac{\mu}{\sigma^2}\theta\right) = \frac{1}{\Gamma\left(\frac{\mu^2}{\sigma^2}\right)}\int_0^{\frac{\mu}{\sigma^2}\theta} u^{\frac{\mu^2}{\sigma^2}-1} e^{-u}\, du$$

First,

$$\int_0^{\theta_i}\left[1 - P\left(\frac{\mu^2}{\sigma^2}; \frac{\mu}{\sigma^2}\theta\right)\right] d\theta$$

$$= \frac{1}{\Gamma\left(\frac{\mu^2}{\sigma^2}\right)}\int_0^{\theta_i} d\theta \int_{\frac{\mu}{\sigma^2}\theta}^{\infty} u^{\frac{\mu^2}{\sigma^2}-1} e^{-u}\, du$$

(changing the order of integration)

$$= \frac{1}{\Gamma\left(\frac{\mu^2}{\sigma^2}\right)}\left\{\int_0^{\infty} u^{\frac{\mu^2}{\sigma^2}-1} e^{-u} du \int_0^{\frac{\sigma^2}{\mu}u} d\theta - \int_{\frac{\mu}{\sigma^2}\theta_i}^{\infty} u^{\frac{\mu^2}{\sigma^2}-1} e^{-u} du \int_{\theta_i}^{\frac{\sigma^2}{\mu}u} d\theta\right\}$$

$$= \frac{1}{\Gamma\left(\frac{\mu^2}{\sigma^2}\right)}\left\{\frac{\sigma^2}{\mu}\Gamma\left(\frac{\mu^2}{\sigma^2}+1\right) - \frac{\sigma^2}{\mu}\Gamma\left(\frac{\mu^2}{\sigma^2}+1\right)\left[1 - P\left(\frac{\mu^2}{\sigma^2}+1; \frac{\mu}{\sigma^2}\theta_i\right)\right]\right.$$

$$\left. + \theta_i\Gamma\left(\frac{\mu^2}{\sigma^2}\right)\left[1 - P\left(\frac{\mu^2}{\sigma^2}; \frac{\mu}{\sigma^2}\theta_i\right)\right]\right\}$$

(using the recurrence formula for the Gamma function $\Gamma(n+1)=n\Gamma(n)$)

$$= \mu P\left(\frac{\mu^2}{\sigma^2}+1; \frac{\mu}{\sigma^2}\theta_i\right) + \theta_i - \theta_i P\left(\frac{\mu^2}{\sigma^2}; \frac{\mu}{\sigma^2}\theta_i\right)$$

So, $$\eta_s(\theta_i) = 1 - P\left(\frac{\mu^2}{\sigma^2}; \frac{\mu}{\sigma^2}\theta_i\right) + \frac{\mu}{\theta_i} P\left(\frac{\mu^2}{\sigma^2}+1; \frac{\mu}{\sigma^2}\theta_i\right)$$

Using the recurrence formula for the incomplete Gamma function

$$P(a+1, x) = P(a, x) - \frac{x^a e^{-x}}{\Gamma(a+1)}$$

we have the simpler form:

$$\eta_s(\theta_i) = 1 - P\left(\frac{\mu^2}{\sigma^2}; \frac{\mu}{\sigma^2}\theta_i\right) + \frac{\mu}{\theta_i}\left[P\left(\frac{\mu^2}{\sigma^2}; \frac{\mu}{\sigma^2}\theta_i\right) - \frac{\left(\frac{\mu}{\sigma^2}\theta_i\right)^{\frac{\mu^2}{\sigma^2}} e^{-\frac{\mu}{\sigma^2}\theta_i}}{\frac{\mu^2}{\sigma^2}\Gamma\left(\frac{\mu^2}{\sigma^2}\right)}\right]$$

$$= 1 - \left(1 - \frac{\mu}{\theta_i}\right) P\left(\frac{\mu^2}{\sigma^2}; \frac{\mu}{\sigma^2}\theta_i\right) - \frac{\mu}{\theta_i} \frac{\left(\frac{\mu}{\sigma^2}\theta_i\right)^{\frac{\mu^2}{\sigma^2}} e^{-\frac{\mu}{\sigma^2}\theta_i}}{\Gamma\left(\frac{\mu^2}{\sigma^2}+1\right)}$$

For long heat regenerators ($1/\sigma_D^2 > 15$), we have:

$$E(\theta) \cong \frac{1}{\sigma\sqrt{2\pi}} e^{-\frac{(\theta-\mu)^2}{2\sigma^2}}$$

and $$U(\theta) \cong \frac{1}{2}\left[1 + \operatorname{erf}\left(\frac{\theta-\mu}{\sqrt{2}\sigma}\right)\right] = 1 - \frac{1}{2}\operatorname{erfc}\left(\frac{\theta-\mu}{\sqrt{2}\sigma}\right)$$

so

$$\eta_s(\theta_i) = \frac{1}{\theta_i}\int_0^{\theta_i}\left[1 - U(\theta)\right] d\theta$$

$$\cong \frac{1}{\theta_i}\int_0^{\theta_i} \frac{1}{2}\operatorname{erfc}\left(\frac{\theta-\mu}{\sqrt{2}\sigma}\right) d\theta$$

(change of variable

$$X = \frac{\theta-\mu}{\sqrt{2}\sigma}$$)

$$= \frac{\sqrt{2}\sigma}{2\theta_i}\int_{-\frac{\mu}{\sqrt{2}\sigma}}^{\frac{\theta_i-\mu}{\sqrt{2}\sigma}} \operatorname{erfc} X\, dX$$

$$= \frac{\sqrt{2}\sigma}{2\theta_i}\left[\int_{-\frac{\mu}{\sqrt{2}\sigma}}^{\infty} \operatorname{erfc} X dX - \int_{\frac{\theta_i-\mu}{\sqrt{2}\sigma}}^{\infty} \operatorname{erfc} X dX\right]$$

(repeated integrals of the error function

$$i^n \operatorname{erfc} Z = \int_Z^{\infty} i^{n-1} \operatorname{erfc} t\, dt$$)

$$= \frac{\sqrt{2}\sigma}{2\theta_i}\left[i\operatorname{erfc}\left(\frac{-\mu}{\sqrt{2}\sigma}\right) - i\operatorname{erfc}\left(\frac{\theta_i-\mu}{\sqrt{2}\sigma}\right)\right]$$

(repeated integrals of the error function

$$i^n \operatorname{erfc} Z = \frac{2}{\sqrt{\pi}}\int_Z^{\infty} \frac{(t-Z)^n}{n!} e^{-t^2} dt$$)

$$= \frac{\sqrt{2}\sigma}{2\theta_i}\left[\frac{2}{\sqrt{\pi}}\int_{\frac{-\mu}{\sqrt{2}\sigma}}^{\infty}\left(t+\frac{\mu}{\sqrt{2}\sigma}\right)e^{-t^2}dt - \frac{2}{\sqrt{\pi}}\int_{\frac{\theta_i-\mu}{\sqrt{2}\sigma}}^{\infty}\left(t-\frac{\theta_i-\mu}{\sqrt{2}\sigma}\right)e^{-t^2}dt\right]$$

$$= \frac{\sqrt{2}\sigma}{\theta_i\sqrt{\pi}}\left\{\frac{1}{2}\left[e^{-\frac{\mu^2}{2\sigma^2}} - e^{-\frac{(\theta_i-\mu)^2}{2\sigma^2}}\right]\right.$$

$$\left. + \frac{\sqrt{\pi}}{2}\left[\frac{(\theta_i-\mu)}{\sqrt{2}\sigma}\operatorname{erfc}\left(\frac{\theta_i-\mu}{\sqrt{2}\sigma}\right) + \frac{\mu}{\sqrt{2}\sigma}\operatorname{erfc}\left(\frac{-\mu}{\sqrt{2}\sigma}\right)\right]\right\}$$

$$= \frac{\sigma}{\theta_i\sqrt{2\pi}}\left[e^{-\frac{\mu^2}{2\sigma^2}} - e^{-\frac{(\theta_i-\mu)^2}{2\sigma^2}}\right]$$

$$+ \frac{1}{2\theta_i}\left[(\theta_i-\mu)\operatorname{erfc}\left(\frac{\theta_i-\mu}{\sqrt{2}\sigma}\right) + \mu\operatorname{erfc}\left(\frac{-\mu}{\sqrt{2}\sigma}\right)\right]$$

$$= \frac{\mu}{2\theta_i}\left[\frac{\theta_i}{\mu} + \operatorname{erf}\left(\frac{\mu}{\sqrt{2}\sigma}\right) - \left(\frac{\theta_i}{\mu}-1\right)\operatorname{erf}\left(\frac{\theta_i-\mu}{\sqrt{2}\sigma}\right)\right]$$

$$- \frac{\sigma}{\theta_i\sqrt{2\pi}}\left[e^{-\frac{(\theta_i-\mu)^2}{2\sigma^2}} - e^{-\frac{\mu^2}{2\sigma^2}}\right]$$

B. Principle of superposition .

—— Equal product of mass flow rate and specific heat, symmetric case .

Input : $t_{in}(\theta) = \sum_{n=0}^{\infty} \left[H(\theta - 2n\theta_i) - H(\theta - (2n+1)\theta_i) \right]$

Output: $t_{ex}(\theta) = \sum_{n=0}^{\infty} \left[u(\theta - 2n\theta_i) H(\theta - 2n\theta_i) - u(\theta - (2n+1)\theta_i) H(\theta - (2n+1)\theta_i) \right]$

thermal efficiency

$$\eta_h(\theta_i) = \frac{1}{\theta_i} \int_{2N\theta_i}^{(2N+1)\theta_i} \left[t_{in}(\theta) - t_{ex}(\theta) \right] d\theta$$

$$= \frac{1}{\theta_i} \sum_{n=0}^{\infty} \left\{ \int_{2N\theta_i}^{(2N+1)\theta_i} \left[1 - u(\theta - 2n\theta_i) \right] H(\theta - 2n\theta_i)\, d\theta - \int_{2N\theta_i}^{(2N+1)\theta_i} \left[1 - u(\theta - (2n+1)\theta_i) \right] H(\theta - (2n+1)\theta_i)\, d\theta \right\}$$

$$= \frac{1}{\theta_i} \sum_{n=0}^{N-1} \left\{ \int_{2(N-n)\theta_i}^{(2(N-n)+1)\theta_i} \left[1 - u(x) \right] dx - \int_{(2(N-n)-1)\theta_i}^{2(N-n)\theta_i} \left[1 - u(x) \right] dx \right\} + \frac{1}{\theta_i} \int_0^{\theta_i} \left[1 - u(x) \right] dx$$

$$= \eta_s(\theta_i) + \frac{1}{\theta_i} \sum_{n=0}^{N-1} \left\{ \int_0^{(2(N-n)+1)\theta_i} \left[1 - u(x) \right] dx - 2 \int_0^{2(N-n)\theta_i} \left[1 - u(x) \right] dx + \int_0^{(2(N-n)-1)\theta_i} \left[1 - u(x) \right] dx \right\}$$

From single pass efficiency, Appendix A,

$$\frac{1}{\theta_i} \int_0^{(2(N-n)+1)\theta_i} \left[1 - u(x) \right] dx = 1 - \left(1 - \frac{\mu}{\theta_i} \right) P\left(\frac{\mu^2}{\sigma^2}; \frac{\mu}{\sigma^2} (2(N-n)+1)\theta_i \right) + 2(N-n) \left[1 - P\left(\frac{\mu^2}{\sigma^2}; \frac{\mu}{\sigma^2} (2(N-n)+1)\theta_i \right) \right] - \frac{\mu}{\theta_i} \frac{\left[\frac{\mu}{\sigma^2} (2(N-n)+1)\theta_i \right]^{\frac{\mu^2}{\sigma^2}} e^{-\frac{\mu}{\sigma^2}(2(N-n)+1)\theta_i}}{\Gamma\left(\frac{\mu^2}{\sigma^2} + 1 \right)}$$

$$\frac{1}{\theta_i} \int_0^{2(N-n)\theta_i} \left[1 - u(x) \right] dx = \frac{\mu}{\theta_i} P\left(\frac{\mu^2}{\sigma^2}; \frac{\mu}{\sigma^2} 2(N-n)\theta_i \right) + 2(N-n) \left[1 - P\left(\frac{\mu^2}{\sigma^2}; \frac{\mu}{\sigma^2} 2(N-n)\theta_i \right) \right] - \frac{\mu}{\theta_i} \frac{\left[\frac{\mu}{\sigma^2} 2(N-n)\theta_i \right]^{\frac{\mu^2}{\sigma^2}} e^{-\frac{\mu}{\sigma^2} 2(N-n)\theta_i}}{\Gamma\left(\frac{\mu^2}{\sigma^2} + 1 \right)}$$

$$\frac{1}{\theta_i}\int_0^{(2(N-n)-1)\theta_i}[1-u(x)]dx = -1+\left(1+\frac{\mu}{\theta_i}\right)P\left(\frac{\mu^2}{\sigma^2};\frac{\mu}{\sigma^2}(2(N-n)-1)\theta_i\right)+2(N-n)\left[1-P\left(\frac{\mu^2}{\sigma^2};\frac{\mu}{\sigma^2}(2(N-n)-1)\theta_i\right)\right]$$
$$-\frac{\mu}{\theta_i}\frac{\left[\frac{\mu}{\sigma^2}(2(N-n)-1)\theta_i\right]^{\frac{\mu^2}{\sigma^2}}e^{-\frac{\mu}{\sigma^2}(2(N-n)-1)\theta_i}}{\Gamma\left(\frac{\mu^2}{\sigma^2}+1\right)}$$

and let j = N-n, then

$$\eta_h(\theta_i)=\eta_s(\theta_i)+\sum_{j=1}^{N}\left\{P\left(\frac{\mu^2}{\sigma^2};\frac{\mu}{\sigma^2}(2j-1)\theta_i\right)-P\left(\frac{\mu^2}{\sigma^2};\frac{\mu}{\sigma^2}(2j+1)\theta_i\right)\right.$$
$$+\frac{\mu-2j\theta_i}{\theta_i}\left[P\left(\frac{\mu^2}{\sigma^2};\frac{\mu}{\sigma^2}(2j-1)\theta_i\right)-2P\left(\frac{\mu^2}{\sigma^2};\frac{\mu}{\sigma^2}2j\theta_i\right)+P\left(\frac{\mu^2}{\sigma^2};\frac{\mu}{\sigma^2}(2j+1)\theta_i\right)\right]$$
$$-\frac{\mu}{\theta_i\Gamma\left(\frac{\mu^2}{\sigma^2}+1\right)}\left[\left(\frac{\mu}{\sigma^2}(2j-1)\theta_i\right)^{\frac{\mu^2}{\sigma^2}}e^{-\frac{\mu}{\sigma^2}(2j-1)\theta_i}\right.$$
$$\left.\left.-2\left(\frac{\mu}{\sigma^2}2j\theta_i\right)^{\frac{\mu^2}{\sigma^2}}e^{-\frac{\mu}{\sigma^2}2j\theta_i}+\left(\frac{\mu}{\sigma^2}(2j+1)\theta_i\right)^{\frac{\mu^2}{\sigma^2}}e^{-\frac{\mu}{\sigma^2}(2j+1)\theta_i}\right]\right\}$$

$$=\eta_s(\theta_i)+\frac{1}{\theta_i}\sum_{j=1}^{N}\left\{\left[-\left((2j-1)\theta_i-\mu\right)P\left(\frac{\mu^2}{\sigma^2};\frac{\mu}{\sigma^2}(2j-1)\theta_i\right)+2\left(2j\theta_i-\mu\right)P\left(\frac{\mu^2}{\sigma^2};\frac{\mu}{\sigma^2}2j\theta_i\right)\right.\right.$$
$$\left.-\left((2j+1)\theta_i-\mu\right)P\left(\frac{\mu^2}{\sigma^2};\frac{\mu}{\sigma^2}(2j+1)\theta_i\right)\right]$$
$$-\frac{\mu}{\Gamma\left(\frac{\mu^2}{\sigma^2}+1\right)}\left[\left(\frac{\mu}{\sigma^2}(2j-1)\theta_i\right)^{\frac{\mu^2}{\sigma^2}}e^{-\frac{\mu}{\sigma^2}(2j-1)\theta_i}\right.$$
$$\left.\left.-2\left(\frac{\mu}{\sigma^2}2j\theta_i\right)^{\frac{\mu^2}{\sigma^2}}e^{-\frac{\mu}{\sigma^2}2j\theta_i}+\left(\frac{\mu}{\sigma^2}(2j+1)\theta_i\right)^{\frac{\mu^2}{\sigma^2}}e^{-\frac{\mu}{\sigma^2}(2j+1)\theta_i}\right]\right\}$$

For long heat regenerators ($1/\sigma_D^2 > 15$), we have:

$$u(\theta)\cong 1-\frac{1}{2}\operatorname{erfc}\left(\frac{\theta-\mu}{\sqrt{2}\sigma}\right)$$

From single pass efficiency, Appendix A,

$$\frac{1}{\theta_h}\int_0^{\theta_h}[1-u(x)]dx=\frac{\sigma}{\theta_h\sqrt{2\pi}}\left[e^{-\frac{\mu^2}{2\sigma^2}}-e^{-\frac{(\theta_h-\mu)^2}{2\sigma^2}}\right]+\frac{1}{2\theta_h}\left[(\theta_h-\mu)\operatorname{erfc}\left(\frac{\theta_h-\mu}{\sqrt{2}\sigma}\right)+\mu\operatorname{erfc}\left(\frac{-\mu}{\sqrt{2}\sigma}\right)\right]$$

so,

$$\frac{1}{\theta_i}\int_0^{(2(N-n)+1)\theta_i}[1-u(x)]dx=\frac{\sigma}{\theta_i\sqrt{2\pi}}\left[e^{-\frac{\mu^2}{2\sigma^2}}-e^{-\frac{((2(N-n)+1)\theta_i-\mu)^2}{2\sigma^2}}\right]$$
$$+\frac{1}{2\theta_i}\left[\left((2(N-n)+1)\theta_i-\mu\right)\operatorname{erfc}\left(\frac{(2(N-n)+1)\theta_i-\mu}{\sqrt{2}\sigma}\right)+\mu\operatorname{erfc}\left(\frac{-\mu}{\sqrt{2}\sigma}\right)\right]$$

similar to $\frac{1}{\theta_i}\int_0^{2(N-n)\theta_i}[1-u(x)]\,dx$ and $\frac{1}{\theta_i}\int_0^{(2(N-n)-1)\theta_i}[1-u(x)]\,dx$

and let j = N-n, then

$$\eta_h(\theta_i)=\eta_s(\theta_i)+\frac{1}{\theta_i}\sum_{j=1}^{N}\left\{\frac{1}{2}\left[\left((2j-1)\theta_i-\mu\right)\operatorname{erfc}\left(\frac{(2j-1)\theta_i-\mu}{\sqrt{2}\sigma}\right)\right.\right.$$
$$\left.-2\left(2j\theta_i-\mu\right)\operatorname{erfc}\left(\frac{2j\theta_i-\mu}{\sqrt{2}\sigma}\right)+\left((2j+1)\theta_i-\mu\right)\operatorname{erfc}\left(\frac{(2j+1)\theta_i-\mu}{\sqrt{2}\sigma}\right)\right]$$
$$\left.-\frac{\sigma}{\sqrt{2\pi}}\left[e^{-\frac{((2j-1)\theta_i-\mu)^2}{2\sigma^2}}-2e^{-\frac{(2j\theta_i-\mu)^2}{2\sigma^2}}+e^{-\frac{((2j+1)\theta_i-\mu)^2}{2\sigma^2}}\right]\right\}$$

C. Principle of superposition.

—— Unequal product of mass flow rate and specific heat, same switching time, unbalanced case.

Input: $t_{in}(\tau) = \sum_{n=0}^{\infty} \left[H(\tau - n\tau_p) - H(\tau - n\tau_p - \tau_h) \right]$

Output: $t_{ex}(\tau) = \sum_{n=0}^{\infty} \left[u_h(\tau - n\tau_p) H(\tau - n\tau_p) - u_c(\tau - n\tau_p - \tau_h) H(\tau - n\tau_p - \tau_h) \right]$

where $\tau_p = \tau_h + \tau_c = \theta_i / u_h + \theta_i / u_c$

Thermal efficiency:

$$\eta_h(\tau_h) = \frac{1}{\tau_h} \int_{N\tau_p}^{N\tau_p + \tau_h} \left[t_{in}(\tau) - t_{ex}(\tau) \right] d\tau$$

$$= \frac{1}{\tau_h} \sum_{n=0}^{N-1} \left\{ \int_{(N-n)\tau_p}^{(N-n)\tau_p + \tau_h} \left[1 - u_h(x) \right] dx - \int_{(N-n)\tau_p - \tau_h}^{(N-n)\tau_p} \left[1 - u_c(x) \right] dx \right\} + \frac{1}{\tau_h} \int_0^{\tau_h} \left[1 - u_h(x) \right] dx$$

$$= \eta_s(\tau_h) + \frac{1}{\tau_h} \sum_{n=0}^{N-1} \left\{ \int_0^{(N-n)\tau_p + \tau_h} \left[1 - u_h(x) \right] dx - \int_0^{(N-n)\tau_p} \left[1 - u_h(x) \right] dx \right.$$
$$\left. - \int_0^{(N-n)\tau_p} \left[1 - u_c(x) \right] dx + \int_0^{(N-n)\tau_p - \tau_h} \left[1 - u_c(x) \right] dx \right\}$$

From single pass efficiency, Appendix A:

$$\eta_s(\tau_h) = 1 - \left(1 - \frac{1}{\tau_h}\right) P\left(\frac{1}{\sigma_{p,h}^2}; \frac{1}{\sigma_{p,h}^2}\tau_h\right) - \frac{1}{\tau_h} \frac{\left(\frac{1}{\sigma_{p,h}^2}\tau_h\right)^{\frac{1}{\sigma_{p,h}^2}} e^{-\frac{1}{\sigma_{p,h}^2}\tau_h}}{\Gamma\left(\frac{1}{\sigma_{p,h}^2} + 1\right)}$$

$$\frac{1}{\tau_h} \int_0^{(N-n)\tau_p + \tau_h} \left[1 - u_h(x) \right] dx = 1 - \left(1 - \frac{1}{\tau_h}\right) P\left(\frac{1}{\sigma_{p,h}^2}; \frac{1}{\sigma_{p,h}^2}\left[(N-n)\tau_p + \tau_h\right]\right) + \frac{(N-n)\tau_p}{\tau_h} \left[1 - P\left(\frac{1}{\sigma_{p,h}^2}; \frac{1}{\sigma_{p,h}^2}\left[(N-n)\tau_p + \tau_h\right]\right) \right]$$
$$- \frac{1}{\tau_h} \frac{\left(\frac{1}{\sigma_{p,h}^2}\left[(N-n)\tau_p + \tau_h\right]\right)^{\frac{1}{\sigma_{p,h}^2}} e^{-\frac{1}{\sigma_{p,h}^2}\left[(N-n)\tau_p + \tau_h\right]}}{\Gamma\left(\frac{1}{\sigma_{p,h}^2} + 1\right)}$$

$$\frac{1}{\tau_h} \int_0^{(N-n)\tau_p} \left[1 - u_h(x) \right] dx = \frac{1}{\tau_h} P\left(\frac{1}{\sigma_{p,h}^2}; \frac{1}{\sigma_{p,h}^2}\left[(N-n)\tau_p\right]\right) + \frac{(N-n)\tau_p}{\tau_h} \left[1 - P\left(\frac{1}{\sigma_{p,h}^2}; \frac{1}{\sigma_{p,h}^2}\left[(N-n)\tau_p\right]\right) \right]$$
$$- \frac{1}{\tau_h} \frac{\left(\frac{1}{\sigma_{p,h}^2}\left[(N-n)\tau_p\right]\right)^{\frac{1}{\sigma_{p,h}^2}} e^{-\frac{1}{\sigma_{p,h}^2}\left[(N-n)\tau_p\right]}}{\Gamma\left(\frac{1}{\sigma_{p,h}^2} + 1\right)}$$

$$\frac{1}{\tau_h}\int_0^{(N-n)\tau_p}[1-u_c(x)]dx = \frac{1}{\tau_h}P\left(\frac{1}{\sigma_{p,c}^2};\frac{1}{\sigma_{p,c}^2}[(N-n)\tau_p]\right)+\frac{(N-n)\tau_p}{\tau_h}\left[1-P\left(\frac{1}{\sigma_{p,c}^2};\frac{1}{\sigma_{p,c}^2}[(N-n)\tau_p]\right)\right]$$
$$-\frac{1}{\tau_h}\frac{\left(\frac{1}{\sigma_{p,c}^2}[(N-n)\tau_p]\right)^{\frac{1}{\sigma_{p,c}^2}}e^{-\frac{1}{\sigma_{p,c}^2}[(N-n)\tau_p]}}{\Gamma\left(\frac{1}{\sigma_{p,c}^2}+1\right)}$$

$$\frac{1}{\tau_h}\int_0^{(N-n)\tau_p-\tau_h}[1-u_c(x)]dx = -1+\left(1+\frac{1}{\tau_h}\right)P\left(\frac{1}{\sigma_{p,c}^2};\frac{1}{\sigma_{p,c}^2}[(N-n)\tau_p-\tau_h]\right)+\frac{(N-n)\tau_p}{\tau_h}\left[1-P\left(\frac{1}{\sigma_{p,c}^2};\frac{1}{\sigma_{p,c}^2}[(N-n)\tau_p-\tau_h]\right)\right]$$
$$-\frac{1}{\tau_h}\frac{\left(\frac{1}{\sigma_{p,c}^2}[(N-n)\tau_p-\tau_h]\right)^{\frac{1}{\sigma_{p,c}^2}}e^{-\frac{1}{\sigma_{p,c}^2}[(N-n)\tau_p-\tau_h]}}{\Gamma\left(\frac{1}{\sigma_{p,c}^2}+1\right)}$$

let j = N-n

$$\eta_h(\tau_h) = \eta_s(\tau_h)+\sum_{j=1}^{N}\left\{-P\left(\frac{1}{\sigma_{p,h}^2};\frac{1}{\sigma_{p,h}^2}[j\tau_p+\tau_h]\right)+P\left(\frac{1}{\sigma_{p,c}^2};\frac{1}{\sigma_{p,c}^2}[j\tau_p-\tau_h]\right)\right.$$
$$+\frac{1-j\tau_p}{\tau_h}\left[P\left(\frac{1}{\sigma_{p,h}^2};\frac{1}{\sigma_{p,h}^2}[j\tau_p+\tau_h]\right)-P\left(\frac{1}{\sigma_{p,h}^2};\frac{1}{\sigma_{p,h}^2}[j\tau_p]\right)\right]$$
$$+\frac{1-j\tau_p}{\tau_h}\left[-P\left(\frac{1}{\sigma_{p,c}^2};\frac{1}{\sigma_{p,c}^2}[j\tau_p]\right)+P\left(\frac{1}{\sigma_{p,c}^2};\frac{1}{\sigma_{p,c}^2}[j\tau_p-\tau_h]\right)\right]$$
$$-\frac{1}{\tau_h\Gamma\left(\frac{1}{\sigma_{p,h}^2}+1\right)}\left[\left(\frac{1}{\sigma_{p,h}^2}[j\tau_p+\tau_h]\right)^{\frac{1}{\sigma_{p,h}^2}}e^{-\frac{1}{\sigma_{p,h}^2}[j\tau_p+\tau_h]}-\left(\frac{1}{\sigma_{p,h}^2}[j\tau_p]\right)^{\frac{1}{\sigma_{p,h}^2}}e^{-\frac{1}{\sigma_{p,h}^2}[j\tau_p]}\right]$$
$$\left.-\frac{1}{\tau_h\Gamma\left(\frac{1}{\sigma_{p,c}^2}+1\right)}\left[-\left(\frac{1}{\sigma_{p,c}^2}[j\tau_p]\right)^{\frac{1}{\sigma_{p,c}^2}}e^{-\frac{1}{\sigma_{p,c}^2}[j\tau_p]}+\left(\frac{1}{\sigma_{p,c}^2}[j\tau_p-\tau_h]\right)^{\frac{1}{\sigma_{p,c}^2}}e^{-\frac{1}{\sigma_{p,c}^2}[j\tau_p-\tau_h]}\right]\right\}$$

$$=\eta_s(\tau_h)+\frac{1}{\tau_h}\sum_{j=1}^{N}\left\{\left[-(j\tau_p-\tau_h-1)P\left(\frac{1}{\sigma_{p,c}^2};\frac{1}{\sigma_{p,c}^2}[j\tau_p-\tau_h]\right)+(j\tau_p-1)P\left(\frac{1}{\sigma_{p,c}^2};\frac{1}{\sigma_{p,c}^2}[j\tau_p]\right)\right.\right.$$
$$+(j\tau_p-1)P\left(\frac{1}{\sigma_{p,h}^2};\frac{1}{\sigma_{p,h}^2}[j\tau_p]\right)-(j\tau_p+\tau_h-1)P\left(\frac{1}{\sigma_{p,h}^2};\frac{1}{\sigma_{p,h}^2}[j\tau_p+\tau_h]\right)\Big]$$
$$-\frac{1}{\Gamma\left(\frac{1}{\sigma_{p,c}^2}+1\right)}\left[\left(\frac{1}{\sigma_{p,c}^2}[j\tau_p-\tau_h]\right)^{\frac{1}{\sigma_{p,c}^2}}e^{-\frac{1}{\sigma_{p,c}^2}[j\tau_p-\tau_h]}-\left(\frac{1}{\sigma_{p,c}^2}[j\tau_p]\right)^{\frac{1}{\sigma_{p,c}^2}}e^{-\frac{1}{\sigma_{p,c}^2}[j\tau_p]}\right]$$
$$\left.-\frac{1}{\Gamma\left(\frac{1}{\sigma_{p,h}^2}+1\right)}\left[\left(\frac{1}{\sigma_{p,h}^2}[j\tau_p+\tau_h]\right)^{\frac{1}{\sigma_{p,h}^2}}e^{-\frac{1}{\sigma_{p,h}^2}[j\tau_p+\tau_h]}-\left(\frac{1}{\sigma_{p,h}^2}[j\tau_p]\right)^{\frac{1}{\sigma_{p,h}^2}}e^{-\frac{1}{\sigma_{p,h}^2}[j\tau_p]}\right]\right\}$$

For long heat regenerators ($1/\sigma_D^2 > 15$), we have:

$$U(\tau) \cong 1 - \frac{1}{2}\operatorname{erfc}\left(\frac{\tau-1}{\sqrt{2}\sigma_D}\right)$$

From single pass efficiency, Appendix A:

$$\eta_s(\tau_h) \cong \frac{\sigma_{D,h}}{\tau_h\sqrt{2\pi}}\left[e^{-\frac{1}{2\sigma_{D,h}^2}} - e^{-\frac{(\tau_h-1)^2}{2\sigma_{D,h}^2}}\right] + \frac{1}{2\tau_h}\left[(\tau_h-1)\operatorname{erfc}\left(\frac{\tau_h-1}{\sqrt{2}\sigma_{D,h}}\right) + \operatorname{erfc}\left(\frac{-1}{\sqrt{2}\sigma_{D,h}}\right)\right]$$

$$\frac{1}{\tau_h}\int_0^{(N-n)\tau_p+\tau_h}[1-u_h(x)]\,dx = \frac{\sigma_{D,h}}{\tau_h\sqrt{2\pi}}\left[e^{-\frac{1}{2\sigma_{D,h}^2}} - e^{-\frac{1}{2\sigma_{D,h}^2}[(N-n)\tau_p+\tau_h-1]^2}\right] + \frac{1}{2\tau_h}\left[[(N-n)\tau_p+\tau_h-1]\operatorname{erfc}\left(\frac{(N-n)\tau_p+\tau_h-1}{\sqrt{2}\sigma_{D,h}}\right) + \operatorname{erfc}\left(\frac{-1}{\sqrt{2}\sigma_{D,h}}\right)\right]$$

$$\frac{1}{\tau_h}\int_0^{(N-n)\tau_p}[1-u_h(x)]\,dx = \frac{\sigma_{D,h}}{\tau_h\sqrt{2\pi}}\left[e^{-\frac{1}{2\sigma_{D,h}^2}} - e^{-\frac{1}{2\sigma_{D,h}^2}[(N-n)\tau_p-1]^2}\right] + \frac{1}{2\tau_h}\left[[(N-n)\tau_p-1]\operatorname{erfc}\left(\frac{(N-n)\tau_p-1}{\sqrt{2}\sigma_{D,h}}\right) + \operatorname{erfc}\left(\frac{-1}{\sqrt{2}\sigma_{D,h}}\right)\right]$$

$$\frac{1}{\tau_h}\int_0^{(N-n)\tau_p}[1-u_c(x)]\,dx = \frac{\sigma_{D,c}}{\tau_h\sqrt{2\pi}}\left[e^{-\frac{1}{2\sigma_{D,c}^2}} - e^{-\frac{1}{2\sigma_{D,c}^2}[(N-n)\tau_p-1]^2}\right] + \frac{1}{2\tau_h}\left[[(N-n)\tau_p-1]\operatorname{erfc}\left(\frac{(N-n)\tau_p-1}{\sqrt{2}\sigma_{D,c}}\right) + \operatorname{erfc}\left(\frac{-1}{\sqrt{2}\sigma_{D,c}}\right)\right]$$

$$\frac{1}{\tau_h}\int_0^{(N-n)\tau_p-\tau_h}[1-u_c(x)]\,dx = \frac{\sigma_{D,c}}{\tau_h\sqrt{2\pi}}\left[e^{-\frac{1}{2\sigma_{D,c}^2}} - e^{-\frac{1}{2\sigma_{D,c}^2}[(N-n)\tau_p-\tau_h-1]^2}\right] + \frac{1}{2\tau_h}\left[[(N-n)\tau_p-\tau_h-1]\operatorname{erfc}\left(\frac{(N-n)\tau_p-\tau_h-1}{\sqrt{2}\sigma_{D,c}}\right) + \operatorname{erfc}\left(\frac{-1}{\sqrt{2}\sigma_{D,c}}\right)\right]$$

and let j = N-n

$$\eta_h(\tau_h) = \eta_s(\tau_h) + \frac{1}{\tau_h}\sum_{j=1}^{N}\left\{\frac{1}{2}\left[(j\tau-\tau_h-1)\,\mathrm{erfc}\left(\frac{j\tau-\tau_h-1}{\sqrt{2}\,\sigma_{p,c}}\right)-(j\tau-1)\,\mathrm{erfc}\left(\frac{j\tau-1}{\sqrt{2}\,\sigma_{p,c}}\right)\right.\right.$$
$$\left.-(j\tau-1)\,\mathrm{erfc}\left(\frac{j\tau-1}{\sqrt{2}\,\sigma_{p,h}}\right)+(j\tau+\tau_h-1)\,\mathrm{erfc}\left(\frac{j\tau+\tau_h-1}{\sqrt{2}\,\sigma_{p,h}}\right)\right]$$
$$\left.-\frac{\sigma_{p,c}}{\sqrt{2\pi}}\left[e^{-\frac{(j\tau-\tau_h-1)^2}{2\sigma_{p,c}^2}}-e^{-\frac{(j\tau-1)^2}{2\sigma_{p,c}^2}}\right]-\frac{\sigma_{p,h}}{\sqrt{2\pi}}\left[e^{-\frac{(j\tau+\tau_h-1)^2}{2\sigma_{p,h}^2}}-e^{-\frac{(j\tau-1)^2}{2\sigma_{p,h}^2}}\right]\right\}$$

D. Principle of superposition for n-stages fluidized bed model.

— Equal product of mass flow rate and specific heat, Symmetric case.

Input: $$t_{in}(\tau) = \sum_{j=0}^{\infty} \left[H(\tau - 2j\tau_i) - H(\tau - (2j+1)\tau_i) \right]$$

Output: $$t_{ex}(\tau) = \sum_{j=0}^{\infty} \left[U(\tau - 2j\tau_i) H(\tau - 2j\tau_i) - U(\tau - (2j+1)\tau_i) H(\tau - (2j+1)\tau_i) \right]$$

where

$$U(\tau) = 1 - \frac{1}{(1+\beta)^n} e^{-\lambda\tau} \sum_{K=1}^{n} \binom{n}{K} \beta^K e_{K-1}(\lambda\tau)$$

Thermal efficiency;

$$\eta_h(\tau_i) = \frac{1}{\tau_i} \int_{2L\tau_i}^{(2L+1)\tau_i} \left[t_{in}(\tau) - t_{ex}(\tau) \right] d\tau$$

$$= \frac{1}{\tau_i} \int_{2L\tau_i}^{(2L+1)\tau_i} \left\{ \sum_{j=0}^{\infty} \frac{1}{(1+\beta)^n} \left[\sum_{K=1}^{n} \binom{n}{K} \beta^K e^{-\lambda(\tau - 2j\tau_i)} e_{K-1}\left(\lambda(\tau - 2j\tau_i)\right) H(\tau - 2j\tau_i) \right.\right.$$

$$\left.\left. - \sum_{K=1}^{n} \binom{n}{K} \beta^K e^{-\lambda(\tau - (2j+1)\tau_i)} e_{K-1}\left(\lambda(\tau - (2j+1)\tau_i)\right) H(\tau - (2j+1)\tau_i) \right] \right\} d\tau$$

$$= \frac{1}{\tau_i} \frac{1}{(1+\beta)^n} \sum_{j=0}^{L-1} \left\{ \sum_{K=1}^{n} \binom{n}{K} \beta^K \int_{2(L-j)\tau_i}^{(2(L-j)+1)\tau_i} e^{-\lambda\chi} e_{K-1}(\lambda\chi) d\chi \right.$$

$$\left. \longrightarrow (\text{let } \chi = \tau - 2j\tau_i) \right.$$

$$- \sum_{K=1}^{n} \binom{n}{K} \beta^K \int_{(2(L-j)+1)\tau_i}^{2(L-j)\tau_i} e^{-\lambda\chi} e_{K-1}(\lambda\chi) d\chi \Big\}$$

$$\longrightarrow (\text{let } \chi = \tau - (2j+1)\tau_i)$$

$$+ \frac{1}{\tau_i} \frac{1}{(1+\beta)^n} \sum_{K=1}^{n} \binom{n}{K} \beta^K \int_{0}^{\tau_i} e^{-\lambda\chi} e_{K-1}(\lambda\chi) d\chi$$

$$= \eta_s(\tau_i) + \frac{1}{\tau_i} \frac{1}{(1+\beta)^n} \sum_{j=0}^{L-1} \left\{ \sum_{K=1}^{n} \binom{n}{K} \beta^K \int_{0}^{(2(L-j)+1)\tau_i} e^{-\lambda\chi} e_{K-1}(\lambda\chi) d\chi \right.$$

$$\left. - \sum_{K=1}^{n} \binom{n}{K} \beta^K 2 \int_{0}^{2(L-j)\tau_i} e^{-\lambda\chi} e_{K-1}(\lambda\chi) d\chi + \sum_{K=1}^{n} \binom{n}{K} \beta^K \int_{0}^{(2(L-j)+1)\tau_i} e^{-\lambda\chi} e_{K-1}(\lambda\chi) d\chi \right\}$$

From single pass efficiency, Equation 4.2.21:

$$\frac{1}{(1+\beta)^n} \sum_{K=1}^{n} \binom{n}{K} \beta^K \int_{0}^{\tau_i} e^{-\lambda\tau} e_{K-1}(\lambda\tau) d\tau$$

$$= \gamma(\tau_i) = n\left[1 - \frac{e^{-\lambda\tau_i}}{n\beta(1+\beta)^{n-1}} \sum_{K=1}^{n} \binom{n}{K} \beta^K \sum_{j=0}^{K-1} e_j(\lambda\tau_i)\right]$$

and let i = L - j

then

$$\eta_h(\tau_i) = \eta_s(\tau_i) + \sum_{i=1}^{L}\left\{\frac{n}{\tau_i}\left[1 - \frac{e^{-\lambda(2i+1)\tau_i}}{n\beta(1+\beta)^{n-1}} \sum_{K=1}^{n} \binom{n}{K} \beta^K \sum_{j=0}^{K-1} e_j(\lambda(2i+1)\tau_i)\right]\right.$$

$$- \frac{2n}{\tau_i}\left[1 - \frac{e^{-\lambda 2i\tau_i}}{n\beta(1+\beta)^{n-1}} \sum_{K=1}^{n} \binom{n}{K} \beta^K \sum_{j=0}^{K-1} e_j(\lambda 2i\tau_i)\right]$$

$$\left. + \frac{n}{\tau_i}\left[1 - \frac{e^{-\lambda(2i-1)\tau_i}}{n\beta(1+\beta)^{n-1}} \sum_{K=1}^{n} \binom{n}{K} \beta^K \sum_{j=0}^{K-1} e_j(\lambda(2i-1)\tau_i)\right]\right\}$$

$$= \eta_s(\tau_i) + \frac{1}{\tau_i} \sum_{i=1}^{L}\left\{\gamma((2i+1)\tau_i) - 2\gamma(2i\tau_i) + \gamma((2i-1)\tau_i)\right\}$$

$$= \frac{1}{\tau_i}\left\{\gamma(\tau_i) - \sum_{i=1}^{L}\left[2\gamma(2i\tau_i) - \gamma((2i+1)\tau_i) - \gamma((2i-1)\tau_i)\right]\right\}$$

E. Principle of superposition for n-stages fluidized bed model.

— Unequal product of mass flow rate and specific heat, Same switching time, unbalanced case.

Input: $$t_{in}(\tau) = \sum_{j=0}^{\infty}\left[H(\tau - j\tau_p) - H(\tau - j\tau_p - \tau_h)\right]$$

Output: $$t_{ex}(\tau) = \sum_{j=0}^{\infty}\left[U_h(\tau - j\tau_p)H(\tau - j\tau_p) - U_c(\tau - j\tau_p - \tau_h)H(\tau - j\tau_p - \tau_h)\right]$$

where $$\tau_p = \tau_h + \tau_c = \theta_i/\mu_h + \theta_i/\mu_c$$

$$U_h(\tau) = 1 - \frac{1}{(1+\beta_h)^n} e^{-\lambda_h \tau} \sum_{K=1}^{n} \binom{n}{K} \beta_h^K e_{K-1}(\lambda_h \tau)$$

$$U_c(\tau) = 1 - \frac{1}{(1+\beta_c)^n} e^{-\lambda_c \tau} \sum_{K=1}^{n} \binom{n}{K} \beta_c^K e_{K-1}(\lambda_c \tau)$$

Thermal efficiency:

$$\eta_h(\tau_h) = \frac{1}{\tau_h}\int_{L\tau_p}^{L\tau_p+\tau_h}\left[t_{in}(\tau) - t_{ex}(\tau)\right]d\tau$$

$$= \frac{1}{\tau_h}\sum_{j=0}^{L-1}\left\{\frac{1}{(1+\beta_h)^n}\sum_{K=1}^{n}\binom{n}{K}\beta_h^K \int_{(L-j)\tau_p}^{(L-j)\tau_p+\tau_h} e^{-\lambda_h \chi} e_{K-1}(\lambda_h \chi)\,d\chi \right.$$

$$\left. - \frac{1}{(1+\beta_c)^n}\sum_{K=1}^{n}\binom{n}{K}\beta_c^K \int_{(L-j)\tau_p-\tau_h}^{(L-j)\tau_p} e^{-\lambda_c \chi} e_{K-1}(\lambda_c \chi)\,d\chi\right\}$$

$$+ \frac{1}{\tau_h}\frac{1}{(1+\beta_h)^n}\sum_{K=1}^{n}\binom{n}{K}\beta_h^K \int_0^{\tau_h} e^{-\lambda_h \chi} e_{K-1}(\lambda_h \chi)\,d\chi$$

$$= \eta_s(\tau_h) + \frac{1}{\tau_h}\sum_{j=0}^{L-1}\left\{\frac{1}{(1+\beta_h)^n}\sum_{K=1}^{n}\binom{n}{K}\beta_h^K \int_0^{(L-j)\tau_p+\tau_h} e^{-\lambda_h \chi} e_{K-1}(\lambda_h \chi)\,d\chi \right.$$

$$- \frac{1}{(1+\beta_h)^n}\sum_{K=1}^{n}\binom{n}{K}\beta_h^K \int_0^{(L-j)\tau_p} e^{-\lambda_h \chi} e_{K-1}(\lambda_h \chi)\,d\chi$$

$$- \frac{1}{(1+\beta_c)^n}\sum_{K=1}^{n}\binom{n}{K}\beta_c^K \int_0^{(L-j)\tau_p} e^{-\lambda_c \chi} e_{K-1}(\lambda_c \chi)\,d\chi$$

$$\left. + \frac{1}{(1+\beta_c)^n}\sum_{K=1}^{n}\binom{n}{K}\beta_c^K \int_0^{(L-j)\tau_p-\tau_h} e^{-\lambda_c \chi} e_{K-1}(\lambda_c \chi)\,d\chi\right\}$$

From single pass efficiency:

$$\frac{1}{(1+\beta_h)^n}\sum_{K=1}^{n}\binom{n}{K}\beta_h^K\int_0^{\tau_h} e^{-\lambda_h\tau}e_{K-1}(\lambda_h\tau)d\tau$$

$$= \gamma_h(\tau_h) = n\left[1-\frac{e^{-\lambda_h\tau_h}}{n\beta_h(1+\beta_h)^{n-1}}\sum_{K=1}^{n}\binom{n}{K}\beta_h^K\sum_{j=0}^{K-1}e_j(\lambda_h\tau_h)\right]$$

and

$$\frac{1}{(1+\beta_c)^n}\sum_{K=1}^{n}\binom{n}{K}\beta_c^K\int_0^{\tau_c} e^{-\lambda_c\tau'}e_{K-1}(\lambda_c\tau')d\tau'$$

$$= \gamma_c(\tau_c) = n\left[1-\frac{e^{-\lambda_c\tau_c}}{n\beta_c(1+\beta_c)^{n-1}}\sum_{K=1}^{n}\binom{n}{K}\beta_c^K\sum_{j=0}^{K-1}e_j(\lambda_c\tau_c)\right]$$

and let i = L - j

then

$$\eta_h(\tau_h) = \eta_s(\tau_h) + \frac{1}{\tau_h}\sum_{i=1}^{L}\left\{\gamma_h(i\tau_p+\tau_h)-\gamma_h(i\tau_p)-\gamma_c(i\tau_p)-\gamma_c(i\tau_p-\tau_h)\right\}$$

$$= \frac{1}{\tau_h}\left\{\gamma_h(\tau_h)-\sum_{i=1}^{L}\left[\gamma_h(i\tau_p)+\gamma_c(i\tau_p)-\gamma_h(i\tau_p+\tau_h)-\gamma_c(i\tau_p-\tau_h)\right]\right\}$$

F. Design Problem

Consider a pair of heat regenerators 30 m high and 4 m in diameter filled with uniformly sized, and close to spherical, basaltic beach stones. The regenerators are to be used to transfer heat from hot waste gases (800°C) leaving a process to cold incoming gases (200°C).

Data:

For the solid: $d_p = 0.08$ m $\qquad K_\rho = 0.5\ W\ m^{-1}\ °K^{-1}$

$\rho_s = 2280\ kg\ m^{-3} \qquad C_{ps} = 1000\ J\ kg^{-1}\ °K^{-1}$

For both hot and cold gas in the regenerator take the average properties at 500°C:

$\mu = 3.5 \times 10^{-5}\ kg\ m^{-1}\ s^{-1} \qquad K_g = 0.05\ W\ m^{-1}\ °K^{-1}$

$\rho_g = 0.5\ kg\ m^{-3} \qquad C_{pg} = 1020\ J\ kg^{-1}\ °K^{-1}$

Different mass flow rates in the regenerator:

$\varepsilon = 0.4 \qquad u_{gh} = 4\ m\ s^{-1}$ (or $\dot{m}_h = 25.14\ kg\ s^{-1}$)

$u_{gc} = 2\ m\ s^{-1}$ (or $\dot{m}_c = 12.57\ kg\ s^{-1}$)

Solution:

1. Find the variance for both heating and cooling period

   (i) Heating period, $\sigma^2_{D,h}$

$$Re_{,h} = \frac{d_p\ u_{gh}\ \rho_g}{\mu} = \frac{(0.08)\ (4)\ (0.5)}{3.5 \times 10^{-5}} = 4.6 \times 10^3 > 10$$

$$Pe = \frac{C_{pg}\ \mu}{K_g} = \frac{(1020)\ (3.5 \times 10^{-5})}{0.05} = 0.714$$

Replacing in one of the recommended correlation

$$\frac{h_{\rho,h}\, d_p}{K_g} = 2 + 1.8\ Re,_h^{1/2}\ Pr^{1/3}$$

then give $h_{\rho,h} = 69.45\ W\ m^{-2}\ °K^{-1}$

Using Equation 6.3.2,

$$\sigma_{D,h}^2 = \frac{1}{30\ (1-\varepsilon)} \frac{u_{gh}\ \rho_g\ C_{pg}\ d_p^2}{K_\rho\ L} + \frac{1}{3\ (1-\varepsilon)} \frac{u_{gh}\ \rho_g\ C_{pg}\ d_p}{h_{\rho,h}\ L} + \frac{d_p}{L}$$

$$= 0.048 + 0.044 + 0.0027 = 0.0947$$

or $1/\sigma_{D,h}^2 = 10.56$

(ii) Cooling period, $\sigma_{D,c}^2$

$$Re,_c = \frac{d_p\ u_{gc}\ \rho_g}{\mu} = \frac{(0.08)\ (2)\ (0.5)}{3.5 \times 10^{-5}} = 2.3 \times 10^3 > 10$$

$$Pe = \frac{C_{pg}\ \mu}{K_g} = 0.714$$

then give $h_{\rho,c} = 49.47\ W\ m^{-2}\ °K^{-1}$

Using Equation 6.3.2,

$$\sigma_{D,c}^2 = \frac{1}{30\ (1-\varepsilon)} \frac{u_{gc}\ \rho_g\ C_{pg}\ d_p^2}{K_\rho\ L} + \frac{1}{3\ (1-\varepsilon)} \frac{u_{gc}\ \rho_g\ C_{pg}\ d_p}{h_{\rho,c}\ L} + \frac{d_p}{L}$$

$$= 0.024 + 0.030 + 0.0027 = 0.0567$$

or $1/\sigma_{D,c}^2 = 17.64$

2. Find the thermal mean residence time for both heating and cooling period

(i) Heating period, μ_h

$$M_s = \rho_s V_s = \rho_s \left(\frac{1}{4}\pi D^2\right) (L) (1-\varepsilon) = 515724 \text{ kg}$$

$$\mu_h = \frac{M_s C_{ps}}{\dot{m}_h C_{pg}} = \frac{(515724)(1000)}{(25.14)(1020)} = 20112 \text{ s} \simeq 5.6 \text{ hr}$$

(ii) Cooling period, μ_c

$$\mu_c = \frac{M_s C_{ps}}{\dot{m}_c C_{pg}} = \frac{(515724)(1000)}{(12.57)(1020)} = 40224 \text{ s} \simeq 11.2 \text{ hr}$$

So we have unequal $\dot{m} C_{ps}'$ for both periods and the ratio is:

$$\mu_h/\mu_c = 0.5$$

3. Find the optimal switching time and maximum overall efficiency for this system

(i) Cocurrent Operation

By the optimization search (similar to Figure 6.1), for the system $1/\sigma_{D,h}^2 = 10.56$, $1/\sigma_{D,c}^2 = 17.64$ and $\mu_h/\mu_c = 0.5$ the optimal switching time should be:

$$\tau_h = 1.52 \text{ and } \tau_c = 0.76$$

$$\text{i.e. } \theta = 30570 \text{ s} \simeq 8.5 \text{ hr}$$

and the corresponding overall efficiency is:

$$\eta_{o,max} = 0.644$$

(ii) Countercurrent Operation

We know that at the same switching time condition countercurrent flow gives higher efficiency than cocurrent flow and the

shorter the switching time the higher will be its thermal efficiency for countercurrent operation, i.e., for the system $1/\sigma_{D,h}^2 = 10.56$, $1/\sigma_{D,c}^2 = 17.64$ and $\mu_h/\mu_c = 0.5$ at switching time $\theta \leq 8.5$ hr the overall efficiency is $\eta_o \geq 0.644$ for countercurrent operation.

(iii) Upper limit for this system

From Figure 2.5

the maximum overall efficiency with $\mu_h/\mu_c = 0.5$ for ideal regenerators for both cocurrent and countercurrent operations is:

$$\eta_{o,max}^{ideal} = 0.667$$

12. VITA

Biographical items on the author of this thesis, Mr. Shih-Ming Lai.

1) Born August 15, 1956.

2) Attended National Taiwan University, Taipei, Taiwan, from September 1974 to June 1978. Received the degree of Bachelor of Science in Chemical Engineering in June, 1978.

3) Platoon Leader (2nd Lt.), Chinese Army, Taiwan, July, 1978 to May, 1980.

4) Teaching Assistant, Department of Chemical Engineering, National Taiwan University, August, 1980 to July, 1981.

5) Attended Washington University from August, 1981 to the present date.

June, 1983